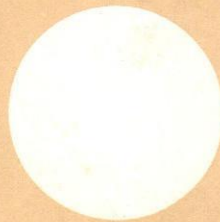


R-J-03

Vol. 03 No. 01 December 1996

TECHNICAL  
**JOURNAL**



**RIVER RESEARCH INSTITUTE  
FARIDPUR**

# TECHNICAL JOURNAL

Vol.03 No.01 December 1996



RIVER RESEARCH INSTITUTE  
FARIDPUR



# TECHNICAL JOURNAL

VOLUME 10, NUMBER 1, 1978



RIVER RESEARCH INSTITUTE  
FARMERS

# TECHNICAL JOURNAL

RIVER RESEARCH INSTITUTE, FARIDPUR

December 1996

## EDITORIAL BOARD

### CHAIRMAN

Syed Abdus Sobhan

### MEMBERS

Md Hanif Mozumder

Dr. Nilufa Islam

Md Abul Ala Moududi

### EXECUTIVE EDITOR

Md Nazrul Islam Siddique

### PUBLICATION ASSOCIATES

Swapan Kumar Das

A M M Motaher Ahmed

Md. Kawser Jamil

Md. Fazlul Karim

Dibakar Chakma

### OFFICE MANAGER

Md Abul Kashem Miah



EDITORIAL BOARD

CHAIRMAN

Prof. John S. Allen

MEMBERS

Mr. David Allen

Dr. John Allen

Mr. John Allen

EXECUTIVE EDITOR

Mr. John Allen

PUBLICATION ASSOCIATES

Mr. John Allen

Mr. John Allen

Mr. John Allen

Mr. John Allen

Mr. John Allen

ONLINE

Mr. John Allen

## TECHNICAL PAPERS

<u>Sl. No.</u>	<u>Title</u>	<u>Page</u>
1.	LOSS OF INACCURATE ESTIMATES OF RETURN PERIOD FOR DESIGN OF FLOOD PROTECTION WORKS	1
	Abu Musa Md Motaher Ahmed	
2.	APPLICATION OF PHYSICAL MODEL APPROACH FOR HYDRODYNAMIC AND MORPHOLOGICAL PREDICTIONS: CASE STUDY ON JAMUNA MULTIPURPOSE BRIDGE PROJECT	10
	Md Badiur Rahman, A M M Motaher Ahmed, Md Abul Ala Moududi & Md Manjurul Hoque	
3.	A CASE STUDY FOR THE PROTECTION OF PANKA NARAYANPUR AREA FROM THE EROSION OF THE GANGES	23
	Syed Abdus Sobhan, Md Nazrul Islam Siddique, Swapan Kumar Das & Mohammed Fazlul Karim	
4.	THE DETERMINATION OF PRECONSOLIDATION PRESSURE FROM CONSOLIDATION TEST AS SIGNIFICANT FOR THE CORRECT EVALUATION OF SETTLEMENT BEHAVIOUR OF SOIL	33
	Md Hanif Mozumder	
5.	ANALYSIS OF ANNUAL EXTREMES OF THE GUMTI RIVER FOR THE DETERMINATION OF 100-YEAR FLOOD MAGNITUDE THROUGH THE DISTRIBUTION FITTINGS	49
	Md Abul Kashem	



6. SCALE MODEL STUDY OF GROYNES FOR THE PROTECTION OF SIMLA AREA FROM THE EROSION OF JAMUNA RIVER 59  
A K M Ashrafuzzaman, Syed Md Anwaruzzaman & Md Nazrul Islam Siddique
7. EFFECTS OF CLAY AND SILT ON THE STRENGTH CHARACTERISTICS OF DIFFERENT TYPES OF SOIL IN BANGLADESH 79  
Mst Anwara Jahan
8. THE KARNAFULI RIVER AND IT'S NAVIGATIONAL FACILITIES FOR THE CHITTAGONG PORT 94  
Md Lutfor Rahman
9. IMPORTANCE OF USING CONE PENETRATION TEST IN SOLVING THE PROBLEMS ASSOCIATED WITH STANDARD PENETRATION TEST 100  
Md Hanif Mozumder & Md Matiar Rahman Mondol
10. STABILITY TEST OF THE PATENGA COASTAL EMBANKMENT NEAR CHITTAGONG 107  
Md Rafiqul Alam
11. DEVELOPMENT OF HEAT AND IT'S DISSIPATION IN HARDENING CONCRETE 117  
Md Sawkat Ali

# Loss of Inaccurate Estimates of Return Period for Design of Flood Protection Works

Abu Musa Md Motaher Ahmed<sup>1</sup>

## Abstract

*The optimum design of flood protection, taken as the height of embankment that maximises the 'net-benefit', depends on a knowledge of flood return periods. Inaccurate estimates will lead to sub-optimum designs. The cost of such inaccuracies is investigated by computer simulation, for a simple scenario based on a published Benefit against Return Period relationship (Parker et al., 1987). Attempts have been made on to the selection of a prospective flood protection works in order to maximising the 'net-benefit'.*

## Introduction

The term 'benefit' comprises the possible outcome of any investment. More specifically, flood prediction benefit is the return from investment in flood protection; benefits include flood losses avoided. The benefits have to be balanced against the cost of investment. Such a comparison is known as a 'cost-benefit analysis'. An important part of a cost-benefit analysis for flood prediction is the estimation of return periods because we are not certain of receiving the good - there is just a chance that we do. In the present study, it is assumed that the optimal design of flood protection, the height of an embankment along a river bank for example, will be when the difference between the benefit and the cost of protection is maximum.

The objective of maximising 'net-benefit'(profit), rather than attempting to provide complete protection or protection of equal value to the expected loss, can be justified because there is always a shortage of money for public investment-there could be more hospitals, better equipped schools and so on and public funds should be spent to maximise the 'net-benefit' i.e. public schemes have to compete against each other, such as, different flood protection projects. Conceptually, if the structure is constructed larger than the optimum design the 'net-benefit' i.e. the difference between the benefit and cost of protection will be reduced and if the structure is smaller, the profit also will be reduced. So, overdesign or underdesign both have the similar shortcomings. At one extreme, if the costs actually exceeds the benefits we have so overdesigned the structure that the design would be criticised under any sensible policy of public spending. On the

---

<sup>1</sup> Scientific Officer, River Research Institute, Faridpur



other hand, if the costs are less than the benefits we have underdesigned the structure to a similar extent. But this may be inevitable if there are no public funds.

The optimum design depends on the probabilities of floods exceeding certain levels. These probabilities can only be estimated approximately. The optimum design return period can be determined by the probabilistic nature of a hydrological event and damage that will result over feasible range of events. As the design return period increases, the cost of construction of a structure increases, but the expected damages decrease because of the better protection afforded. A design return period having maximum 'net-benefit' can be found by 'cost-benefit analysis'. The aim of this study is to investigate the loss that is a consequence of inaccurate estimates of probabilities. The loss is the difference between maximum 'net-benefit' and the difference between the cost of construction and the actual benefits achieved from it. The analysis has not been attempted to follow through the whole process of a specific actual cost-benefit analysis.

## Methodology

The estimation of flood extent incorporates a relationship between hydrological analysis of the frequency of flood discharges and the economic analysis of flood protection benefits. Floods can be defined in terms of stage or discharge. The general relationship between these are non-linear (e.g.  $Q \propto H^{3/2}$  for a rectangular channel). As a simplification it is assumed that they are linearly related. A 'loss-probability' relationship can be established by combining 'stage-damage' relationships with return period or probability of exceedance. Such a relationship links expected event damages to probability of exceedance. By integrating the area under the loss-probability curve, the average annual benefits of protecting upto a specified design standard can be determined. Assessment of event losses for some return period events are used to estimate the shape of the loss-probability curve and calculate the area under the curve. Expected annual value of benefits can be estimated as the mean damage expected between two successive flood stages at each flood level is multiplied by its interval probability of exceedance. The expected annual value of benefits afforded by protection of any particular flood stage are the cumulative annual benefits to that flood stage. Flood prediction in terms of probability of exceedance with a certain return period is a basic tool to the protection needed for that level of flood which causes severe damages as because the benefits are very sensitive to the return period event at which flooding occurs. It is inevitable require to calculate 'loss-probability' curves without scheme and with scheme situations and thus the difference between the two curves represents the benefits of flood protection.

A numerical example is based on a catchment for which it is assumed that the probability that the stage exceeds 2.97 scaled units is 0.05. The design which gives a maximum 'net-benefit' is compared with designs based on maximising 'net-benefit' when the probability of exceeding 2.97 is incorrectly estimated at 0.01, 0.03, 0.08, 0.10, 0.2 and so on.



## Data requirements

The three data components essential to the evaluation comprise flood probability data, often derived from river flow or hydrographic records, data on flood stage for given probabilities and flood damage data for different flood stages.

### Damage-discharge relationship:

Combining the 'stage-damage' and 'stage-discharge' relationships yields a 'damage-discharge' relationships for various protection levels.

### Damage-probability relationship:

Combining 'damage-discharge' relationships with the return period or exceedance probability data yields 'probability-damage' data.

### The loss-probability relationship:

By combining 'stage-damage' relationships with return period or exceedance probability data a 'loss-probability' relationship may be established (Figure.1). This figure is originally taken from an example of 'loss-probability' relationship (Parker et.al., 1987, Figure 1.3) for which the physical details of the catchment were not given and is used to calculate annual average flood losses. Such a relationship links expected event damages to exceedance probability. By integrating the area under the loss probability curve over  $P_r = 0$  to 1, the average annual value of protecting upto a specified design standard can be determined.

### The value of accuracy in flood prediction

For simulation, it is assumed that flood stage and corresponding discharge are linearly related and it is also assumed that scaled flood stage (heights) are distributed with an EV1 distribution with a mean of 0 and a standard deviation of 1. The results are unaffected by this scaling, since everything is in relative terms, and 0 and 1 are convenient parameters of the EV1 distribution to work with. It is also assumed from Figure 1 that the embankment will prevent flood damage for floods with a return period of up to 50 years (1/0.02), where 0.02 is the probability of exceedance because residual loss starts there. This corresponds to a scaled height of 3.9 which is the solution of following equations:

$$F(Y) = [\exp\{-\exp(-Y)\}] \dots (I)$$

$$\text{or, } Y = -\ln(-\ln(0.98)) \dots (II)$$

Where, Y is the height of embankment, F(Y) is the probability of non-exceedance which equals 1-P(Y) and P(Y) is the probability of exceedance of flood of same magnitude.



It is further assumed after extending the without curve towards right in Figure 1 that, the flood of 5-year return period (i.e. probability of exceedance 0.20) does not damage to the property and only damages start from the flood of return periods higher than that.

### Calculation of benefits:

The annual value of an embankment of height 3.9 is estimated from Figure 1 as 23.21 (in million Taka). The calculation of the values of embankment height of 3.9 when the probability of exceeding 2.97 = 0.05 is shown in Table-1. In this investigation, the designs are based on estimated probabilities of exceeding 2.97. If the probability of exceeding 3.9 is 0.02 then the probability of exceeding 2.97 is 0.05. The value here, comprises the savings of money by protecting the floods of 50 year return period providing an embankment comparing without that.

The value of accuracy of estimation has been investigated by fixing the probability of exceeding 2.97 as 0.05 and it is also assumed that this probability estimate turns out the maximum 'net-benefit' at the height of 3.9.

The value of the height of 3.9 is now estimated for different assumed probability of exceeding 2.97 in the same procedure and presented in Table-2. This table shows that when the probability of exceeding 2.97 increased, the value of 3.9 also increased because the corresponding probabilities of exceeding as well as interval probabilities increased. Similarly, the value decreased with decreasing probabilities of exceeding 2.97.

The values of different heights are now estimated as above by assuming the probability of exceeding 2.97 as 0.01 and the procedure is repeated for other probabilities. The values of different heights are plotted against assumed probability of exceeding 2.97. Here, the scheme is designed to protect the maximum flood level of 3.9 where 2.97 corresponds probability of exceedance 0.05. It is evident that the value of the embankment of a height of 3.9 is much higher for higher probabilities of exceeding 2.97 and lower for low probabilities. However, in the simulation experiment it is assumed that the real probability of exceeding 2.97 is 0.05. The changes in value are the misleading quantities that will be calculated if the probability of exceeding 2.97 is incorrectly estimated. Actually, overestimating in probability of exceeding reduces the magnitude of return period and implies a higher value of the embankment of a given height. Similarly, underestimating probability ultimately increases the return period with higher flood and as a result the structures are undervalued.

The benefit is then compared to the cost of construction and it is then justified on the basis of economic consideration whether or not the scheme is economically worthful to protect the flood of designed level.

Table-1:

Return Period (Years)	Prob. of Exceed.	Interval Prob.	Damage without	Damage with	Benefit	Average benefit	Annual benefit	Cumu. benefit
5	0.2		0	0	0			
		0.033				10	0.33	0.33
5.98	0.167		20	0	20			
		0.067				30	2.01	2.34
10	0.1		40	0	40			
		0.05				75	3.75	6.09
20	0.05		110	0	110			
		0.025				165	4.13	10.22
40	0.025		220	0	220			
		0.005				255	1.28	11.49
50	0.02		290	0	290			
		0.007				342.5	2.40	13.89
76.92	0.013		420	25	395			
		0.01				615	6.15	20.04
333.33	0.003		885	50	835			
		0.003				1057.5	3.17	23.21
$\infty$	0		1380	100	1280			

\*\* All damage and benefit figures are in Million Taka.

Table-2:

Value of 3.9 (in million Taka)	5.92	9.82	14.1	23.2	38.2	49.3	80.5	117.2
Pr( $X > 2.97$ )	0.01	0.02	0.03	0.05	0.08	0.10	0.15	0.20



### Cost calculation:

A plausible cost curve has been based on two basic assumptions:

1. The cost is of the form:

$$C = a + bh^3$$

Where,  $a$  is a fixed cost element,  $b$  is a constant of variable cost component and  $h$  is the height of the embankment. The variable cost or marginal cost increases with the volume of structure.

2. The height of 3.9 is an optimum, in so much as the difference between the benefit and cost is a maximum, when the probability of exceeding 2.97 is the assumed real value of 0.05.

A plausible cost curve has been assumed which crossed the benefit curve when height,  $h=6.0$  and the assumed cost model is expressed as the following equation:

$$C = 4.74 + 0.088h^3$$

This equation shows that if a cost curve and benefit curves are given, a value can then put on the accuracy of probability calculations.

### Cost-benefit comparison:

Scheme benefits and costs for different height of defence are plotted for probability of exceeding 2.97 = 0.05 which is real curve and shown in Figure 2 and the 'real net-benefit' for optimum strategy is found at the embankment height of 3.9.

It is worthwhile to construct an embankment of height of 3.9 because it maximises the 'net-benefits'. However, the embankment can be made at height 6.0 where benefit equals cost but extra savings from the height beyond the design height of 3.9 are less than the extra cost of construction. Similarly, the height of less than design reduces the 'net-benefit' since the reduction in cost is less than the decrease in benefit. So, these two alternatives has similar effects rather than to select a design height. In economic point of view, it is worthful to save money because there may be fund constraints for public welfare but it is well recommended to design a scheme with maximising 'net-benefit'. If the 'net-benefit' is less than maximum and construction cost for height less than 3.9 saves extra money, then it is justified to construct it. If the benefits and costs are plotted for different incorrect estimated probabilities of exceeding 2.97, then the maximum wrongly estimated 'net-benefits' are estimated and the heights which maximise those wrong 'net-benefits' have been identified. The 'net-benefits' for identified heights are extracted from real curve(Figure 2) simply by read-off the values from the curve and termed as 'estimated net-benefits' for optimum strategy. The 'net-benefits' for the optimum design



strategy are then plotted against different probabilities of exceeding 2.97 and 'Profit-Probability' relationship for optimum strategy has been found.

An alternative 'Profit-Probability' curve is then constructed by a policy that tends towards overdesign and a 'Profit-Probability' curve using the nearly optimum design strategy has been established. The strategy of overdesign is on the basis of taking an optimum region of heights within 10% of maximum 'net-benefits' for each estimated probabilities of exceeding 2.97 and the middle of that region corresponds to nearly optimum strategy 'net-benefits'. The point is that whilst this is not as good if the probability of exceeding 2.97 is estimated exactly at 0.05- it is better when probabilities are incorrectly estimated. The real 'nearly optimum net-benefits' are found from Figure 2 and the estimated nearly optimum strategy 'net-benefits' are obtained as before. The estimated nearly optimum strategy 'net-benefits' are plotted against estimated probabilities of exceeding 2.97 and the 'Profit-Probability' curve for nearly optimum strategy has been established. These two 'Profit-Probability' curves are then compared which is shown in Figure 3 to select a design which would satisfy the scheme objectives. The designer might select optimum strategy or nearly optimum strategy because this is less sensitive to the accuracy of the probability estimates.

### Conclusions and Recommendations

There may be a number of schemes where the benefit exceeds cost and it is a question to the decision makers which is to be implemented. The decision can be encapsulated by examining the marginal increase of benefits with increasing costs. Here, it is assumed that the design would be constructed to maximise 'net-benefit'. In practice, the best value for money if budgets are limited would be the schemes where the ratio of 'net-benefit' to cost is maximum. However, this does not affect the design parameters for a project, it does affect whether the project is implemented.

Before implementation of expensive flood protection projects, economic evaluation of flood prediction with accuracy in terms of cost-benefit analysis is a must. Because there may be uncertainty in flood predictions and it is not easy to predict the extent of flood.

Since the aim is to provide effective flood embankment to protect people and property against flooding, the risks should be minimised to get maximum 'net-benefit'. This goal can be achieved by comparing optimum and sub-optimum design strategies.

The nearly optimum design strategy is less sensitive to the estimates with less risk and eventually the expected 'net-benefit' from the protection is higher than the optimum design strategy. Since the accuracy of the estimation of flood risk is of concern, it is recommended to design a flood embankment based on sub-optimum strategy which also will maximise the 'net-benefit' and cost ratio.



## References

1. AHMED, A.M.M.M. (1994) *M.Sc Engineering Thesis entitled 'Economic Benefit of Improving the Accuracy and Precision of Flood predictions'*, Published from Civil Engineering department, University of Newcastle upon Tyne, England.
2. BARI, M.F. (1994) Flood Proofing Potentials in Bangladesh Flood Management, In White, W.R. and Watts, J. (eds.), paper presented at *2nd International Conference on River Flood Hydraulics*, Wallingford Ltd., Wallingford, Oxon, John Wiley and Sons Ltd, UK. pp 553-560.
3. CHATTERTON, J.B. and FARREL, S.J. (1977) *Nottingham Flood Warning Scheme: Benefit Assessment*, Middlesex Polytechnic Flood Hazard Research Centre, Enfield, England.
4. FLOOD ACTION PLAN (1992) *North West Regional Study (FAP 2), Vol 13, Draft Final Report*, Government of the People's Republic of Bangladesh.
5. HAQUE, M.M. (1994) Evaluating Design Characteristics of Floods in Bangladesh, In White, W.R. and Watts, J. (eds.), paper presented at *2nd International Conference on River Flood Hydraulics*, Wallingford Ltd., Wallingford, Oxon, John Wiley and Sons Ltd, UK. pp 553-560.
6. PARKER, D.J., GREEN, C.H. AND THOMPSON, P.M. (1987) *Urban Flood Protection Benefits : A Project Appraisal Guide*, Aldershot, Hampshire. Gower Technical Press/Saxon House, London.

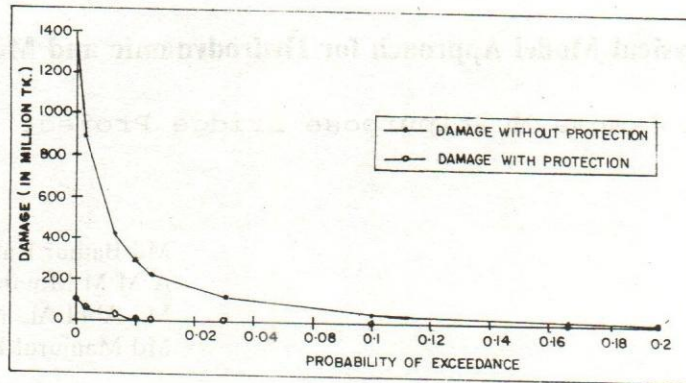


FIGURE 1: LOSS-PROBABILITY RELATIONSHIP (AFTER PARKER et al., 1987)

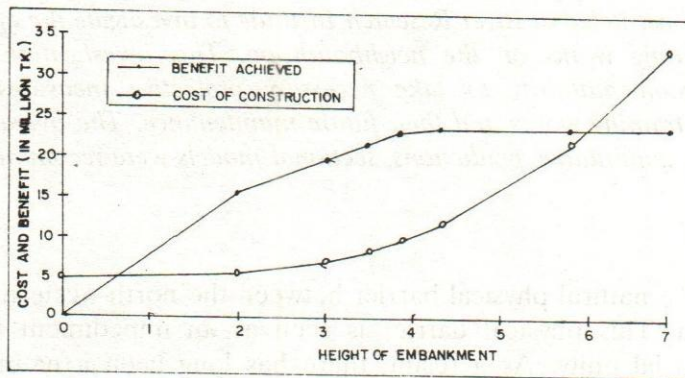


FIGURE 2: BENEFIT-COST RELATIONSHIP WHEN  $\Pr(X > 2.97) = 0.05$

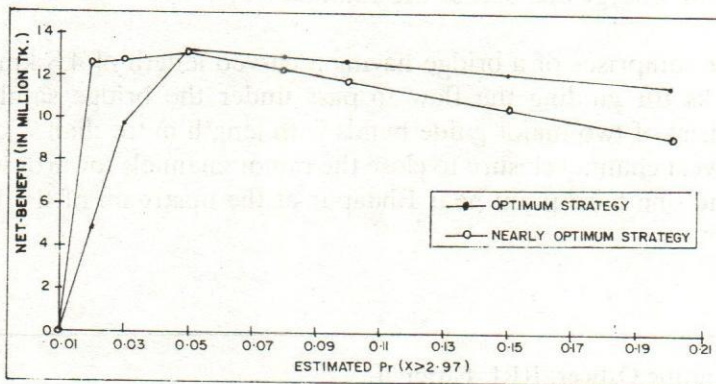


FIGURE 3: COMPARISON OF OPTIMUM STRATEGY AND NEARLY OPTIMUM STRATEGY NET-BENEFIT WITH ESTIMATED PROBABILITIES OF EXCEEDING 2.97



## **Application of Physical Model Approach for Hydrodynamic and Morphological Predictions:**

### **case Study on Jamuna Multipurpose Bridge Project**

Md Badiur Rahman<sup>1</sup>

A M M Motaher Ahmed<sup>2</sup>

Md Abul Ala Moududi<sup>3</sup>

Md Manjurul Hoque<sup>4</sup>

### **Abstract**

*This paper describes the possible hydrodynamic and morphological changes during the construction and maintenance phases of jamuna bridge construction. An overall fixed bed physical model was constructed at River Research Institute to investigate the effect of bridge along with river training works on the neighbourhood. This investigation enables the construction supervision authority to take necessary protective measures during the construction of river training works and their future maintenance. The overall predictions were qualitative. For quantitative predictions, sectional models were recommended.*

### **Introduction**

The river Jamuna is a natural physical barrier between the north-western and eastern parts of Bangladesh. This physical barrier is seen as an impediment to economic development and social unity. As a result, there has long been a natural desire to establish this permanent link between the east and the north-west. The construction of Jamuna Multipurpose Bridge has been undertaken to establish a permanent link between the two parts of the country. The proposed bridge which is under construction and is located about 8 km downstream of the existing ferry ghat near Bhuapur and provide for transfer of road, rail, energy etc. across the Jamuna river.

The bridge project comprises of a bridge having a curved length of 4.8 km and several river training works for guiding the flow to pass under the bridge safely. The river training works consist of two major guide bunds with length more than 2 km each, one large dike named west channel closure to close the minor channels towards western bank (Sirajgonj side) and one hard point near Bhuapur at the upstream of the bridge.

---

<sup>1</sup>Senior Scientific Officer, RRI, Faridpur.

<sup>2,3&4</sup>Scientific Officer, RRI, Faridpur.

The river Jamuna is a multi-channeled river with typically 2 to 4 channel and maximum discharge of about 90000 m<sup>3</sup>/s. The river flows through fluvial deposits of fine sand and traces of silt. This dynamic river changes its planform from year to year resulting in major shifts of main channel in braiding belt. The continuous morphological changes may affect the progress of the construction works and disrupting the maintenance of the bridge and river training structures. The physical model study was undertaken to forecast hydrodynamic and morphological changes during the construction phases of different river training structures.

In this study, the model was operated at different scenarios of flooding to check the robustness of the construction methodology followed by the contractors and to ascertain the needs/options for temporary protective measures prior to completion of the project works.

### **The study area**

The study area is about 135 km downstream of Bangladesh border of the Jamuna river. The latitude and longitude of the study area lies between 24°21'N to 24°31'N and 89°41'E to 89°51'E. The main bridge along with the components are shown in Figure 1. The eastern part of the project area is located under Tangail district and western part under Sirajgonj district. The area comprised of flood plains, mega-chars(stable chars), unstable chars where the people lives. Crops are grown on these lands which is the main source of income generation. Several numbers of mega-chars are situated within the study area.

### **Aspects of the study**

The study deals with a view to meet the following objectives:

- to determine the flow velocities and flow fields in order to determine the effect of bridge construction on the entire river training works;
- to find out the difference in water level between upstream and downstream of the closure due to closing of the four minor channels towards western bank and to see the robustness of the construction methodology; to determine the effect of west guide bund on the east bank; and
- to forecast possible morphological changes around the bridge due to the construction of different river training structures.

### **Theoretical considerations**

For long stretches of either a canal or a river in which the actual changes in bed configuration are not critical, are usually studied in fixed bed models. Unless an unusually large model is involved, a distortion of slope is required the followings:



- To offset the disproportionately high resistance
- To obtain a sufficiently high value of the Reynold's number which will ensure turbulent flow or
- To accommodate the model in the available space

In the first case, the vertical exaggeration is designed to compensate for the high model resistance. In other cases, extra or, artificial model roughness may be required to compensate for the exaggerated model slope.

The required distortion of slope can be computed with sufficient precision from the empirical Manning's formula:

$$V = \frac{1}{n} R^{\frac{2}{3}} S^{\frac{1}{2}}$$

Where, V=Velocity, R= Hydraulic radius and S= Slope and n is the Manning's roughness co-efficient. In order that the velocity ratio will vary with the square root of the depth scale as required by the Froude law:

$$V_r = \sqrt{y_r} = \frac{R_r^{2/3} S_r^{1/2}}{n_r}$$

Substituting  $y/L$  for S results in the expression,

$$\sqrt{y_r} = \frac{R_r^{2/3} y_r^{1/2}}{n_r L_r^{1/2}}$$

or

$$\frac{y_r}{L_r} = \frac{n_r^2 y_r}{R_r^{\frac{4}{3}}}$$

If n is known for model and prototype,  $n_r$  is also known and the exaggeration  $y_r/L_r$  can be computed for a given depth y and hydraulic radius R. In models for which the slope distortion is dictated by other considerations, an adjustment of model roughness is required to simulate prototype conditions. If the distortion and value of n for the prototype are known, the required value of n for model can be computed from the above equation.

The model with roughness adjusted for a particular depth will yield dependable results for flow at or near that depth. If a problem involves several depths, the model roughness should be adjusted to give an average friction that is approximately right for each depth

or the roughness may be varied with depth for a closer approximation at all depths. The fact is that the Manning's  $n$  is strictly a roughness characteristic, and that the Manning's formula applies only at sufficiently high values of  $R$  for viscous effects to be negligible.

The relative roughness of model and prototype are kept same to get geometric similitude. For dynamic similitude, the Froude's number and Reynold's number should be the same in model and prototype. But it is impossible to satisfy both criteria in model. However, the viscous effect (expressed by Reynold's number) is minimized by ensuring rough turbulent flow in the model.

### **Data acquisition**

To carry out the overall fixed bed physical model study of Jamuna river at Jamuna bridge project area, the following information/data were collected from different sources and were used for the study:

- **Topographic data :**

The bathymetric survey was carried out by Surface Water Modelling Centre (SWMC) during September-October, 1995. In this survey a total 118 numbers of cross-section were surveyed at an interval of 100 m and 300 m covering 15 km upstream 5 km downstream of the bridge axis in which sounding depth were measured at an interval of 50 m along each cross section. At the same period, chars were also surveyed.

- **Hydrometric data:**

Hydrometric data such as water level, discharge, average velocity were collected from Surface Water Modelling Centre (SWMC), FAP 24 and Construction Supervision Consultants (CSC).

- **Bed material data:**

A number of bed material samples were collected from different location of the surveyed area and analyzed.

- **Design data :**

Design of West Channel Closure, East and West guide bunds, bridge and hard points etc. were collected from Jamuna Multipurpose Bridge Authority (JMBA) and CSC.



### Model set up and scale ratios

In the frame work of the model study, an overall fixed bed model covering 15 km at upstream and 5 km at downstream of the bridge axis was reproduced with a view to forecast the possible hydrodynamic and morphological changes around the bridge site due to construction of bridge and different river training structures. The extent of the model area is shown in Figure 2. The geometric scales are given in Table - 1.

Table-1 : Geometric Scales

Parameters	Unit	Scale factor
Length	m	280
Width	m	280
Depth	m	80

The other scale ratios were determined based on Froude's model law to achieve geometric and dynamic similarity in the model and are presented in Table-2.

Table-2: Model Scale Ratios

Parameters	Unit	Scale factor
Discharge	m <sup>3</sup> /s	200351
Flow velocity	m/s	8.94
Water surface slope	-	1/3.5
Relative roughness(k/h)	-	0.0233
Chezy's co-efficient (C)	m <sup>0.5</sup> /s	1.87
Manning's co-efficient (n)	s/m <sup>0.33</sup>	1.11

### Model construction

The model bed was constructed as per bathymetric data collected by SWMC. A layer of brick was placed over the sand bed and then plastered by 30 mm thick sand-cement

mortar. Finally, brick chips were placed to reproduce prototype roughness in the model as per model design.

### Boundary conditions

For a fixed bed overall model, two types of boundary conditions are needed.

- a) An upstream boundary condition at the inflow of the model
- b) A downstream boundary condition at the outflow of the model

The upstream boundary condition is the discharge distribution along the upstream section of the model. The downstream boundary condition is the water level along the downstream of the model boundary. The upstream discharge distribution and downstream water level were collected from 2-D mathematical model which was carried out by Danish Hydraulic Institute(DHI) in association with Surface Water Modelling Centre (SWMC). This discharge distribution was ensured at the upstream of the model boundary by several trails and the downstream water level was controlled by tail gates.

### Calibration and Verification

#### Discharge and Velocity

For better representation of the model results, a medium discharge of  $74,918 \text{ m}^3/\text{s}$  was considered for model calibration. This flow was measured by FAP-24 in July 1995. The model was calibrated at the bridge corridor where the flow was separated by two distinct channels. The individual flow for these channels were  $62,431 \text{ m}^3/\text{s}$  and  $12,487 \text{ m}^3/\text{s}$  for channel 1 (main channel) and channel 2 (combined four minor channels) respectively. The corresponding average velocities were measured as  $1.95 \text{ m/s}$  and  $1.86 \text{ m/s}$ .

#### Bed roughness

The Chezy's roughness value of the Jamuna river at Sirajgonj varies between  $40 \text{ m}^{0.5}/\text{s}$  for low flow and  $100 \text{ m}^{0.5}/\text{s}$  for flood condition (Klaassen et.al. 1988). In the Jamuna bridge project study, it was found that the Chezy number varies between  $40 \text{ m}^{0.5}/\text{s}$  for low flow and  $100 \text{ m}^{0.5}/\text{s}$  for flood based on Bangladesh Water Development Board (BWDB) discharge measurement (RPT-NEDECO-BCL, August 1989). In that study, it was mentioned that the Chezy's roughness value varies with water depth. On the basis of these studies, the Chezy's roughness value of  $70 \text{ m}^{0.5}/\text{s}$  and  $64 \text{ m}^{0.5}/\text{s}$  for  $62,431 \text{ m}^3/\text{s}$  and  $12,487 \text{ m}^3/\text{s}$  respectively were considered. For fulfillment of geometric and dynamic similitude in the model, the model bed was made with unfinished concrete to reproduce prototype behaviour. The bed roughness in the model was adjusted by trail and error.



The model was calibrated and verified based on the measured prototype values of water level, discharge distribution and average velocity at the calibration section. After calibration, the results found in the model are presented in Table 3 and 4.

Table 3: Comparison of model and prototype data after calibration for channel 1

Parameters	Unit	Prototype data	Observed value in model	Scale factor	Observed value in Prototype
Average water depth	m	7.96	0.091	80	7.28
Design discharge	m <sup>3</sup> /s	62,431	0.297	200350	59,504
Flow velocity	m/s	1.95	0.257	8.94	2.297
Relative roughness height (k/h)	-	0.0026	0.118	0.023	0.00271
Chezy's Co-efficient(C)	m <sup>0.5</sup> /s	70	37.01	1.87	69.2
Manning's co-efficient(n)	s/m <sup>0.33</sup>	0.021	0.0181	1.11	0.020
Water surface slope	-	0.000063	0.000151	1/3.5	0.00053

Table 4: Comparison of model and prototype data after calibration for channel 2

Parameters	Unit	Prototype data	Observed value in model	Scale factor	Observed value in prototype
Average water depth	m	5.15	0.074	80	5.95
Design discharge	m <sup>3</sup> /s	12,487	0.078	200350	15,627
Flow velocity	m/s	1.85	0.177	8.94	1.58
Relative roughness height(k/h)	-	0.0044	0.254	0.023	0.0058
Chezy's Co-efficient(C)	m <sup>0.5</sup> /s	64	32.63	1.87	61
Manning's co-efficient(N)	s/m <sup>0.33</sup>	0.020	0.018	1.11	0.019
Water surface slope	-	0.000063	0.000151	1/3.5	0.00053

It is evident from Table 3 and 4 that the observed values in prototype were found close to the measured values.

### Model testing

Several number of tests were carried out for different scenarios of flooding with different changes in river morphology around the bridge corridor which was regularly monitored



by CSC. Firstly, the water level differences and changes in velocity in pre and post closing of four minor channels towards western bank were examined. Secondly, the effect of west channel closure and west guide bund on east bank and possible hydrodynamic and morphological changes were investigated for design discharge of 91,000 m<sup>3</sup>/s.

### Data analysis and interpretation

Firstly, water level was measured at upstream and downstream of the west channel closure for different scenarios of flooding from which the differences were found. Velocity data were analysed and possible sedimentation and erosion were predicted based on critical velocity for initiation of sediment movement. Critical velocity for bed material movement lies between 0.2-0.4 m/s and the value is 0.36 m/s for bank erosion of Jamuna river (FAP-21/22, Klaassen et.al. 1988). Float tracking were performed from which flow concentration as well as attacking nature of flow towards the banks were envisaged.

### Findings of the study:

The results of the physical model study are given below:

Due to the construction of the west channel closure and west guide bund, the following results were found :

- The difference in water level between upstream and downstream of the closure were 0.48 m for 30000 m<sup>3</sup>/s, 1.02 m for 75000 m<sup>3</sup>/s and 1.36 m for 91000 m<sup>3</sup>/s.
- A channel was formed at the immediate downstream of the west channel closure which was linked with the western channel.
- Water level difference between upstream and downstream of the closure is reduced by 0.46 m for design discharge providing short-cut channel.
- Afflux in the main channel were found within the range of 13 cm-20 cm for design discharge at different morphological conditions.
- Bank erosion along right bank was observed which started at 1.3 km downstream of the west guide bund and extended towards downstream direction up to 3.0 km. The char downstream of west guide bund will partly be washed away.
- Erosion along right bank at immediate downstream of the closure may occur due to continuous wave attacking from east side.
- Erosion along left bank had taken place from 3 km downstream of the East Guide Bund (EGB) and extended towards further downstream direction.



- Sedimentation occurred in front of work harbor and at the nose of new Dhaleswary off- take.
- Dredged filled chars at the upstream and downstream of work harbor may be eroded away in future.
- Flooding may occur at the upstream of the closure and may extend up to 7.5 km upstream with a decreasing trend of water levels along right bank for bankful discharge.

The possible locations of erosion, sedimentation and scour are shown in Figure 3.

### Conclusions

Some important forecasts through physical modelling have been made relating to construction of west channel closure and west guide bund which were found with a very good agreement with field conditions. The important forecasts such as changes in water level, velocity, afflux, flow concentration etc were found close to the practical observation prevailed during different phases of construction. Forecasts of possible morphological changes in terms of bank erosion, channel formation, migration and bifurcation, sedimentation, char erosion, formation of new char etc. were very close to the reality and the predictions helped the contractors to take prospective protective measures.

### Recommendations

The case study revealed that fixed bed physical modelling approach is a tool for hydrodynamic and morphological predictions. Although the predictions were qualitative, the results would have been used for planning and implementation of construction of such a big project. This physical modelling tool has a great importance to the planners as well as engineers for planning and execution of hydraulic structures. This approach itself have some limitations due to down scaling the parameters. Physical processes like local scour, effect of helical flow etc. are not possible to observe in the fixed bed model. To overcome these shortfalls, sectional mobile bed models were recommended.

### Acknowledgement

The authors like to express their gratitude to Bangladesh University of Engineering and Technology (BUET) advisory team without whose valuable suggestions and collaboration it would certainly not have been possible. Special thanks are due to the Jamuna Multipurpose Bridge Authority who supplied data and financial support for this study. Works of RRI personnel those involved in this study are gratefully acknowledged.

## References

1. Ahmed, M. F and Badruzzaman, A.B.M. (1995) Construction related environmental impacts of the Jamuna Multipurpose Bridge. *Journal of the Civil Engineering Division*, Vol. CE 23, No. 1, PP-1, The Institution of Engineers, Bangladesh.
2. Bank Protection and River Training (AFPM) Pilot Project, FAP 21/22,1993) *Physical model tests*, Draft final report, Planning study, Volume VI, pp A14-12,1993, FPCO, Government of Bangladesh.
3. Klaassen,G. J., Vermeer, K. & Uddin, N.(1988) *Sedimentological processes in the Jamuna (Lower Brahmaputra)River*, Bangladesh, Proc. Intern. Conf. on Fluvial Hydraulics, Budapest, Hungary.
4. Rendel, Palmer and Tritton/NEDECO/BCL (1989) *Jamuna Bridge Project, Phase II, Study Feasibility Report*,Volume II,Annexure B: River Morphology, August 1989.
5. River Survey Project (FAP-24, 1995) *Routine Measurements*, Survey bulletin no.160, 173, 174, 8011 and 8018, FPCO, Dhaka,GOB.
6. RRI (1996) "Scale Model Study of Jamuna River at Jamuna Bridge Project Area", *1st interim report*, Government of Bangladesh, Jamuna Multipurpose bridge authority, Client: River Research Institute, Faridpur, Adviser: BUET, Dhaka.
7. RRI (1996) "Scale Model Study of Jamuna River at Jamuna Bridge Project Area", *2nd interim report*, Government of Bangladesh, Jamuna Multipurpose bridge authority, Client: River Research Institute, Faridpur, Adviser: BUET, Dhaka.
8. Warnock, J. E. (1949 ) " Hydraulic similitude", Published in Engineering Hydraulics, Rouse, H. (eds), Proc. of the Fourth Hydraulics conf., IOWA, Institute of Hydraulic Research, John Wiley & Sons, Inc. New York.



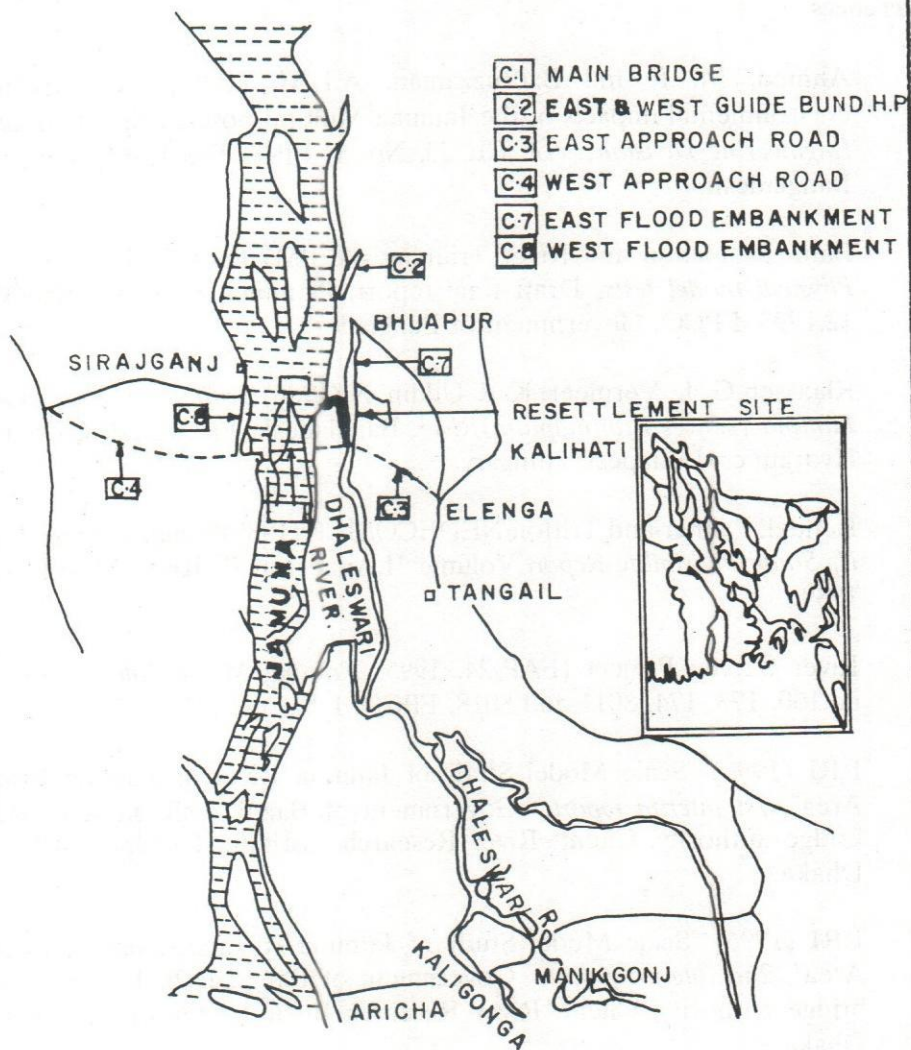


FIG. 1: LOCATION OF JAMUNA BRIDGE AND ITS COMPONENTS

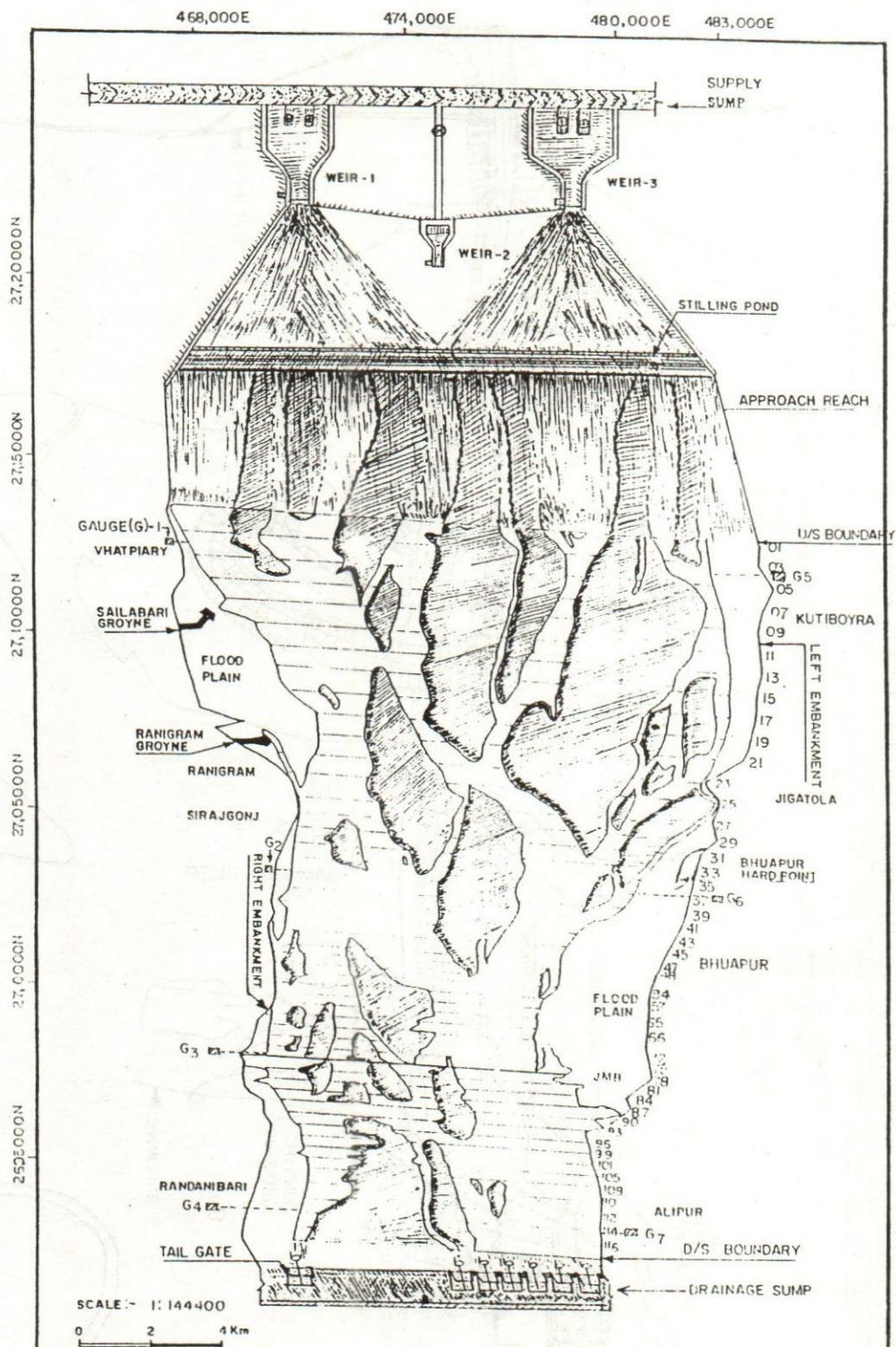
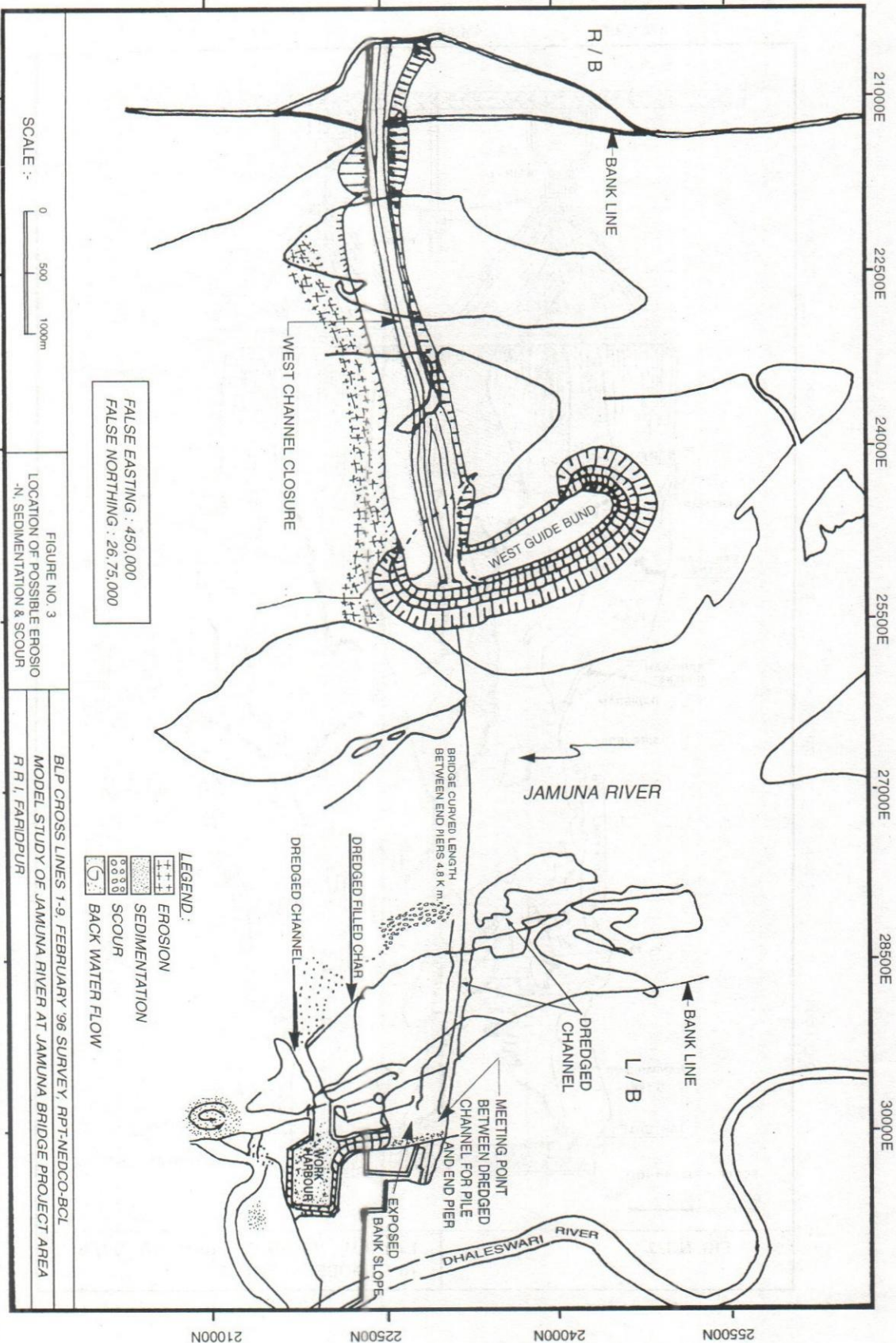


FIG. NO. 2

LAYOUT PLAN OF JAMUNA OVER  
ALL MODEL, R R I





## A Case Study for the Protection of Panka Narayanpur Area From the Erosion of the Ganges

Syed Abdus Sobhan<sup>1</sup>  
Md. Nazrul Islam Siddique<sup>2</sup>  
Swapan Kumar Das<sup>3</sup>  
Mohammed Fazlul Karim<sup>4</sup>

### Abstract

*River bank erosion is the common natural phenomenon in Bangladesh. Groyne and Revetment types of river training works are generally constructed for the protection of river bank. A physical model study was done for the protection of Ganges' left bank at Panka Narayanpur area using series of impermeable groynes. This study was conducted in a 60mX30m open air model bed at River Research Institute. An undistorted length scale ratio of 75 was used for the model construction. In the scaling procedure, Froude's model law was used for the geometric, kinematic and dynamic similarity in the model and prototype. Some fourteen tests were carried out with groynes changing length, location and number. The results show that each groyne can be considered acceptable for the protection of river bank upto 4.5 to 5 times its projected length perpendicular to the channel when used in a series. On the basis of test results a total of 10 groynes were suggested for the protection of 2.7 km river bank. It was also recommended for armoring the river bank between the groynes as there exist a reversible velocity near bank.*

### Introduction

Bangladesh is a riverine country comprising three major rivers and several hundred small rivers and rivulets. One of the major rivers is the Ganges river. Many important towns, cultivable land units, homestead, irrigation projects and others valuable structures are situated on the bank of this river. The continual erosion and sedimentation of this river create numerous problems in the vicinity of the river bank.

Panka and Narayanpur, which are situated on the right bank of the Ganges, are the first level administrative unit under Nowabganj district. These are the most vulnerable area in which major part of the area is now flashed out by the Ganges. One of the country's ancient high school at Panka is now disappeared due to the shifting of river bank. Captain Mohiuddin Zahangir College, which is the only institution for higher education in that region, is now threatened due to degradable nature of the Ganges. Recently, Bangladesh water development board (BWDB) has undertaken a development project for the protection of that area. This study is a part of that project.

---

<sup>1</sup>Director General, <sup>2</sup>Principal Scientific Officer,

<sup>3</sup>Senior Scientific Officer, <sup>4</sup>Scientific Officer, RRI



## **The Ganges River**

The Ganges is one of the major rivers in Bangladesh and is also noted for its massive water discharge and huge sediment load. Among the three major rivers in Bangladesh, the Ganges River has the highest drainage basin of some 1.1 million km<sup>2</sup>, yet its water yield is the least of the three rivers. Other notable characteristics of the Ganges are its wide meandering planform (Fig. 1), a bed-level slope of  $5 \times 10^{-5}$ , and an average bed material grain size of about 0.12mm (Barua, 1994). It is more sinuous in the upper reaches and less sinuous tending to straight braided pattern in the lower reaches (Hossain, 1989).

## **An over View of Groynes as a Bank Protective Device**

Groynes are stone, gravel, rock, earth or pile structures, constructed transverse to the river flow and extend from the bank into the river. It serves one or more of the following functions: (a) training the river along a desired course by attracting, deflecting or repelling the flow in a channel. (b) protection of the river bank by keeping the flow away from the bank (c) improvement of depth for navigation by contracting the river width. Depending on the purposes, groynes can be used singly or in series. They can also be used in combination with other training works. The alignment of groynes may be either perpendicular to the bank line or to the thalweg, or at an angle pointing upstream or downstream. A groyne pointing upstream has the property of repelling the river flow away from it and pointing downstream attracts the river flow towards it (Joglekar, 1971). In the study of Sastry (1962) it is shown that a groyne angled upstream produce greater scour depth than those normal to the flow direction and a groyne angled downstream caused the least depth of scour.

## **Study Zone**

A total of 2.7 km river length was of interest because of our desire to protect the Captain Mohiuddin college and its vicinity effectively. The Captain Mohiuddin College was taken as a key point while 1.5 km in the upstream and 1.2 km in the down stream were considered for the study. A total of 650m river width was considered in the model as the available pump capacity and model bed restrict the total width of the river for consideration.

## **Model Setup**

### **a) Collection of Data**

An index map of the river reach showing river position, bank line, flood embankment was collected from the BWDB. Bathymetric data were supplied by the Surface Water Modelling Centre (SWMC). Water level and discharge data of 25 years recorded at the Hardinge bridge and water level of 4 years recorded at Panka Narayanpur were collected. Some soil samples of river bed and bank material were collected and tested for gradation and grain size analysis.



### b) Assessment of Discharge

There was no discharge measurement station at Panka-Narayanpur area. Only a station at Hardinge bridge was available in the Ganges river which is about 138 km downstream of the study area. In the assessment of discharge at Panka Narayanpur area, recorded discharge at Hardinge bridge and the water level at the study area were used. The discharge value was assessed using both Chezy's and Manning's formula. The corresponding discharge value for the highest flood level of 23.19m PWD was  $56500\text{m}^3/\text{s}$  for Manning's formula and  $42500\text{m}^3/\text{s}$  for Chezy's formula. The value of maximum discharge  $56500\text{m}^3/\text{s}$  was used for the study which was more representative in comparison to the maximum discharge at Hardinge Bridge.

### c) Preparation of Model Bed

An open air model bed having the dimension 60m X 30 m was used for this model study. Some 13 nos of cross sections (Pk08 to Pk20) covering approximately 2700m river length and average river width 650m was reproduced in the model. The model was designed and constructed in such a way that separation of flow does not occur during the model test. The model was constructed having fixed bed, 13m in the upstream and 4m in the downstream, and a mobile bed of 30m in the middle. A standard sharp crested weir was installed in the upper end for the measurement of the inflow water. A point gauge was installed at a sufficient distance upstream of the weir to measure water depth over the weir for discharge calculation. At the end of the model bed four nos of tail gates having the length of 1.8 m each were installed to control desired water level in the model. Three point gauges were constructed along the right bank to measure water level in different section during model run. The layout plan of the model is shown in Figure 2.

### Operation of the Model

The water supplied to the model from a constant head sump. The water passed over a 1.78 m long sharp crested weir. A well gauge installed upper side of the weir was used to measure the water depth flowing over the weir. Then the model discharge was measured using the Rehbock's formula for discharge calculation. The water head corresponding to desired discharge was fixed up first, then the flow was allow to flow over the weir. The model was executed with design discharge first and then for higher discharge in each test. Design discharge was used to investigate the velocity distribution, near bank velocity and stream lines. The higher discharge was used for the scour simulation. As the representative bed material could not reproduce in the model with the selected scale, higher discharge value was selected in such a way that it produced the same results on higher resistive bed material.



### a) Model Calibration

The setup of the model were verified for velocity distribution and water level. The distribution of the velocity along the cross section were verified at x-section no 9, with the computed elemental velocity. Observed velocity was not available at Panka-Narayanpur area, so the model was calibrated with computed discharge at section Pk-09.

### b) Test run

In the study a total of 12 tests were executed changing groyne length, location and number for the same bathymetric and hydraulic condition. At the beginning of each test run the bed was remoulded such that same bathymetric condition was exist. The discharge value for each test was kept same so that the outcome of the model study represent a quantitative results. After, starting the flow over the model it takes a period varying between 1 to 3 hrs for attaining equilibrium by adjusting the bed slope. Again, in the study of Garde et al.(1961) it is shown that change in bed level become zero with in 3 to 5 hrs after introduction of the model. Hence in the present study, the model run was continued for almost 8 hrs in each test. In each test the water was allowed to flow for a period of 8hrs for design discharge and 8hrs for higher discharge. In the study of Liu and Skinner (1960) it was found that for all practical purposes the maximum scour depth was attained after 3 to 5 hrs. After this the lowering of the model bed was too slow to record with the available equipment. During the test run, velocity was measured along the x-section with an interval of 25cm in the model. The velocity also measured around the groyne and along the bank between two groynes. The recording of bed level was continued until the bed reading changed so slowly with time that it was difficult to record a change. In Table-1 maximum near bank velocity and maximum scour depth for each test is given.

## Results and Discussion

The near bank velocity of the third test using recommended design in which 30m long groyne each at 6.5 times spacing was found 1.02m/s which is greater than the erodible velocity. In this test flow in the reverse direction was found in some places near the bank. The test results showed that the length of the groyne was not sufficient to deflect the axis of the flow along a convenient path. Then six other tests were done increasing groynes length and for different spacing ratio. In these test reverse velocity reduced slightly but not totally. At this stage, some three tests were done for smaller length of groyne and higher spacing ratio. The stream lines deviated towards the bank resulting flow velocity more than 1.5 m/s in these tests. Hence, finally two other test were done for moderate length and relatively smaller spacing ratio. The last test showed better results, though there was existence of reverse flow. Hence, the length and location of the groynes (Fig. 3) used in this test were recommended.



Table 1: Summary of the tests with proposed groynes

Test no	Test description	Maximum near bank velocity(m/s)	Maximum scour depth at groyne no. 1 (m)
T1	Proving test		
T2	Calibration test		
T3	With proposed groynes, each length 30m, (spacing 6.5 times)	1.02	17.25
T4	With proposed groynes, each length 39m, (spacing 5 times)	-1.20	21.90
T5	With proposed groynes, G1-G6 48m (spacing 4 times), G7-G12 39m length (spacing 5 times)	-1.31	21.95
T6	With proposed groynes, G1-G6 65m (spacing 3 times), G7-G12 48m length (spacing 4 times)	-1.12	22.82
T7	With proposed groynes, G1-G4 65m (spacing 3 times), G5-G11 48m length (spacing 4 times), G4 to G5 distance 390m (6times), embankment setback distance was increased to 30m	-1.20	23.16
T8	With proposed groynes, G1-G4 97m length(spacing 2 times), G5-G11 65m length (spacing 3 times), G4 to G5 distance 390m (spacing 4times).	-0.85	25.00
T9	With proposed groynes, G1-G6 60m length. G1-G3(spacing 5 times), G3-G6 (spacing 6 times),	-0.78	22.34
T10	With proposed groynes, G1-G5 30m length(spacing 10 times).	1.65	16.55
T11	6 nos of groynes. G1- G6 length 30m and (spacing 12 times)	1.80	16.62
T12	6 nos of groynes. G1- G3 length 40m(spacing 9 times), G4-G6 length 36m (spacing 10times). Distance between two groyne 360m.	1.78	18.50
T13	7 nos of groynes. G1- G7 length 40m(spacing 7.5 times). Distance between two groyne 300m.	1.50	19.30
T14	10 nos of groynes. G1- G5 length 50m (spacing 4.5 times), G6-G10 length 45m (spacing 5times).	-0.65	20.78

- sign indicates flow in the reverse direction

## Conclusion and Recommendation

In this study it was observed that there was always existence of reversible velocity near bank. In some cases the reversible velocity was higher than the erodible velocity. Again, a direct flow was developed near the bank when spacing to length ratio six or higher. This results would be helpful for the designers to design the parameters of groynes to be used for the bank protection.



Based on the test results the following recommendations were made to the client (BWDB) for the protection of 2.7km river bank at Panka Narayanpur area:

- a. The length of the groynes from G1 to G5 is 50m and from G6 to G10 is 45m
- b. The distance between two successive groynes is 225m
- c. All the groynes are perpendicular to the bank
- d. Exposed bank between two groynes should be covered by armoring materials.
- e. The construction of all the groynes should be completed before the next monsoon.

### Acknowledgement

The authors would like to thank all the officers and staff of RRI those are involved in this study. The financial support provided by the BWDB, Northern Zone, Rajshahi is greatly acknowledged.

### References

1. **Ahmed M. (1953)**, 'Experiment on design and Behaviour of Spur-Dike', Proceeding, I.A.H.R., ASCE, Joint Meeting, University of Minnesota.
2. **FAP 21/22 (1992)**, 'Bank Protection and River Training Pilot Project', Physical model tests, Draft final report, Planning Study, Volume VI.
3. **Garde R.J., Subramanya K., Nambudripad K.D.(1961)**, "Study of Scour Around Spur-Dikes", Journal of the Hydraulic Division, ASCE.
4. **Hossain M.M. (1989)**, 'Geometric Characteristic of the Padma upto Brahmaputra confluence', final Report, R 02/89, IFCDR, Dhaka.
5. **Jogleker D.v. (1969)**, 'Manual on River Behaviour Control and Training', Publication No.60, Central Board of Irrigation and power, Page 215-242.

6. **Khan Z.H. and Barua D.K.(1994),**'Seasonal Variation of Certain Hydraulic Parameters of the Ganges River', 39th Annual convention of IEB, Chittagong, Bangladesh.
7. **Liu H. K.and Skinner M. M. (1960),**'Laboratory Observation of Scour at Bridge Abutment', Highway Research BD, Bulletin No. 242.
8. **Montensen P. (1984),**'Physical Modelling Of Open channel Flow', Lecture Notes, Danish Hydraulic Institute.
9. **Sir William Halcrow& Partners Ltd (1993),**'River Training Studies of the Brahmaputra River, GOB, Report on model studies, volume IV.
10. **Raudkivi, A. J. (1989),**' Scour at Bridge Piers', H.N.C., Breusesers, pp 61-63
11. **Surface Water Modelling Centre (1996),**'Bathymetric Survey on the Ganges River at Panka Narayanpur', Final Report.
12. **Sharpe J.J. (1981),** Hydraulic Modelling, The Buttersworth group, Billing and sons, England.
13. **Sastry C.L.N.(1962),**'Effect of Spur-Dike Inclination on Scour Characteristic', Thesis presented to the University of Roorkee, at Rookee, India in Partial fulfillment of the requirements for the degree of Master of Engineering.
14. **Tesaker E. (1986),**' Some Aspect of Hydraulic Modelling', Lecture Notes for RRI, UNDP/DTCD Project.



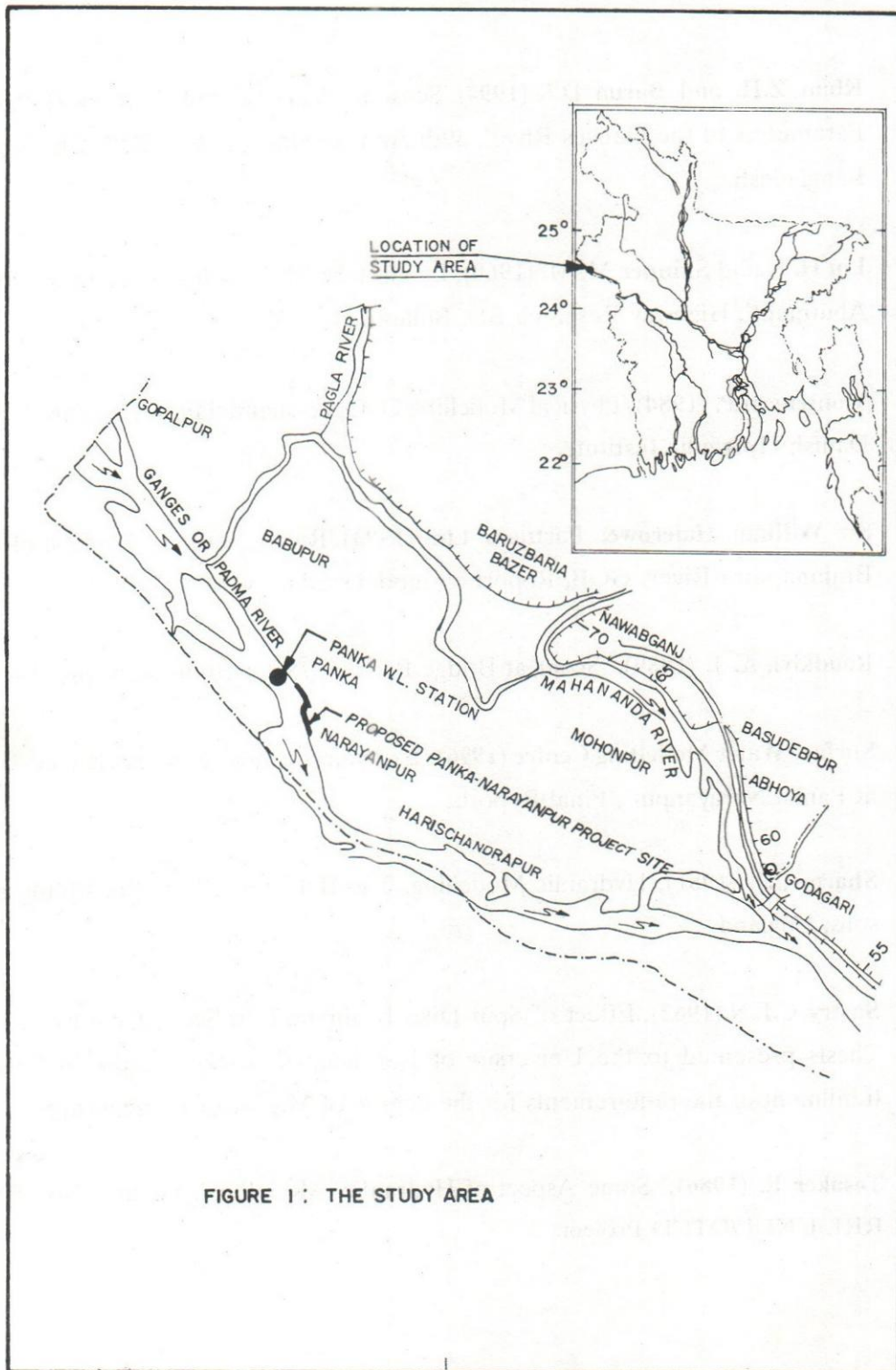


FIGURE 1 : THE STUDY AREA

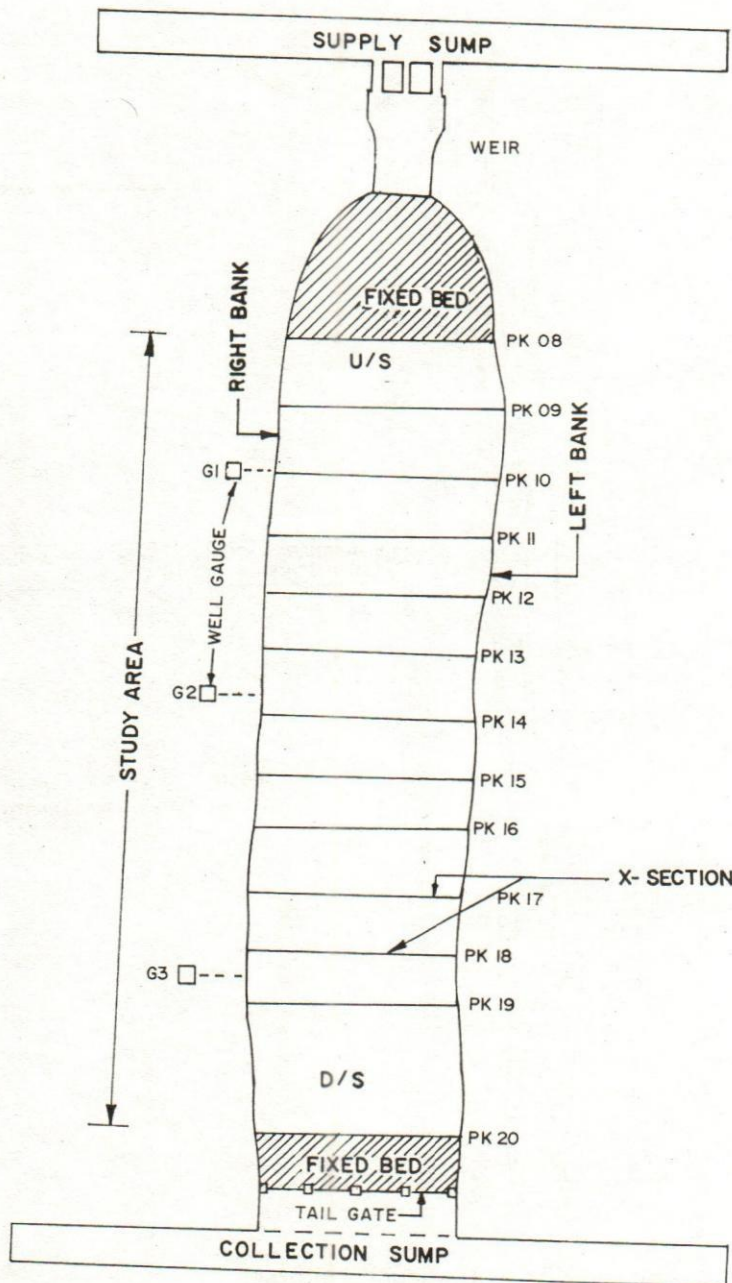
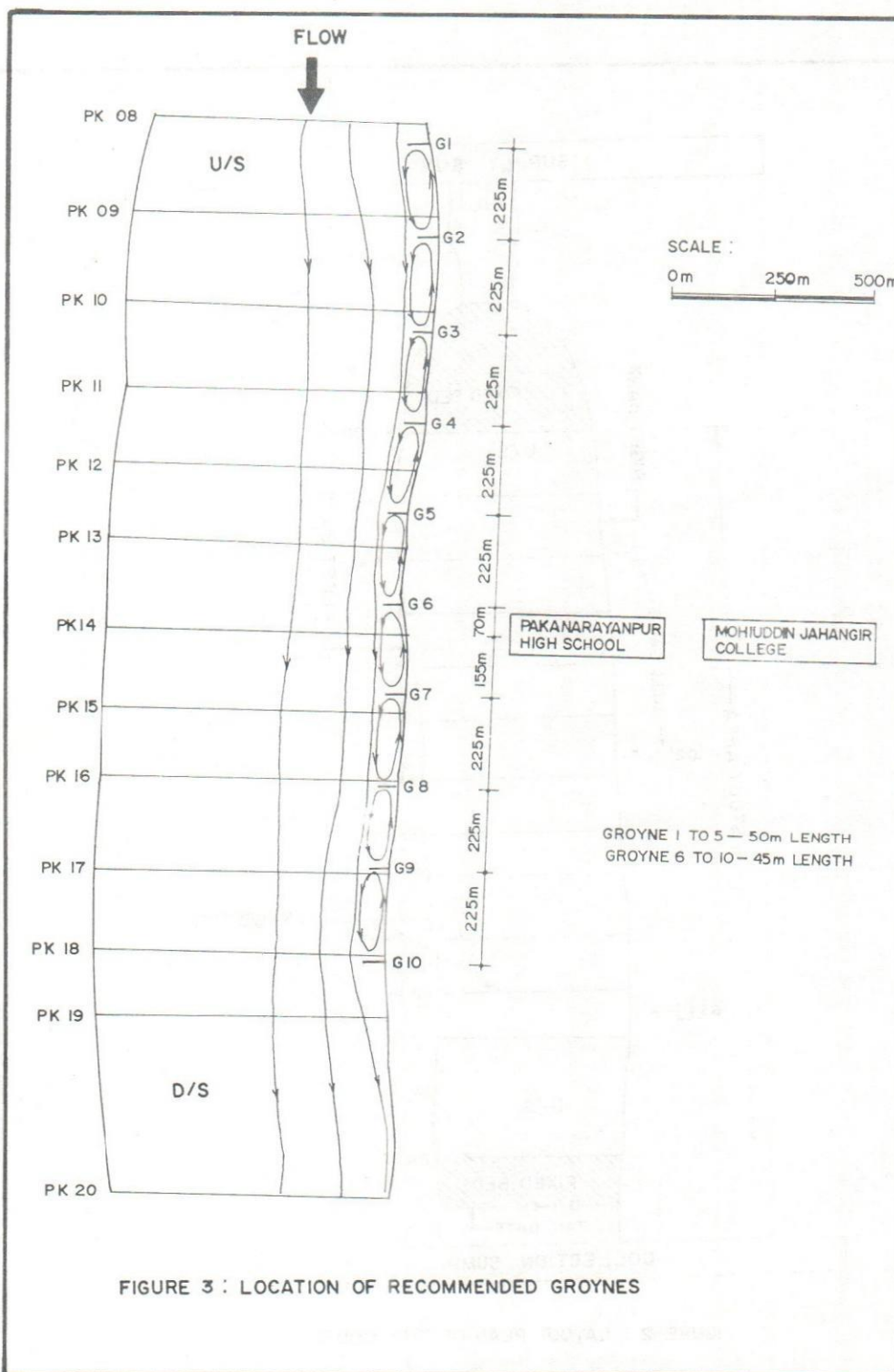


FIGURE 2 : LAYOUT PLAN OF THE MODEL





## **The Determination of Preconsolidation Pressure from Consolidation Test as Significant for the Correct Evaluation of Settlement Behaviour of Soil**

Md. Hanif Mazumder<sup>1</sup>

### **Abstract**

*Settlement behaviour of relatively low permeable soil types can be predicted from the results of consolidation test. The correct determination of preconsolidation pressure,  $\sigma'_p$  is essential for better prediction of settlement behaviour of soil. The preconsolidation value should not exceed the natural preconsolidation in-situ. Attempt has been made in this paper for the determination of preconsolidation pressure adopting different methods by the right performance of consolidation tests. It has been observed that there is a moderate preconsolidation in some of the soils of Bangladesh. The preconsolidation pressure should be considered during the evaluation of settlements for better prediction of settlement behavior of soils.*

### **Introduction**

Determination of settlement of structures is mainly based on the results of consolidation tests performed on undisturbed soil samples collected in Shelby tubes or plastic liner, tested in the soil mechanics laboratory in consolidation test apparatus. The samples are collected from borings by drilling rigs, planned and executed by boring agency/party. During sampling, storing and transportation a degree of disturbances of soil samples is unavoidable but can be increased by inappropriate handling. Even in the laboratory a degree of disturbance will occur during preparation of the sample for executing the consolidation test. On the other hand, it is important to know the actual soil conditions in situ and try to restore them in the sample during testing in the laboratory. This can be implemented by means of the application of most correct laboratory procedures, before using the results for calculating settlements.

The purpose of consolidation test is to determine the one-dimensional consolidation characteristics (deformation properties) of selected soil types of low permeability. The two parameters normally required are: 1) The compressibility of the soil expressed in terms of the co-efficient of volume compressibility; also known as modulus of volume change, which is a measure of the amount by which the soil will compress when loaded and allowed to consolidate, 2) The time related parameter expressed in terms of co-efficient of consolidation which indicates the rate of compression and hence the time period over which consolidation settlement will take place.

---

<sup>1</sup>Principal Scientific Officer, Geotechnical Research Directorate, RRI, Faridpur.



According to the knowledge gained from extensive experience in connection with laboratory consolidation tests and also from the training course " Practical training in Soil Mechanics " at Danish Geotechnical Institute (DGI), Denmark it can be concluded that use of a correct preconsolidation pressure value  $\sigma'_p$  is essential during the evaluation of settlement. This preconsolidation value should not exceed the natural preconsolidation in situ. Consolidation properties include stress-strain and time strain relationships and also permeability and secondary consolidation.

The correct evaluation of preconsolidation stress value and over consolidation value is important for the determination of settlements, because load increments lower than the over consolidation value is a reloading problem which gives much lesser settlements than for normally consolidation. The compression index value ( $C_c$ ) is only valid for load increments greater than preconsolidation values,  $\sigma'_p$ .

So, it is essential to consider the determination of preconsolidation value,  $\sigma'_p$  in consolidation test for correct evaluation of settlements.

### Normally Consolidated Clay and Silt

The consolidation tests are executed with stepwise loading of the samples from an initial load of 20 to 30 kN/m<sup>2</sup> upto a load of 800 to 1000 kN/m<sup>2</sup>.

Water is added to the specimen before deformation readings are started and the first small load increment is put on. This can result in a quick expansion of the sample. It can be avoided by starting with an initial vertical stress of 5-10 kN/m<sup>2</sup> and taking the first readings on the deformation gauge before adding water.

If the expansion is registered, it is usually recommended to increase the stress quickly until the expansion stops.

The mean characteristics of the deformation property of a normally consolidated clay or silt deposit is the compression index-  $C_c = \frac{(\Delta e)}{(\log \sigma')}$ . This value of  $C_c$  which is derived

from the straight line in an  $e=f(\log \sigma')$  graph, Fig No. 3 is only moderately influenced by sample disturbance. The line and  $C_c$  expresses the consolidation of the soil i.e, the reduction in void ratio- $e$  for increasing stresses above the previous stress level, which has ever been applied on the sample in situ or in the laboratory.

For example, clay sample taken from boring no.3 in Mahluma Khal Bridge Project (soil testing report no. 9(86) of River Research Institute). The boring is situated in the river bed having ground water level in ground level which is not surveyed. Soil profile, classification tests and Special Penetration Test(SPT) values are shown in Fig. No. 1 and explanation of signs on Fig. No. 2. The boring logs show the water content  $W$ , the plasticity limits ( $W_L$  and  $W_p$ , the content of clay (% CLAY) and the number of blows per



foot from the SPT tests, together with the soil description. The grain weight density for  $U_1$  is  $\gamma_s = 26.78 \text{ kN/m}^3$  and Unconsolidated Undrained(UU) test gave  $C_u = 17 \text{ kN/m}^2$ , ( $q_u = 34 \text{ kN/m}^2$ ).

The vertical, effective, in situ stress is  $\sigma'_0 = 45 \text{ kN/m}^2$  for the undisturbed sample U-1.

As already mentioned, is the value of  $C_c$  rather well determined from consolidation tests, even if the sample is disturbed to some extent but still has the original void ratio and water content. This can especially expected for clays due to very low permeability.

If the clay and silt deposits really is normally consolidated (NC), the determination of settlement should be rather accurate.

### Preconsolidation

Since the stress history of clay is important to its stress-strain characteristics, it is essential to be able to determine the maximum past effective stress i.e, the preconsolidation stress value ( $\sigma'_p$ ) for the clay. In some cases the maximum past effective stress may be estimated from geologic evidence, however, this is rarely the case. Casagrande (1936) developed a method for estimating the past effective stress from the laboratory compression curve of consolidation test. Examination of consolidation test from a number of soil testing reports of River Research Institute- 114(84), 143(85) and 159(85), 2(86) to 9(86) & 14(86) & many other reports indicate the possible existence of a certain preconsolidation.

There are several reasons to expect a moderate preconsolidation in the alluvial deposits which is of main interest of Bangladesh.

- i) Preconsolidation due to secondary consolidation and the age of the deposits.
- ii) Consolidation due to varying effective stresses from variation in the ground level of several meters.
- iii) Negative pore water pressure in the upper layer due to evaporation in dry seasons. Mainly is an upper layer, preconsolidated, dry crust.
- iv) Preconsolidation from now eroded soil layer by River activities.
- v) Chemical reactions or cementation.

The classical way of determining the preconsolidation from consolidation tests is the Casagrande construction where the point with the smallest radius of curvature of the laboratory compression curve is taken and a horizontal line is drawn at the point on the curve and a line tangent to the curve is also drawn. The angle between this two lines is



bisected. Projection of straight line portion of the laboratory compression curve which intersects the bisector of the angle and this point of intersection approximates the maximum past effective stress shown in Fig. No. 3. Based on this approach, there are indications of certain preconsolidation  $\sigma'_p{}_C$  in many RRI test results and hence the over consolidation ( $\sigma'_p{}_C - \sigma'_0$ ) where  $\sigma'_0$  is the effective vertical stress in situ. The over consolidation range between 0-100 kN/m<sup>2</sup>, but the determination is very sensitive to sample disturbances.

Another method for estimating the preconsolidation value is to study the variation of the secondary consolidation. This deformation is straight lined in a logarithmic line scale & can be expressed as percent sample deformation during a time decade,  $\epsilon_s$ . The increasing loading steps (stresses) indicates an increasing secondary consolidation rate in the consolidation tests (% / decade). The determination of these values are discussed in section-4, Time curves.

The resulting time curves from a specific consolidation test are shown in Fig. no. 4 & 5 and transferred to Fig. no. 3. The Casagrande construction indicates a preconsolidation  $\sigma'_p{}_C = 65$  kN/m<sup>2</sup> ( $\sigma'_p{}_C - \sigma'_0$ ) = 65-45 = 20 kN/m<sup>2</sup>), while the  $\epsilon_s$  method indicates value  $\sigma'_p{}_C = 100$  kN/m<sup>2</sup> ( $\sigma'_p{}_C - \sigma'_0$ ) = 55 kN/m<sup>2</sup>).

The correct evaluation of the over consolidation is important for the determination of settlements, because load increments lower than the over consolidation value, is a reloading problem, which gives much lesser settlements than for normally consolidation.

The  $C_c$ -value is actually only valid for load increment greater than  $\sigma'_p{}_C$ .

### Time Curves

Deformation in a consolidation test during a load step as a function of time is known to be proportional to the square root of time during primary consolidation and to the logarithm of time during the secondary consolidations. At River Research Institute or elsewhere the time curves are reproduced graphically in a square root and/or log time diagram.

It is suggested to use a combination as shown on Fig. no. 4 & 5, which is the standard performance at the Danish Geotechnical Institute. The scales for 0 to 10 minute and the decade of time (log 10) is chosen in such a way that the intersection between  $\sqrt{t}$  and log t scales is smooth, Fig. no. 4 & 5. Using the graph, the straight line part of the  $\sqrt{t}$  curve indicates the starting point  $\delta_0$  (after a possible initial settlement) and the intersection between the  $\sqrt{t}$  and log t lines is defined as  $\delta_{100}$  (100% primary consolidation). These values give the possibility to determine  $\delta_{50}$  and  $t_{50}$  (deformation



calculation of the Co-efficient of permeability and consolidation.

The time diagrams on Fig. 4 & 5 are shown with a change from  $\sqrt{t}$  to  $\log t$  at 10 minutes, this will be convenient in many tests but the intersection between the straight lines in the  $\sqrt{t}$  and  $\log t$  sections should be reasonable close to border line ( $3 < t < 30$  min.). If not, the time scales should be changed by a multiplication factor to secure an intersection of the lines nearer the border line (time curve for load step = 400 kN/m<sup>2</sup> on Fig. no.5). The new dotted lines appears from a rotation of the  $\sqrt{t}$  line and a parallel transformation of the  $\log t$  line as shown on Fig. no. 5, the variation of  $t_{50}$  and  $(\delta_{100} - \delta_{50})$  is unimportant in the actual case.

### Estimation of the Preconsolidation

The classical way of estimating the preconsolidation, as mentioned in section-3, is the Casagrande construction, Fig. no. 3 and 6. The result is rather sensitive to sample disturbance.

The rate of secondary consolidation,  $\epsilon_s$ , seems less sensitive to sample disturbance.

The variation of  $\epsilon_s$  with  $(\epsilon_s = f(\sigma))$  is shown on Fig. no. 3 and 6 for a clay sample.  $\epsilon_s$  is increasing (after a straight line in an arithmetic delineation) until it reach a constant value at vertical stresses greater than the preconsolidation value. This variation is also expected for organic materials.

For silt and silty clay deposits the variation of secondary ( $\epsilon_s$ ) consolidation more often shows small values of increases below  $\sigma'_p$ , followed by an increasing, straight lined variation in the logarithmic scale above  $\sigma'_p$ , Fig. no. 7 & 8 (results from the RRI soil testing report no. 2(86) Kalkapur).

For the clay sample, Fig. no.3, the value of preconso-lidation is estimated to  $\sigma'_p = 100$  kN/m<sup>2</sup>, ( $\sigma'_0 = 45$  kN/m<sup>2</sup>) and for the silt, Fig. no.7,  $\sigma'_p = 120$  kN/m<sup>2</sup> ( $\sigma'_0 = 113$  kN/m<sup>2</sup>, which means nearly normally consolidated).

### Testing Procedure and Presentation

The normal procedure used in River Research Institute is to add water to the sample and increase the load stepwise from 20-30 kN/m<sup>2</sup> to 800-1000 kN/m<sup>2</sup> in 6 steps. Water must be added after implementation of a low stress step (5-10 kN/m<sup>2</sup>) during 5 minute to check bedding effects or expansion tendencies.

Every step has a duration of about 24 hours for determining the time settlement curve. The load is then finally decreased in two 24 hours steps.



In many cases 100% consolidation ( $\delta_{100}$ ) is reached with in 10 to 20 minute having the standard sample height in the consolidometer 20 to 25 mm. Readings during the first two hours (120 minute) will give a reasonable good indication of the primary and secondary consolidation, in which two steps loading a day could be a possible procedure for increasing the number of test performed with the existing equipment.

The second, daily step will have a more longer secondary deformation (1300 minute) and cause some variations in the resulting consolidations curve, using the last reading from these time curves. This minor problem, can be eliminated by using more correct value for 100% consolidation ( $\delta_{100}$ ) as reference or generally the 120 minute reading in all steps.

A comparison between the last (1440 minute) reading and the 100% consolidation reading is shown on Fig. no. 6. The resulting evaluation of the settlement properties will not vary essentially using the one or the other curve.

Instead of representing the deformation properties in the consolidation test as a function of the void ratio,  $e[\sigma = f(e)]$  Fig. no. 3, it is suggested to use the relative deformation  $\epsilon = 100 \times \Delta h / h [\sigma = f(\epsilon)]$  Fig. no. 6. Fig. no. 9 shows a test performance on a clay sample where the preconsolidation is expected to be 250 kN/m<sup>2</sup> and where the sample is situated at a depth equal to an effective overburden pressure,  $\sigma'_0 = 60 \text{ kN/m}^2$ .

In this case the soil sample should be preconsolidated (in the test as in situ) to  $\sigma'_p = 250 \text{ kN/m}^2$  and afterwards unloaded to the in-situ, vertical stress,  $\sigma'_0 = 60 \text{ kN/m}^2$ . Then a reloading to  $\sigma'_p$  and loadings above this value will represent deformation characteristics of an undisturbed preconsolidated ( $\sigma' < \sigma'_p$ ) and normally consolidated ( $\sigma' > \sigma'_p$ ) soil sample.

The test on this undisturbed sample indicates a preconsolidation  $\sigma'_p \sim 200 \text{ kN/m}^2$  determined by the Casagrande method, the value  $\sigma'_p \sim 250 \text{ kN/m}^2$  by  $\epsilon_s$ -(secondary consolidation) method.

## Conclusion

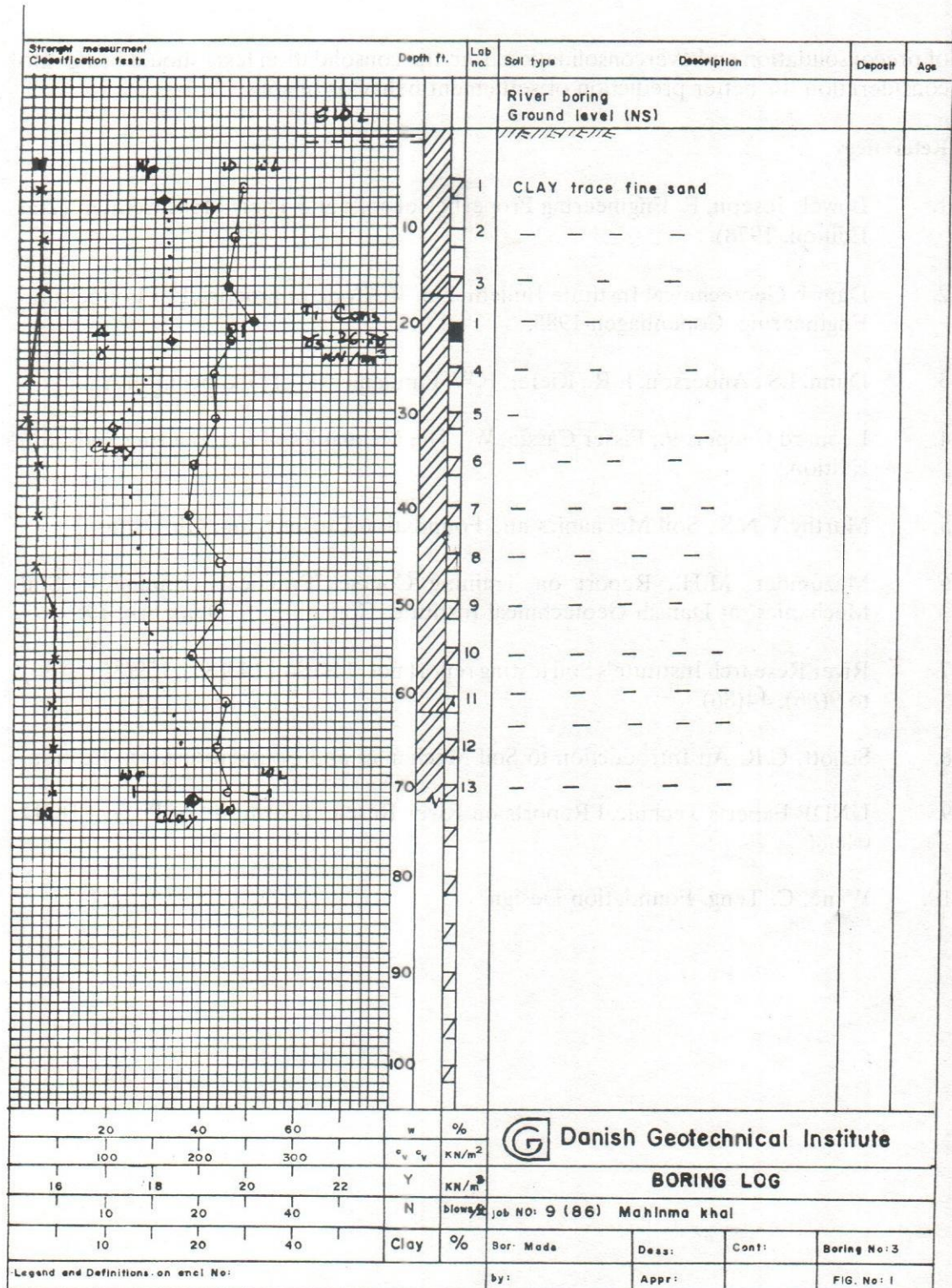
The main part of the soil deposits of Bangladesh as used for support in construction work is of young geological age of Recent or Holocene Alluvial soils. Soils deposits at greater depths or soils of border areas found to be of pleistocene age. These young soils can be normally consolidated causing substantial settlement problems. However, the above mentioned observations indicates a moderate preconsolidation of soils. So, it is suggested for the correct determination of preconsolidation stress  $\sigma'_p$  by the right performance of consolidation test on undisturbed soil samples and the tests data and information should present in the data sheets as used in the different figures. The results

of preconsolidation and overconsolidation from the consolidation tests should bring into consideration for better prediction of settlement behavior of soils.

## References

1. Bowels Joseph, E. Engineering Properties of soils and Their Measurement (2nd Edition, 1978).
2. Danish Geotechnical Institute Bulletin No. 36, Code of practice For Foundation Engineering. Copenhagen-1985.
3. Dunn, I.S., Anderson, L.R., Kiefer, F.W. Fundamental of Geotechnical Analyses.
4. Leonard Capper, P., Fisser Cassie, W., The Mechanics of Engineering Soils. 6th Edition.
5. Murthy, V.N.S., Soil Mechanics and Foundation Engineering. 4th Edition.
6. Mazumder, M.H., Report on Training Course "Practical Training in Soil Mechanics" at Danish Geotechnical Institute, Copenhagen, Denmark, 1989.
7. River Research Institute's Soil testing report nos. 114(84), 143(85), 159(85), 2(86) to 9(86), 14(86).
8. Scoott, C.R. An Introduction to Soil Mechanics and Foundations, 3rd Edition.
9. UNDP Experts Technical Reports on River Research Institute of Project BGD 046/86.
10. Wane, C. Teng. Foundation Design.





### Soil signs

Guide	sign	designation and grain size	sign	designation
		cobbles		fill
		gravel		topsoil
		sand		moor peat
		silt		peaty mud
		clay		organic soils
		limestone or chalk		shells
		rock		
	signs can be combined			
		glacial till (clayey silty sand cobbles)		
		glacial till (sandy clay with gravel and cobbles)		

### Boring sections

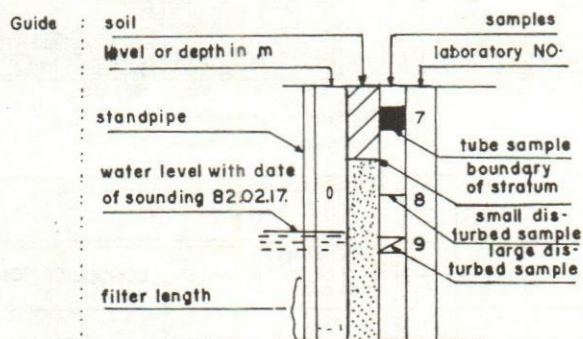
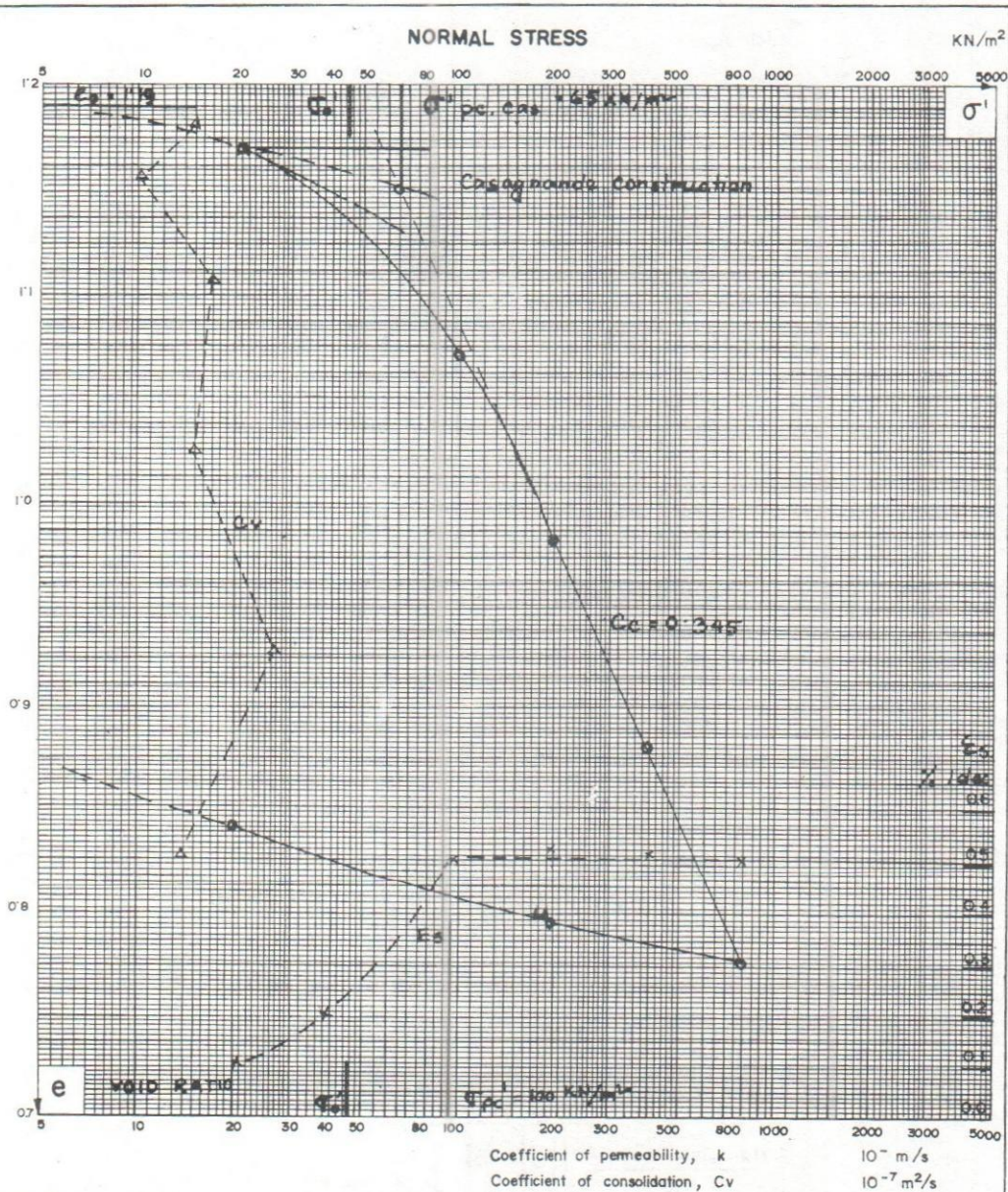



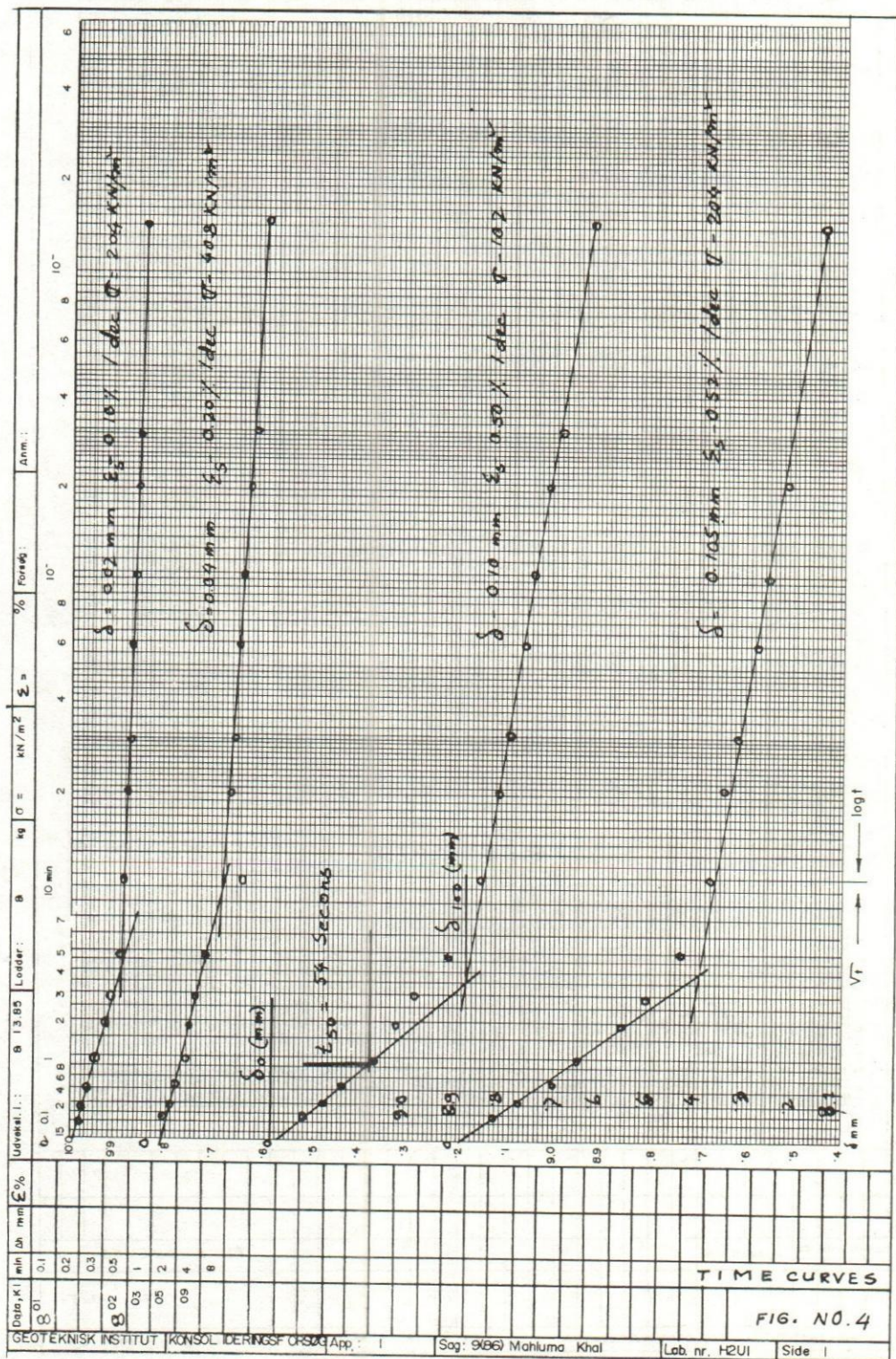
FIG. NO-2



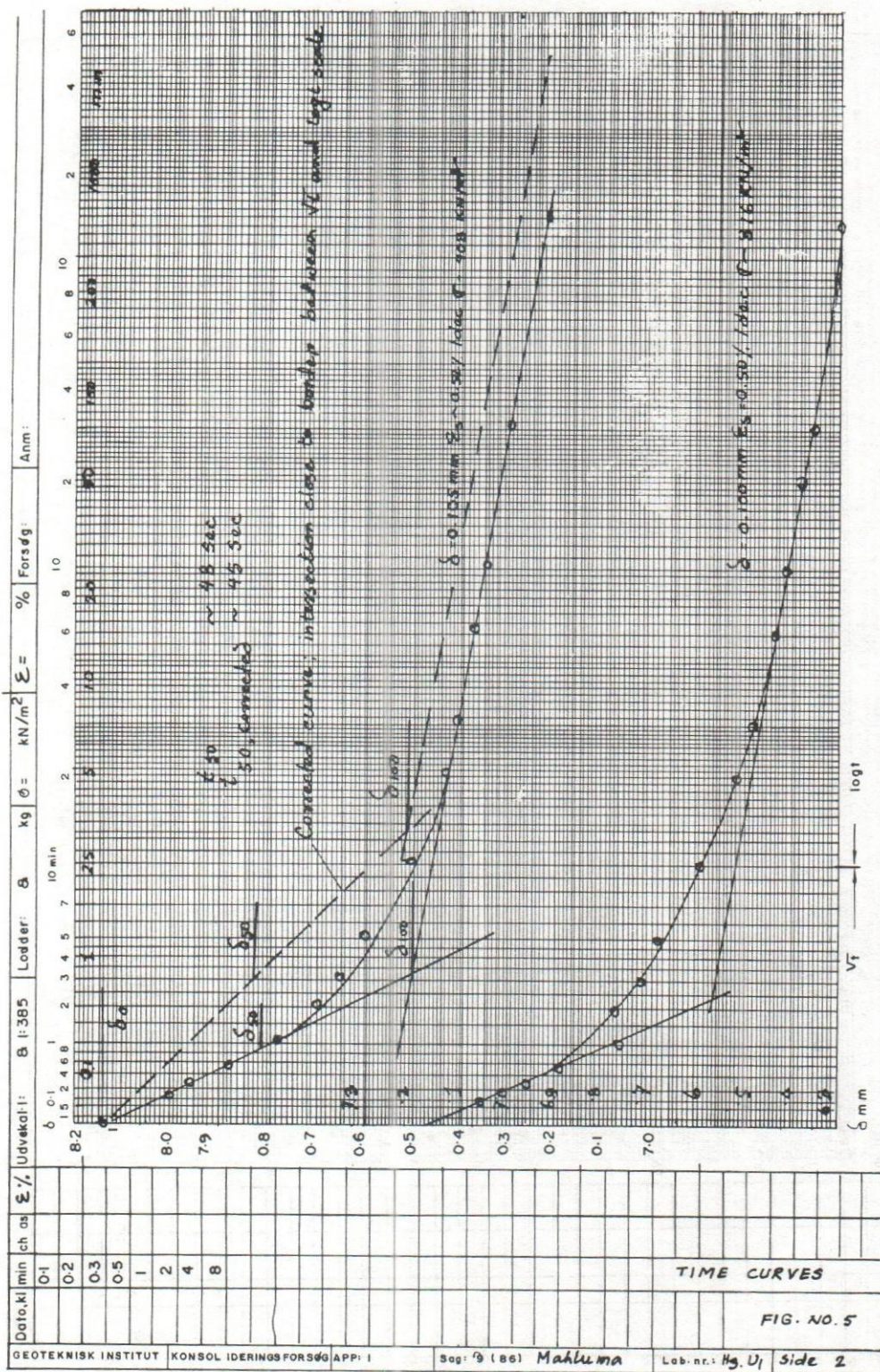


Height of sample	1.98	cm	Soil description : CLAY, trace Fine sand	
Pressure area	14.34	cm <sup>2</sup>		
Void ratio before consolidation	1.192		<div style="display: flex; align-items: center;"> <div style="text-align: center; margin-right: 10px;">  <b>DANISH GEOTECHNICAL INSTITUTE</b> </div> <div> <b>CONSOLIDATION TEST</b> </div> </div>	
Bulk density before consolidation	17.12	kN/m <sup>3</sup>		
Water content before consolidation	43.2	%	Test	Job no 9(86) Mahluma
Water content after consolidation	31.5	%	Design	Boring no H3
Undrained shear strenght, UU-test	17	kN/m <sup>2</sup>	Checked	Elev:      Depth : 6.4 m
Vertical effective stress in situ $\sigma'_0$	45	kN/m <sup>2</sup>	Approved	Lab. no. U1      FIG. NO. 3

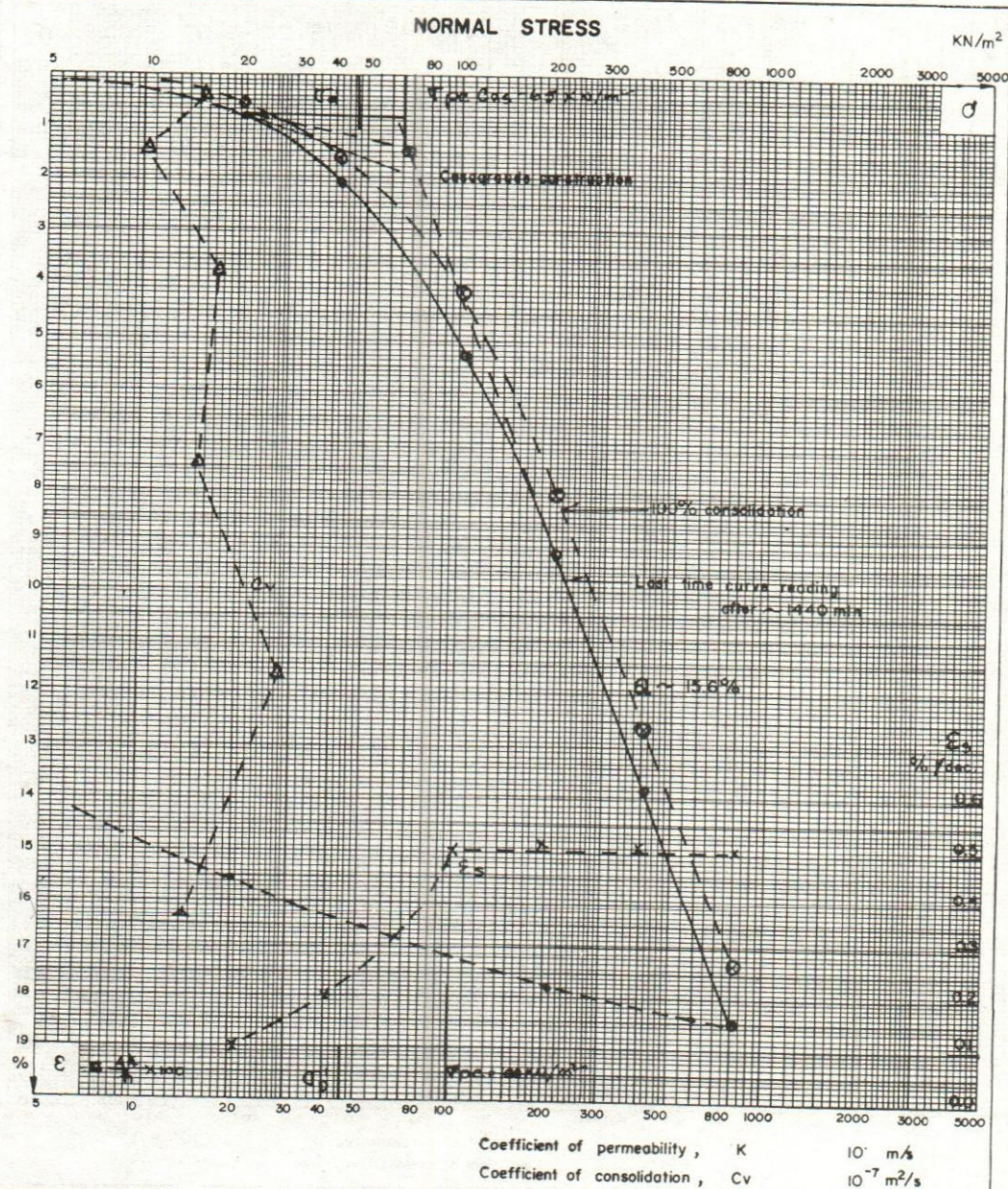






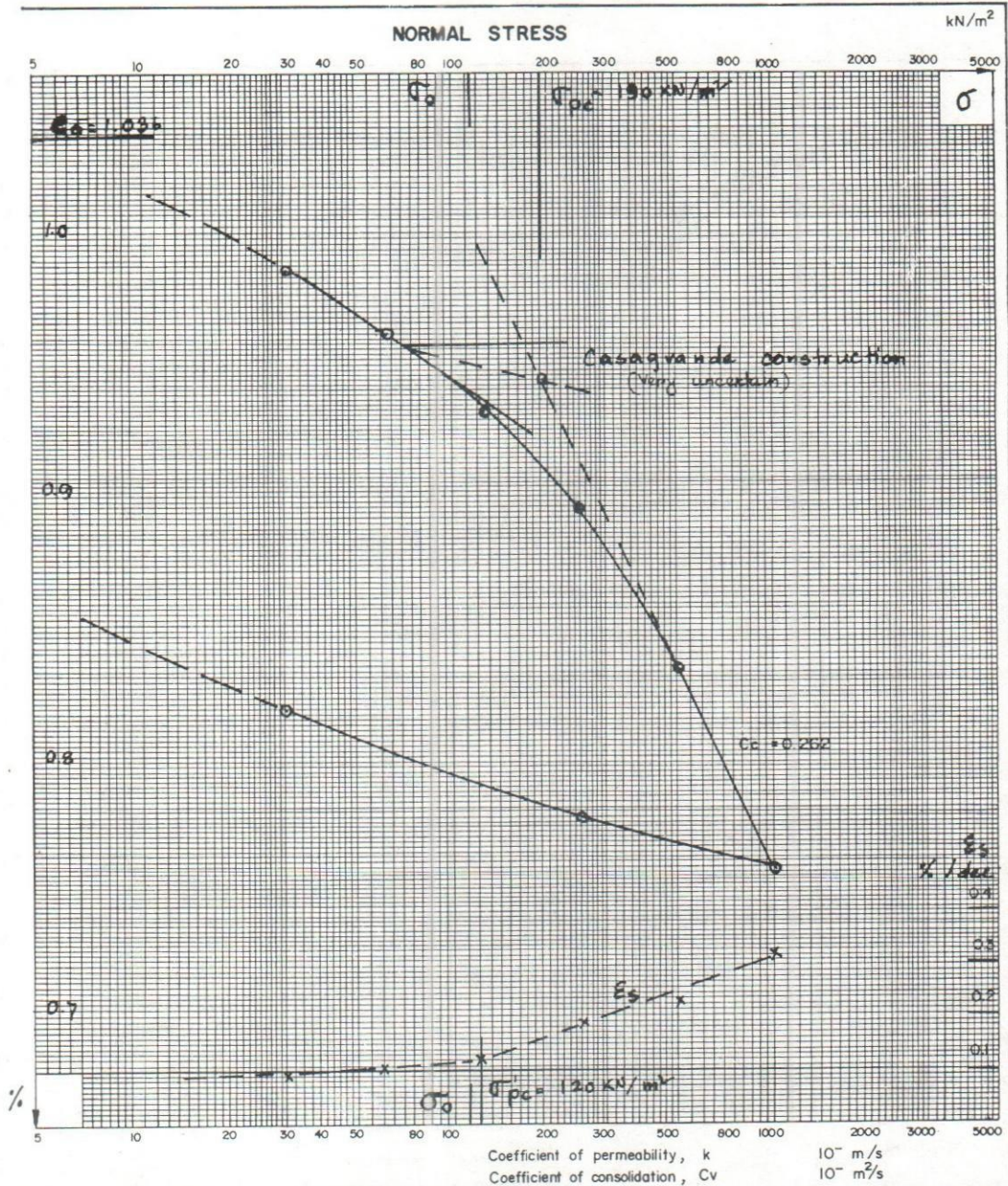







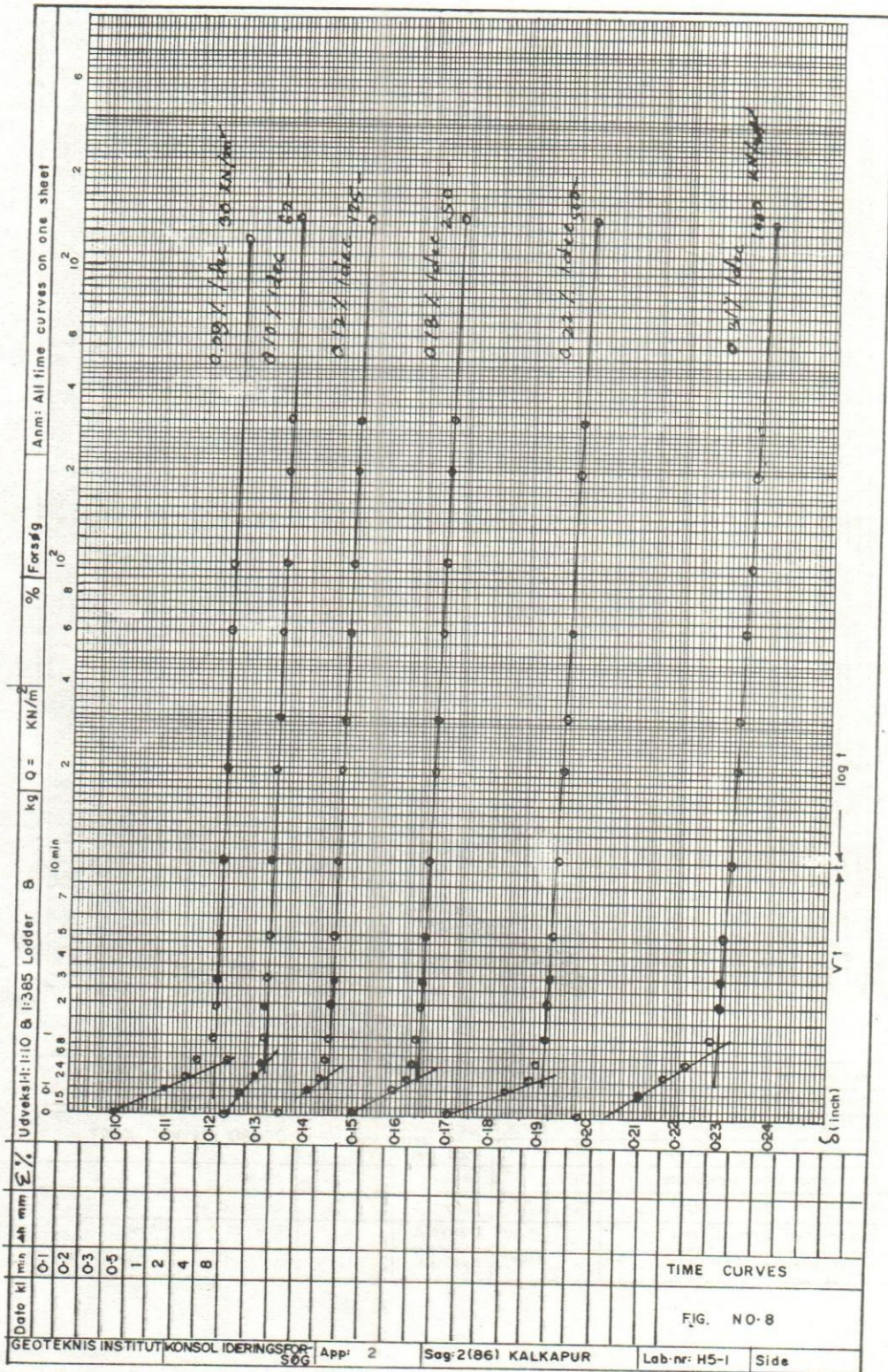
Height of sample	1.98	cm	Soil description: CLAY, trace Fine sand	
Pressure area	19.14	cm <sup>2</sup>		
Void ratio before consolidation	1.192		<div style="display: flex; align-items: center;"> <div style="border: 1px solid black; padding: 2px; margin-right: 5px;">G</div> <div> <b>DANISH GEOTECHNICAL INSTITUTE</b> </div> </div>	
Bulk density before consolidation	17.12	KN/m <sup>3</sup>		
Water content before consolidation	43.2	%	Test	Job no 9 (86) Mähluma
Water content after consolidation	31.5	%	Design	Boring no. H3
Undrained shear strength, UU-test	17	KN/m <sup>2</sup>	Checked	Elev: . . . Depth: 64m
Vertical effective stress in situ	$\sigma_0$ 45	KN/m <sup>2</sup>	Approved	Lab. no. U1 FIG. NO. 6



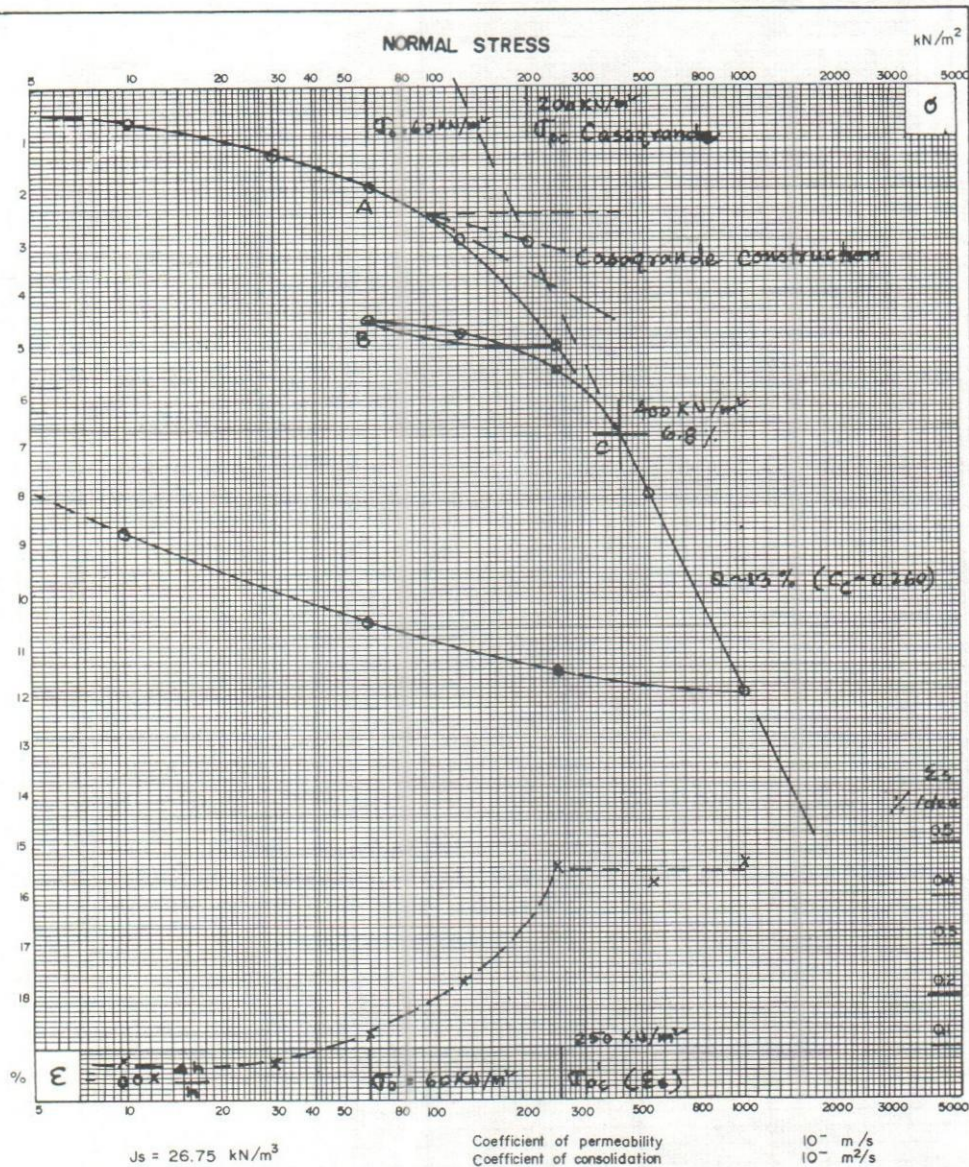


Height of sample	2.54	cm	Soil description : SILT, trace Fine sand	
Pressure area	40.32	cm <sup>2</sup>		
Void ratio before consolidation	1.036		<div style="display: flex; align-items: center;"> <div style="flex: 1;">  <div>                     DENISH GEOTECHNICAL INSTITUTE                 </div> </div> <div style="flex: 1; text-align: center;"> <b>CONSOLIDATION TEST</b> </div> </div>	
Bulk density before consolidation	17.76	kN/m <sup>3</sup>		
Water content before consolidation	38.37	%	Test	Job. no. 2 (86) KALKAPUR
Water content after consolidation	28.44	%	Design	Boring no. H5
Undrained shear strength, UU-test	65	kN/m <sup>2</sup>	Checked	Elev. N.D.      Depth : 7.9 m
Vertical effective stress in situ $\sigma'_0$	113	kN/m <sup>2</sup>	Approved	Lab. no. U1      FIG. NO. 7









Height of sample	2.00	cm	Soil description:			
Pressure area ( $\varnothing 5.0 \text{ cm}$ )	19.64	$\text{cm}^2$				
Void ratio before consolidation	1.00		<div style="display: flex; align-items: center;"> <div style="border: 1px solid black; padding: 2px; margin-right: 5px;">G</div> <div> <b>DANISH GEOTECHNICAL INSTITUTE</b> </div> </div>			
Bulk density before consolidation	18.4	$\text{kN/m}^3$				
Water content before consolidation	37.4	%	Test		Job no.	
Water content after consolidation	31.1	%	Design		Boring no	
Undrain shear strenght, vane		$\text{kN/m}^2$	Checked		Elev :	Depth :
Vertical effective stress in situ $\sigma'_0$		$\text{kN/m}^2$	Approved		Lab. no.	FIG. NO. 9



# **Analysis of Annual Extremes Of The Gumti River For The Determination of 100- Year Flood Magnitude Through The Distribution Fittings**

Md. Abul Kashem<sup>1</sup>

## **Abstract**

*For the design of hydraulic structures or forecasting flood magnitude, frequency analysis is widely used for the determination of flood magnitude corresponding any given year returned periods especially for 100-year. A frequency analysis of annual extremes (discharges) of the River Gumti is presented in this paper for the determination of 100 years flood magnitude including some comments for other returned periods or Probabilities of exceedance.*

## **Introduction**

For hydrological practices, frequency analysis is widely used for the determination flood magnitude corresponding to given returned periods or probabilities of exceedance which is useful for the purpose of flood forecasting or design of hydraulic structures.

A frequency analysis of annual extremes (discharges) of the Gumti River which comes from the Indian hilly province of Tripura, recorded at the border station Comilla [23°28'N and 91°15'E] for 28 years was carried out for the selection of flood magnitude for 100-year returned periods.

## **Analysis of extremes**

The analysis of annual extremes (maximum discharges) of the Gumti River was carried out on available data for twenty eight years. The basic statistics of the historical flood frequency are given in the Table 1.

---

<sup>1</sup>Scientific Officer, RRI, Faridpur.



**Table-1** Basic statistics of the annual maximum discharge of the Gumti River recorded at the station comilla.

Basic statistics	Value
Mean $[X]$	516.75
Standard deviation $[S]$	205.80
Variance $[s^2]$	42353.64
Skewness $[C_s]$	1.39
Kurtosis $[C_k]$	5.42

**Table- 2** Some Criteria for the selection of Probability distribution [after Shahin, 1993].

Distribution	Criteria
Normal distribution	$C_s=0$ $C_k=3$
Two parameter Lognormal distribution	For $C_s \sim +ve$ only $C_s=3C_v+C_v^3$ where $C_v= s/\bar{x}$ or $Log C_s=0$ $Log C_k=3$ . Number of data between $\bar{x}+s$ and $\bar{x}-s$ $= 2/3 * \text{total number of data}(n)$ :
Gamma distribution 1 parameter 2 parameter 3 parameter	$\bar{x}=s^2$ $C_s=2C_v$ $C_s=3C_v+C_v^3$
Pearson Type-III	$C_s \sim +ve$ (-ve for Log Pearson III) $C_k=1.5C_s^2+3$
Gumbel Extreme Value Type-I [Gumbel EVI]	$C_s=1.14$ $C_k=5.4$

Note:  $\bar{x}$ =mean,  $C_v$ = Co-efficient of variation,  $S$ =Standard deviation,  $S^2$ = Variance,  $C_s$ =Skewness,  $C_k$ =Kurtosis

From the basic statistics [Table-1.1], the value of the Skewness and the Kurtosis were found as 1.39 and 5.42 respectively which were not too different from the standard values 1.14 and 5.4 respectively for the Gumbel EV1 distribution [Tab.-1.2]. It is quite resonable to think of fitting Gumbel EV1 distribution to the selected data.

Again, from the criteria for the Pearson Type-III distribution, Kurtosis  $C_k=1.5C_s^2+3$  [Tab.-1.2], the Kurtosis [ $C_k$ ] was found as 6.65 for  $C_s=1.56$ , which was not too different from the value of kurtosis,  $C_k=5.42$  and also, the Skewness is positive [Tab.-1.1]. So, it might also be thought of fitting a Pearson Type-III to the selected data.

However, for the analysis of the annual extremes, the Gumbel EVI distribution and the Pearson Type-III distribution were selected. From the comparison of the results of these two distributions, the 100-year flood magnitude was determined.

### The Gumbel EVI distribution

The relation according to the Gumbel EVI distribution between the variables [ $X_{Gum}$ ] and the reduced variate [ $Y$ ] [de Laat and Savenije, 1994] is:

$$X_{Gum} = \bar{X}_{ext} + \frac{S_{ext}}{\sigma_n} (Y - \bar{Y}_n) \quad (1.1)$$

where

$\bar{X}_{ext}$  = Mean of annual extremes  
 $X_{Gum}$  = estimated value from the Gumbel distribution  
 $S_{ext}$  = standard deviation of extremes  
 $\sigma_n$  = standard deviation of reduced variate

$\bar{Y}_n$  = mean of reduced variate  
 $Y$  = reduced variate which is defined by

$$Y = -\ln(-\ln(F_i)) \quad (1.1a)$$

$F_i$  = plotting probability . According to the Gringorton formula [NERC 1975, Cunnane 1978, and Hall 1993], it is defined by:

$$F_i = \frac{i - 0.44}{n + 0.12} \quad (1.1b)$$

where

$n$  = total number of data  
 $i$  = the rank of a value in the ascending order



**Table- 3** The analysis of the Gumbel Type-1 distribution for annual maximum discharges.

Rank i	$X_{ext}$ m <sup>3</sup> /s]	$F_i$	Y	$X_{gum}$ [m <sup>3</sup> /s]
1	241.00	0.020	-1.365	162.89
2	246.00	0.055	-1.062	219.38
3	274.00	0.091	-0.874	254.39
4	281.00	0.127	-0.726	281.96
5	348.00	0.162	-0.598	305.73
6	370.00	0.198	-0.483	327.23
7	372.00	0.233	-0.375	347.28
8	422.00	0.269	-0.273	366.39
9	425.00	0.304	-0.173	384.90
10	436.00	0.340	-0.076	403.06
11	439.00	0.376	0.021	421.09
12	450.00	0.411	0.118	439.14
13	464.00	0.447	0.216	457.40
14	488.00	0.482	0.316	476.01
15	504.00	0.518	0.418	495.13
16	505.00	0.553	0.525	514.95
17	532.00	0.589	0.636	535.67
18	537.00	0.624	0.753	557.53
19	552.00	0.660	0.878	580.56
20	562.00	0.696	1.013	606.00
21	580.00	0.731	1.161	633.53
22	582.00	0.767	1.326	664.17
23	649.00	0.802	1.513	699.03
24	653.00	0.838	1.732	739.88
25	657.00	0.873	2.000	789.77
26	730.00	0.909	2.349	854.85
27	1010.00	0.945	2.863	950.66
28	1160.00	0.980	3.906	1144.94
		<b>0.990</b>	<b>4.600</b>	<b>1274.21</b>

Mean  $[\bar{X}_{ext}] = 516.75$

Standard deviation  $[S_{ext}] = 205.80$

Total number of data  $[n] = 28$

Plotting Probability  $[F_i] = (i-0.44)/(28.12)$

Mean of reduced variate  $[y_n] = 0.5343$

Std. deviation of reduced variate  $[\sigma_n] = 1.1047$

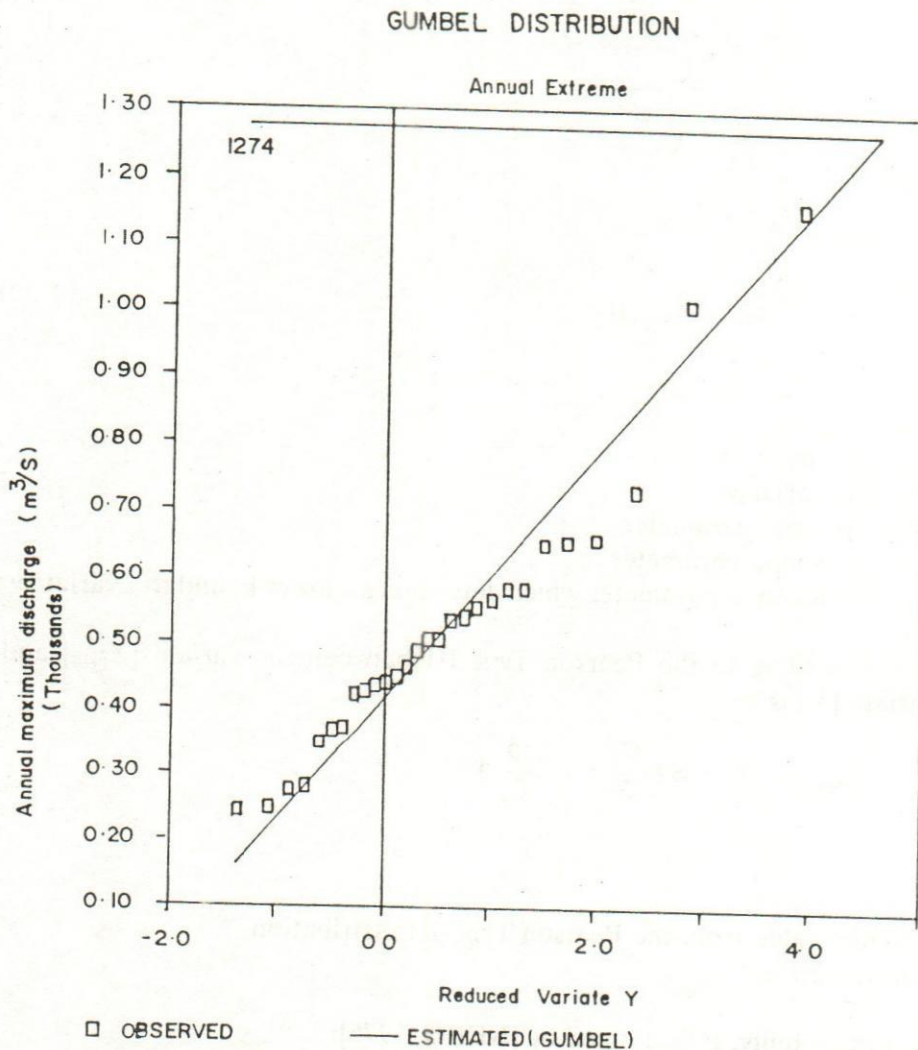
For any returned periods:

$$\bar{X}_{Gum} = \bar{X}_{ext} + S_{ext}/\sigma_n * (Y - Y_n)$$

$$= 516.75 + 205.8/1.1047 * (Y - 0.5343) \text{ [m}^3\text{/s]}$$

For 100-year returned period  $X_{100} = 1274 \text{ m}^3\text{/s}$

The analysis of the Gumbel distribution for annual maximum discharges is given in the Table-1.3. The parameters of this distribution were estimated by the method of moments. The distribution fittings is shown in Fig.-1.1.



**Fig. 1.1** The fit of the Gumbel EVI distribution for the annual extreme of the Gumti River.

From the distribution fittings, a 100-year flood magnitude was found 1274 m<sup>3</sup>/s.



### 1.2.2 Pearson Type-III distribution

The Pearson Type-III was also considered for fitting the data of annual extremes. The three parameters:  $\beta, \gamma$  and  $x_0$ , of the Pearson Type-III distributions are defined by:

$$\gamma = \left( \frac{2}{C_s} \right)^2 \quad (1.2)$$

$$\beta = \sqrt{\frac{S^2}{\gamma}} \quad (1.2a)$$

and

$$x_0 = \bar{X} - \beta\gamma \quad (1.2b)$$

Where

$\bar{X}$	= mean
$S^2$	= variance
$\beta$	= scale parameter
$\gamma$	= shape parameter
$x_0$	= location parameter which determines a lower bound to variate value.

The relation according to the Pearson Type-III between the variate  $[X_{\text{pear}}]$  and the reduced variate  $[Y]$  is:

$$X_{\text{pear}} = \bar{X} + S \left( \frac{C_s}{2} Y - \frac{2}{C_s} \right) \quad (1.3)$$

where

$X_{\text{pear}}$  = estimated value from the Pearson Type-III distribution

$Y$  = reduced variate

The Plotting probability,  $F_i$  is defined by [NERC, 1975]:

$$F_i = \frac{i - 0.4}{n + 0.2} \quad (1.3a)$$

where

$n$  = total number of data and  $i$  = the rank of a value in the ascending order.

**Table-1.4** The analysis of the Pearson Type-III distributions for annual maximum discharges.

Rank i	$X_{ext}$ [m <sup>3</sup> /s]	$F_i$	Y	$X_{Pear}$ [m <sup>3</sup> /s]
1	241.00	0.021	-0.467	147.36
2	246.00	0.057	0.047	250.59
3	274.00	0.092	0.374	296.97
4	281.00	0.128	0.561	326.89
5	348.00	0.163	0.654	356.81
6	370.00	0.199	0.739	365.79
7	372.00	0.234	0.748	371.77
8	422.00	0.270	0.757	379.25
9	425.00	0.305	0.832	386.73
10	436.00	0.340	0.841	388.23
11	439.00	0.376	0.935	401.69
12	450.00	0.411	1.028	416.65
13	464.00	0.447	1.075	434.60
14	488.00	0.482	1.215	461.53
15	504.00	0.518	1.309	476.49
16	505.00	0.553	1.496	503.42
17	532.00	0.589	1.589	521.38
18	537.00	0.624	1.683	536.34
19	552.00	0.660	1.776	551.30
20	562.00	0.695	1.870	570.75
21	580.00	0.730	1.963	588.70
22	582.00	0.766	2.150	611.14
23	649.00	0.801	2.244	641.06
24	653.00	0.837	2.524	670.98
25	657.00	0.872	2.711	727.83
26	730.00	0.908	3.085	790.67
27	1010.00	0.943	3.552	955.24
28	1160.00	0.979	4.431	1045.00
		<b>0.990</b>	<b>6.170</b>	<b>1239.49</b>

Mean  $\bar{X}_{ext} = 516.75$ Standard deviation  $[S_{ext}] = 205.80$ Skewness  $[C_s] = 1.56$ Plotting Probability  $[F_i] = (i-0.4)/(28.2)$ Parameters:  $\gamma = 1.65$ ,  $\beta = 160.03$  and  $x_0 = 252.08$ 

For any returned periods:

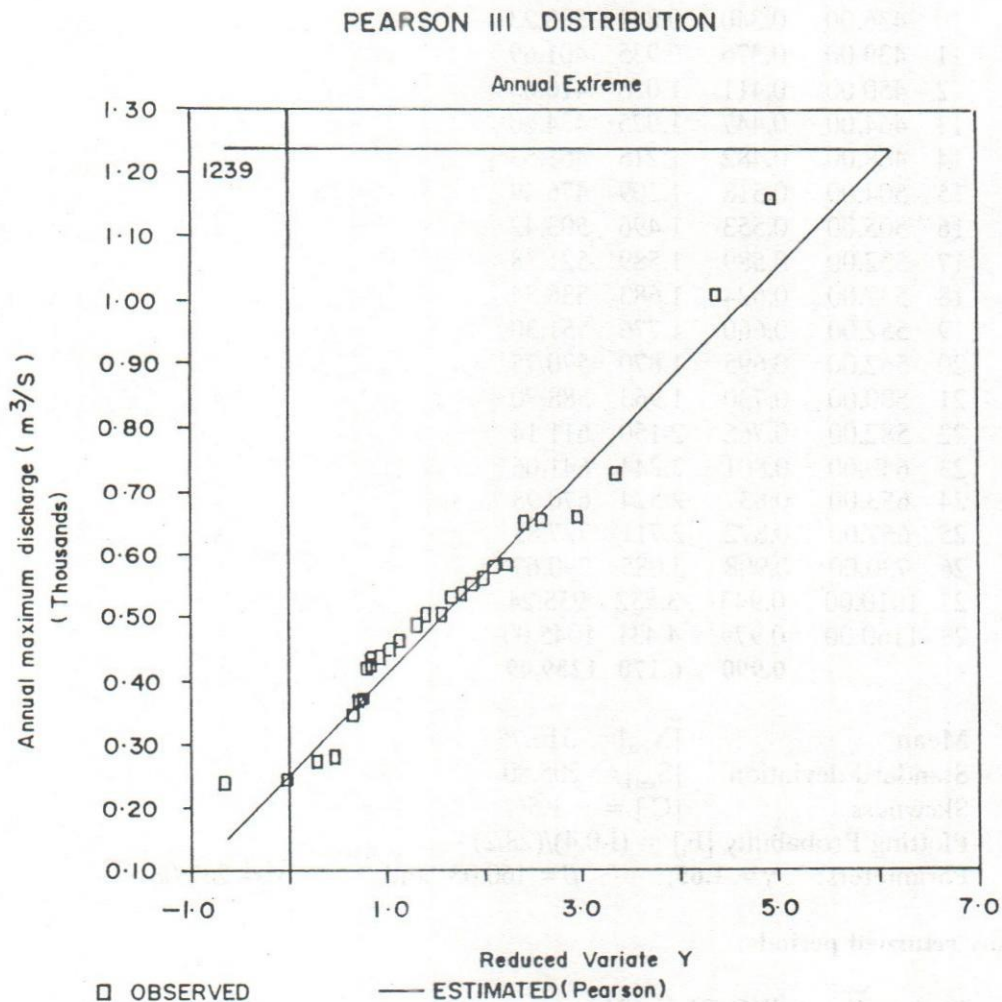
$$X_{Pear} = \bar{X}_{ext} + S(C_s/2 * Y - 2/g)$$

$$= 516.75 + 205.804 * (0.7776 * Y - 1.286)$$

For 100-year returned period  $X_{100} = 1239 \text{ m}^3/\text{s}$



The analysis of Pearson Type-III is given in the Table-1.4, and also, the distribution fittings is shown in Fig.-1.3. The three parameters were determined by the method of moments, i.e., by using the equations 1.2, 1.2a and 1.2b. The reduced variate [Y] was determined for  $\gamma = 1.65$  from the Table-1.5 which was prepared by Harter for the determination of the reduced variate (Y) with respect to different  $\gamma$  value and Probabilities of Non-exceedance [G(y)] [NERC, 1975].



**Fig.1.2** The fit of the **Pearson Type-III** distribution for the annual extreme of the Gumti River.

**Table-5** Percentage points of standardised gamma variates [NERC, 1975]

$G(y)$	$\gamma = 1$	$\gamma = 2$	$\gamma = 5$	$\gamma = 10$	$\gamma = 20$
0.10	0.105[Y]	0.532	2.433	6.221	14.53
0.20	0.223	0.824	3.090	7.289	16.17
0.30	0.357	1.097	3.634	8.133	17.44
0.40	0.511	1.376	4.148	8.904	18.57
0.50	0.693	1.678	4.671	9.669	19.67
0.60	0.916	2.022	5.237	10.476	20.81
0.70	1.204	2.439	5.890	11.387	22.08
0.80	1.609	2.994	6.721	12.519	23.63
0.90	2.303	3.890	7.994	14.206	25.90
0.95	2.996	4.744	9.154	15.705	27.88
0.99	4.605	6.638	11.605	18.783	31.85

Note:  $G(y)$  = Probability of Nonexceedence,  $Y$  = Reduced variate

From the distribution fittings of the Pearson Type-III, a 100-year flood magnitude was found at 1239 m<sup>3</sup>/s.

### Conclusion and Recommendation

From the analysis of the Gumbel EVI and the Pearson Type-III distributions two different 100 years flood magnitudes, respectively 1274 m<sup>3</sup>/s and 1239 m<sup>3</sup>/s, were found. Nevertheless, these two values were close to each other. Hence, a 100-year flood magnitude [discharge] at the border station, Comilla, was chosen in between these two values, at 1250 m<sup>3</sup>/s.

Moreover, this frequency analysis method should be an example for the determination of flood magnitude corresponding to any given returned periods or probabilities of exceedance for other rivers.



## Reference

1. **Cunnane C.**, (1978), Unbiased plotting positions- A review, *Journal of Hydrology*, 37: 205-222.
2. **de Laat P. J. M. and Savenije H. H. G.**, (1994), Principles of Hydrology, Lecture note, IHE, Delft, The Netherlands.
3. **Hall M. J.** 1993, Statistics and Stochastic Processes in Hydrology, Lecture note, IHE, Delft, The Netherlands.
4. **Kashem Md. A.** (1995) Flood Forecasting System for the River Gumti in Bangladesh, M.Sc. Thesis, H.H. 250, IHE, Delft, The Netherlands.
5. **Natural Environmental Research Council [NERC]**, London, U.K., (1975), Flood Studies Report, Volume 1, Hydrological Studies.

## Scale Model Study of Groynes for the Protection of Simla Area from the Erosion of Jamuna River

A.K.M. Ashrafuzzaman<sup>1</sup>  
Syed Md. Anwaruzzaman<sup>2</sup>  
Md.Nazrul Islam Siddique<sup>3</sup>

### Abstract

*This paper presents the results of scale model investigation in connection with the protection of Simla area from the erosion of Jamuna river. In this study attempt was made to find out a solution of the erosion problem which should be justified from technical as well as economical stand point. The behavior & effectiveness of T-headed groynes as bank protection devices were the key interest of this study. The model was undistorted & designed according to the Froude's model law. Different test runs have been carried out in this model study. Test no. 1 was conducted with existing condition and the model was calibrated in this test. Each test run (with varying no. of groynes, length of shank & T-head, location, orientation, inclination of T-head with shank) was designed analyzing the results of the previous test. In each test run depth averaged flow velocity, flow lines, and scour depth around the groynes (excluding Test no. 1) were measured. On the basis of test results, two groynes were recommended which were supposed to be economically justified & sufficient to save river bank of about 3000 m.*

### Introduction

Simla is situated on the right bank of Jamuna river under Sadar Thana of Sirajgonj district. Many villages, cultivable lands and a small town are there. The economy of that area is mainly based on agriculture. But the erosion of Jamuna river causes unmitigable losses of properties and unbearable sufferings to the people and the continuous bank erosion threatens the whole area to be devoured by the river.

Fig.1 shows the bank line shifting of Jamuna river at Simla from 1985 to 1995, from which one can easily visualize the nature of devastation of bank erosion. Realizing the

---

<sup>1</sup> & <sup>2</sup>Scientific Officer, River Research Institute, Faridpur.

<sup>3</sup>Principal Scientific Officer, RRI, Faridpur.



facts and to save the agrarian economy of the region, BWDB planned to undertake a project for the protection of that area and formally proposed to RRI to carry out a scale model investigation to find out a viable solution. This study is a part of that project. Fig.2 shows index map of the study area.

### **The Jamuna River**

In Bangladesh, the Brahmaputra river is also named as the Jamuna. It is the country's largest as well as rank two among the largest rivers of the world. The Brahmaputra originates from the Tibetan Himalayas at an elevation of 5,150 meters near the Nepal-China border. It first drains the dry northern side of the Himalayas, flows eastward under the Chinese name of Tsango. Through a succession of rapid turning southward, it enters into India taking the name the Brahmaputra. Further, turning westward, it drains the very humid Assam valley. It turns once again southward, round the Garo hills and enters into Bangladesh near Noonkhawa.

The Brahmaputra moved to its present course (inside Bangladesh) about 200 years ago (1787). In Bangladesh, the width of the river in general varies between 8 to 10 km, but at few places the river is 15 to 20 km wide. It drains a total area of about 5,80,000 km<sup>2</sup> of which about 10% lies within Bangladesh.

The Jamuna is a highly braided river with multiple channels without fixed bank. The shifting of course and bank lines is very much frequent. Maximum annual average peak flow at Bahadurabad is about 65,400 m<sup>3</sup>/s while the maximum peak discharge observed in 1988 was 98,600 m<sup>3</sup>/s which is highest ever recorded. The average annual sediment load at Bahadurabad was observed as 449 million ton. The slope of Jamuna river varies from 5 to 9 cm/km with an average of about 7.5 cm/km. The bed material of Jamuna consists of fine sand with median diameter of about 0.18 mm.

### **Objectives of the Model Study**

The overall objectives of the present model study were as follows:

- 1) To check the effectiveness of the groyne proposed by BWDB
- 2) To suggest a suitable means to combat erosion at Simla
- 3) To furnish design parameters such as velocity, scour depths etc. for the finalization of design of the river training works.

### **Data Collection and Assessment of Discharge for the Model**

Hydrological Dte. of BWDB records both discharge and water level data at Bahadurabad and only water level is measured at Sirajgonj. Bahadurabad is located at 89 km upstream from Simla. As per requirement of RRI, Morphological division of BWDB collected river



bathymetry and carried out a plain table survey to prepare a index map of the river reach to be modelled. About 3.5 km of the river width was considered during data collection.

A frequency analysis has been carried out to find out the discharges and corresponding water levels for different return periods at Bahadurabad. The discharge & corresponding water level is found 91,000 cumecs & 21.26 m+PWD respectively for 100 years return period. Water levels at Sirajgonj corresponding to the different return period has also been calculated through frequency analysis and the water level corresponding to 1 in 100 years flood is 14.95 m+PWD. Distance of Simla from Sirajgonj is about 10 km and the average water surface slope of Jamuna is about 7.5 cm/km. Thus the water level at Simla corresponding to 1 in 100 years flood is calculated as 14.70 m+PWD. In the model, about 2.5 km of the river width was reproduced and the discharge within this width corresponding to 1 in 100 years flood with water level 14.70 m+PWD was estimated as 35,000 cumecs.

### Design of the Model

If the model is properly designed and verified, the results obtained from the model study may be transformed easily to prototype and can be used successfully in the field. In the scaling procedure, Froude's model law was used and an un-distorted sectional model with scale of 1:100 was selected. The following simulation criteria were verified during model design:

#### (a) Simulation of flow pattern and flow velocity in the model

##### 1) Fulfillment of the Froude's model law

According to the Froude's model law, the Froude's number in the model and prototype should be equal. Froude's number is given by the following equation:

$$F = \frac{V}{\sqrt{gh}}$$

Equating the Froude's number in the model and prototype the velocity ratio has been calculated as

$$V_r = \sqrt{H_r} = 10$$

Velocity in the model,  $V_m = 2.1$  m/s

$$Q_r = A_r V_r = h_r^2 \sqrt{H_r} = h_r^{5/2} = 100000$$

Discharge in the model = 350 l/s



## 2) Turbulent flow in the model

Depending upon the Reynold's number, the flow in the river can be classified as laminar and turbulent. In laminar flow the viscous force is dominant and in the turbulent flow the effect of viscous force is small. In laminar flow,  $R < 500$  and in turbulent flow  $R > 2000$  and in the transitional zone  $500 < R < 2000$ . Most of the river flow is turbulent and thus to simulate flow pattern, the flow in the model should also be turbulent. The Reynold's number can be defined as

$$R = \frac{Vh}{\nu}$$

Here,  $\nu$  = Kinematic viscosity =  $1.10 \times 10^{-6}$   
 Reynold's number in the prototype

$$R_p = \frac{2.1 \times 7.3}{0.95 \times 10^{-6}} = 16136842$$

Which confirms turbulent flow in the prototype  
 Reynold's number in the model

$$R_m = \frac{0.21 \times 0.073}{0.95 \times 10^{-6}} = 16137$$

Which confirms turbulent flow in the model

## 3) Rough turbulent flow in the model

According to the equivalent roughness height, the flow can be classified as hydro-dynamically smooth and rough. In hydro-dynamically smooth flow, the thickness of the viscous sub-layer ( $\delta$ ) is greater than the roughness height ( $K_s$ ) and viscous force may affect the velocity distribution. And thus to avoid this effect, the flow in the model should be rough turbulent i.e hydro-dynamically rough.

The flow will be hydro-dynamically rough if  $\delta < K_s$ .

During the proving test of the model the slope of the water surface measured as  $S_m = 0.0006$ . From this measured slope, the Chezy's coefficient in the model calculated from the following equation

$$C_m = \frac{V_m}{\sqrt{h_m S_m}} = \frac{0.21}{\sqrt{0.073 \times 0.0006}} = 31.73$$

Corresponding Manning's roughness calculated as

$$n_m = \frac{h_m^{1/6}}{C_m} = \frac{0.073^{1/6}}{31.73} = 0.02$$

From Stricler's equation, the roughness height can be calculated as

$$K_s = (26 n_m)^6 = (26 * 0.02)^6 = 0.0198$$

The friction factor in the model calculated from the following equation

$$f_m = (2.21 + 2.03 \log \frac{h_m}{K_s})^{-2}$$

$$= (2.21 + 2.03 \log \frac{0.073}{0.0198})^{-2} = 0.089$$

Particle Reynold's number in the model can be calculated as

$$R_{*m} = R_m \left( \frac{f_m}{8} \right)^{1/2} \left( \frac{K_s}{h_m} \right)$$

$$= 13936 \left( \frac{0.089}{8} \right)^{1/2} * \frac{0.0198}{0.073} = 399$$

The viscous sub-layer in the model may be calculated from the following equation:

$$\delta_m = 11.6 \frac{K_s}{R_{*m}} = 11.6 * \frac{0.0198}{462} = 0.000576$$

The value of  $\delta_m$  is less than the value of  $K_s$ , which means that the flow in the model will be rough turbulent.

#### (b) Simulation of roughness in the model

As the material distortion was allowed in the model, the quantitative equalization of roughness in the prototype and model was not possible, but effort was made to ensure similar pattern and forms of roughness in the prototype and model. As for instance, the form roughness dominates and controls flow distribution in the prototype and thus the form roughness should also dominate in the model. The roughness due to viscosity is negligible in the prototype and this should also happen in the model.

#### (c) Simulation of scouring in the model

As Jamuna river carries sediment laden water, the model was designed corresponding to the live bed condition. In an un-distorted model, the sediment transport can be reproduced in the model at scale if the  $D_{50}$  is reproduced at the length scale. The sediment of Jamuna river is fine sand. If this sand is scaled at the length scale, the diameter of the model sand will become equal to the diameter of silt or clay. However,



the properties and transportation characteristics of sand and clay particles are completely different from the properties and the transportation characteristics of sand. Therefore the sand of the Jamuna river can not be scaled in the model to reproduce the sediment transport intensity in the model.

Many Researchers worked on the local scour around the bridge piers and it was found that scour depth at an obstacle becomes independent of flow velocity when the average flow velocity is greater than the critical velocity of the sediment for initiation of threshold motion. However, in the model study of Flood Action Plan (FAP), it is opined that the scour depth becomes independent of flow velocity if  $V_m > 2V_{cr}$ . This means that the maximum scour depth does not depend on the flow velocity in the model if  $V_m > 2V_{cr}$ , where  $V_m$  is the average flow velocity and  $V_{cr}$  is the critical velocity. Only the time period in which this maximum scour depth will be reached, will decrease if the model flow velocity increases.

The critical flow velocity for the initiation of bed load movement can be calculated from the following equation:

$$V_{cr} = 0.19 (D_{50})^{0.10} \text{Log} \left( \frac{12 R_b}{3 D_{90}} \right) \text{ for } 100 < D_{50} < 500 \mu m$$

$$V_{cr} = 8.5 (D_{50})^{0.60} \text{Log} \left( \frac{12 R_b}{3 D_{90}} \right) \text{ for } 500 < D_{50} < 2000 \mu m$$

Critical velocity in the prototype is

$$V_{crp} = 0.19 (0.00018)^{0.10} \text{Log} \left( \frac{12 * 7.30}{3 * 0.00026} \right) = 0.41 \text{ m/s}$$

Critical velocity in the model is

$$V_{crm} = 0.19 (0.000185)^{0.10} \text{Log} \left( \frac{12 * 0.073}{3 * 0.000284} \right) = 0.24 \text{ m/s}$$

Thus the material available at RRI's model bed will be used and the model will be designed for live bed condition and model discharge simulate the local scour can be calculated as follows:

$$V_{ms} = 1.4 * V_{crm}$$

$$= 1.4 * 0.24 = 0.336 \text{ m/s}$$

$$Q_{ms} = A_m * V_{ms}$$

$$= 1.69 * 0.336 = 0.568 \text{ cumecs}$$

## Model Construction

An open air model bed of RRI with the area of 60 m x 30 m was selected. The river reach of 4 km from C/S-15 (Ch.156 km) to C/S-49 (Ch.160 km) and the width of 2.5 km of the river from the right bank line of 1995 were reproduced in the model. The model was a sectional model and the mid river boundary was constructed in such a way that no flow separation would be occurred during model operation. The movable bed extended from C/S-17 to C/S-47 and was constructed according to the bathymetry. The upstream part (from weir to C/S-17) and the downstream part (from C/S-47 to C/S-49) of the model bed were fixed. Tail gates each having a length of 1.8 m were installed at the downstream end of the model along the C/S-49 to regulate water level in the model. Two point gauges were constructed and during model operation water level was measured with these point gauges and the water surface slope was found out.

## Measurements

Discharge was measured with a standard sharp crested weir (length=1.78m) installed at the u/s end of the model. A point gauge was also constructed to measure water level over the crest of the weir at a sufficient distance from the weir to avoid curvature effect. The following Rehbock's formula was used to determine the model discharge:

$$Q = (0.403 + 0.053 \frac{h_w}{P}) \times b \sqrt{2g} \left[ \left( h_w + \frac{V_a^2}{2g} \right)^{1.5} - \left( \frac{V_a^2}{2g} \right)^{1.5} \right]$$

Where, Q=Discharge in m<sup>3</sup>/s

$V_a$  = Velocity of approach in m/s

P = Height of the weir in m

$h_w$  = Head over the weir in m

b = Length of weir in m

P = Height of the weir in m

g = Acceleration due to gravity m/s<sup>2</sup>

Depth averaged point velocity was measured with an A-OTT type horizontal axis current meter.

## Calibration of the Model

In a sectional model where whole width of the outflanking channel is not considered, three boundary conditions are necessary to be satisfied. Boundary conditions are normally adjusted in the model comparing with measured prototype information.



## Boundary Conditions

Upstream boundary condition is the discharge distribution along the upstream limit of the model. The measured discharge distribution of Jamuna at or near the upstream limit was not available and the model was calibrated against computed discharge distribution at C/S-25. Table-2 shows comparison between computed and measured depth averaged flow velocity at C/S-25. Downstream boundary condition is the water level controlled by tailgates at the downstream end of the model. Water level was measured with point gauge. The prototype water level is 15.70 m+PWD and the water level measured in the model is 15.65 m+PWD. The lateral boundary condition is the location and alignment of the left boundary of the model. This boundary is not the left bank of the out flanking channel, but it is a flow line of the prototype in order to represent a portion of the river where the discharge is constant. Two criteria are important during construction of the lateral boundary: (a) The width of the model should be sufficient to prevent any influence by the groynes on this flow line. (b) The curvature of the boundary wall should be as smooth as possible to avoid flow separation.

## Test Results and Discussion

Seven test runs were carried out in this model study. Table-3 shows the summary of test descriptions. During each test run depth averaged flow velocity at different cross-sections, flow lines and scour depths (excluding Test no. 1) were measured. Tests (T-2 to T-7) were carried out with the groyne(s). Comparison of depth average flow velocity up to 150 m in different tests are shown in Table-4. The flow lines from Test no. 1 to 7 are shown in Fig. 3 to 9.

Test no. 1 was conducted with existing condition (with no groyne). Velocity measured in this test will be compared with the velocities from next tests to check the reduction of near bank flow velocity. Five flow lines were recorded and will be compared with the flow lines from next tests to assess the influence of proposed groyne on flow direction. The flow lines have a tendency to move toward the right bank at the downstream indicating severe bank erosion in the downstream areas which justifies the correct similitude of flow pattern in the model because severe bank erosion took place (Fig. 1) in those areas during last flood.

Test no. 2 was carried out with the groyne proposed by Bangladesh Water Development Board (BWDB). Velocities at the downstream of this groyne were tremendously reduced upto C/S-37. Velocities from C/S-41 to the downstream were much more to cause bank erosion. The flow lines still had a tendency to move toward the right bank at the downstream. The flow direction remained unchanged in spite of construction of a groyne at C/S-26. Another groyne may be necessary to reduce the flow velocity in the region of C/S-41 to the downstream and to change the converging tendency of flow in the said areas.

Test no. 3 was planned to conduct with a single smaller sized groyne at C/S-26 to observe the effectiveness of this groyne on velocities and flow direction in the downstream area.



No remarkable change in flow direction was observed and flow lines followed approximately the same path as that for Test no. 2. The overall performance of groyne in Test no. 3 was better than that for Test no. 2 as the groyne in Test no. 3 was shorter. Flow concentration near C/S-46 was remained unchanged.

Test no. 4 was planned to conduct with two groynes, one at C/S-26 and another at C/S-41 keeping the size of groyne at C/S-26 unaltered. Velocities in between the groynes were substantially reduced. Velocities near C/S-47 and to the downstream were slightly higher and to reduce the velocity in those areas, groyne G-2 may need to be shifted from C/S-41 towards downstream. Flow direction was changed in the downstream areas and concentration of flow near C/S-46 was reduced. Test no. 4 produced better results in comparison with Test no. 3. Situation of flow concentration near C/S-46 was improved but considerably high velocity was observed at C/S-47 and to the downstream. Velocity in between the groynes was fairly reduced.

Test no. 5 was conducted with location of groyne G-2 was at C/S-43 and with increased length of T-head and the length of shank & T-head of groyne G-1 (C/S-26) was reduced. Velocities in between the groynes and also near C/S-47 to the downstream were substantially reduced. Test no. 5 produced better results in comparison with Test no. 4. Near bank flow Velocity was reduced remarkably from C/S-26 to C/S-47 and also better deflection of flow was observed in this test. But to economize the solution further, following modifications were made to the groynes in the next test (Test no. 6): (a) Size of shank & T-head of the groyne G-1 (at C/S-26) were reduced (b) Size of shank & T-head of the groyne G-2 (at C/S-43) were also reduced. Velocities in between the groynes from C/S-31 to C/S-39 were increased which might be enough to cause bank erosion. Velocities downstream of groyne G-2 were also increased. Direction of flow aggravated and was moved close to the bank in between the groynes. Test no. 6 produced bad results in comparison with Test no. 5. Near bank flow Velocity was increased substantially which may cause bank erosion. Flow lines were moved towards the river bank in between the groynes. Following modifications were made for the next test:

- (a) Length of shank & T-head of the groyne G-1 (at C/S-26) were increased
- (b) Length of shank & T-head of the groyne G-2 (at C/S-43) were also increased

Near bank flow velocities were fairly reduced and this test was produced comparatively better results. Flow lines were deviated from the river bank towards the mid river and this test produced comparatively better results. Table-5 shows velocity around the groynes G-1 & G-2 respectively and Table-6 shows bed level around the groyne G-1 & G-2 respectively.



## Conclusions & Recommendations

Test no. 7 was produced best results in comparison with the other tests. The two groynes proposed in this test were supposed to be sufficient to save bank erosion from C/S-26 to the some distance downstream of C/S-47. The near bank flow velocities were quite low to cause bank erosion and near bank flow were fairly shifted towards the middle of the river. The distance between the groynes G-1 & G-2 was 1800 m which is about 5 times of the shank length of groyne G-1 and the groynes proposed in this test were economically justified. Thus the results of the Test no.7 were finally accepted and groynes constructed in this test will be recommended to construct in the field to save Simla area from the erosion of Jamuna river. Length of falling apron can be decided from the equilibrium bed levels around the groynes presented in Table-6.

During model study, following area were found to be protected by the recommended groynes:

- (a) River bank (in between the groynes) from C/S-26 to C/S-43 (about 1800 m)
- (b) River bank of about 1000 m (downstream of G-2) from C/S-43 to the downstream
- (c) Some distance upstream of the groyne G-1

Two groynes having a joint hydrodynamic effect should be constructed at the same time. The groynes should be perpendicular to the present bank line. Groyne G-1 should be extended from river bank to the existing flood embankment & Groyne G-2 should also be extended from river bank to the proposed flood embankment. The groynes should be constructed before next monsoon because the model study was conducted on the basis of the river geometry/bathymetry collected in the post monsoon of 1995 and river geometry/bathymetry may be changed after the next monsoon.

## References

1. Ahmed M.(1953), "Experiment on Design and Behaviour of Spur-Dike", Proceedings of IAHR, ASCE, Joint Meeting, University of Minnesota.
2. FAP-21/22, FPCO, (1993), "Bank Protection and River Training (AFPM) Pilot Project, Draft Final Report, Planning Study, Volume VI, Annex-14
3. FAP 21/22 (1992), "Bank Protection and River Training Pilot Project", Physical Model Tests, Draft Final Report, Planning Study, Volume VI.
4. FAP-5B, IDA Credit 1870BD, Part D, (1990), "Meghna River Bank Protection", Short Term Study, Final Report, Volume IV, Annex-D
5. Garde R.J., Subramanya K., Nambudripad K.D.(1961), "Study of Scour Around Spur-Dikes", Journal of the Hydraulic Division, ASCE.

6. Jogleker D.V.(1994), "Manual on River Behaviour Control and Training", Publication No.60, Central Board of Irrigation and Power, Page 215-242.
7. Liu H. K.and Skinner M. M. (1960), "Laboratory Observation of Scour at Bridge Abutment", Highway Research BD, Bulletin No. 242.
8. Montensen P.(1984), "Physical Modelling of Open Channel Flow", Lecture Notes, Danish Hydraulic Institute.
9. Raudkivi, A. J. (1989), "Scour at Bridge Piers", H.N.C., Breusesers, pp 61-63
10. Rijn, L.C.van, "Sediment Transport, Part III: Bed Forms and Alluvial Roughness", Journal of Hydraulic Engineering, Volume 110, No. 12, December, 1984, ASCE.
11. Sharpe J.J. (1981), "Hydraulic Modelling", The Buttersworth Group, Billing and Sons, England.
12. Sastry C.L.N.(1962), "Effect of Spur-Dike Inclination on Scour Characteristic", Thesis presented to the University of Roorkee, Roorkee, India in Partial fulfillment of the requirements for the degree of Master of Engineering.
13. Sir William Halcrow & Partners Ltd (1993), "River Training Studies of the Brahmaputra River", GOB, Report on Model Studies, Volume IV.
14. Tesaker E. (1986), "Some Aspect of Hydraulic Modelling", Lecture Notes for RRI, UNDP/DTCD Project.



Table-1: Characteristics design parameter

Parameters	Prototype	Scale factor	Model
Length(m)	4000	100	40
Width(m)	2500	100	25
Average depth(m)	7.30	100	0.073
Discharge(m <sup>3</sup> /s)	35000	100000	0.350
Cross-sectional area(m <sup>2</sup> )	16,908	10000	1.69
Average velocity(m/s)	2.10	10.0	0.21
Critical velocity(m/s)	0.41	-	0.24
Reynold's number	13936363	1000	13936
Froude's number	0.248	1.0	0.248

Table-2: Comparison of computed and measured velocity at C/S-25

Distance from R/B in m	Computed velocity in m/s	Measured velocity in m/s	Percentage of error
150	2.29	2.41	-5.24
355	1.13	1.21	-7.07
808	1.69	1.75	-3.50
1000	1.13	1.20	-6.19
1300	1.81	1.72	+4.97
1500	2.20	2.14	+2.72
1600	2.62	2.51	+4.19
1800	3.01	2.95	+2.00

Table-3 : Summary of test descriptions

Test no.	Test description	
T-1	Existing condition	
T-2	A single groyne proposed by BWDB the specification of which were as follows: Location & orientation: c/s-26, perpendicular to the river bank Length of shank & T-head: 800 m, 350 m Alignment of T-head: 71° perpendicular to the shank Berm level: 16.00 m+PWD Crest level : 17.50 m+PWD Crest width: 8.00 m Side slope: 1 in 3	
T-3	Location & orientation: c/s-26, perpendicular to the river bank Length of shank & T-head: 500 m, 350 m Alignment of T-head: 71° perpendicular to the shank Berm level: 16.00 m+PWD Crest level : 17.50 m+PWD Crest width: 8.00 m Side slope: 1 in 3	
T-4	Two groynes the specification of which were as follows:	
	G-1	G-2
	Location & orientation: c/s-26, perpendicular to the riverbank Length of shank & T-head: 500 m, 350 m Inclination of T-head: 90 deg. with shank Berm level: 16.00 m+PWD Crest level : 17.50 m+PWD Crest width: 8.00 m Side slope: 1 in 3	Location & orientation: c/s-41, perpendicular to the river bank Length of shank & T-head: 400 m, 100 m Inclination of T-head: 70 deg. with shank at u/s side Berm level: 15.85 m+PWD Crest level : 17.35 m+PWD Crest width: 8.00 m Side slope: 1 in 3
T-5	Two groynes the specification of which were as follows:	
	G-1	G-2
	Location & orientation: c/s-26, perpendicular to the riverbank Length of shank & T-head: 400 m, 150 m Inclination of T-head: 70 deg. with shank at u/s side Berm level: 16.00 m+PWD Crest level : 17.50 m+PWD Crest width: 8.00 m Side slope: 1 in 3	Location & orientation: c/s-43, perpendicular to the river bank Length of shank & T-head: 400 m, 150 m Inclination of T-head: 70 deg. with shank at u/s side Berm level: 15.85 m+PWD Crest level : 17.35 m+PWD Crest width: 8.00 m Side slope: 1 in 3
T-6	Two groynes the specification of which were as follows:	
	G-1	G-2
	Location & orientation: c/s-26, perpendicular to the riverbank Length of shank & T-head: 250 m, 100 m Inclination of T-head: 90 deg. with shank Berm level: 16.00 m+PWD Crest level : 17.50 m+PWD Crest width: 8.00 m Side slope: 1 in 3	Location & orientation: c/s-43, perpendicular to the river bank Length of shank & T-head: 300 m, 100 m Inclination of T-head: 90 deg. with shank at u/s side Berm level: 15.85 m+PWD Crest level : 17.35 m+PWD Crest width: 8.00 m Side slope: 1 in 3
T-7	Two groynes the specification of which were as follows:	
	G-1	G-2
	Location & orientation: c/s-26, perpendicular to the riverbank Length of shank & T-head: 350 m, 150 m Inclination of T-head: 70 deg. with shank at u/s side Berm level: 16.00 m+PWD Crest level : 17.50 m+PWD Crest width: 8.00 m Side slope: 1 in 3	Location & orientation: c/s-43, perpendicular to the river bank Length of shank & T-head: 350 m, 150 m Inclination of T-head: 70 deg. with shank at u/s side Berm level: 15.85 m+PWD Crest level : 17.35 m+PWD Crest width: 8.00 m Side slope: 1 in 3





Table-5: Velocity around groynes G-1 & G-2

Distance from shank axis (m)	Velocity (m/s)													
	Distance from T-axis (m)													
	200.00	150.00	100.00	50.00	0.00	-50.00	-100.00	200.00	150.00	100.00	50.00	0.00	-50.00	-100.00
	G-1							G-2						
150.00	3.18	2.96	4.23	3.79	2.58	1.36	0.73	3.52	3.90	4.01	4.29	2.03	-1.03	-1.14
100.00	2.63	2.96	4.71	3.4	3.68	0.76	0.67	3.46	3.79	4.11	4.70	2.00	1.50	0.80
50.00	2.63	3.18	3.68	4.56	T-head axis	0.70	0.70	3.85	3.90	3.90	3.29	T-head axis	1.00	0.70
0.00	3.02	2.74	4.23	3.79		Shank axis		3.24	3.57	3.66	3.24		Shank axis	
-50.00	2.47	2.90	4.29	3.79	Shank axis		1.00	3.46	3.63	3.24	3.26	Shank axis		0.00
-100.00	2.90	2.69	3.07	4.07	3.57	1.14	1.03	2.90	3.46	2.80	2.91	2.25	1.50	0.50
-150.00	2.85	2.47	3.13	2.85	2.36	1.36	1.00	2.69	3.29	1.86	2.03	1.25	1.00	0.80

(-) sign indicates distance from the shank axis in u/s direction and distance from the T-head axis towards the river bank  
Velocity with negative sign indicates eddy



Table-6: Equilibrium bed levels around groynes G-1 & G-2

Distance from shank axis (m)	Bed levels (m+PWD)													
	Distance from T-axis (m)													
	200.00	150.00	100.00	50.00	0.00	-50.00	-100.00	200.00	150.00	100.00	50.00	0.00	-50.00	-100.00
	G-1							G-2						
150.00	8.50	2.50	2.00	1.50	7.50	15.30	14.90	0.50	-5.70	-8.90	-5.00	-9.70	3.00	3.70
100.00	9.70	1.80	-6.10	1.80	1.40	9.30	10.10	0.50	-7.30	-15.40	-3.70	11.70	4.50	5.50
50.00	8.20	1.20	-4.10	1.00	T-head axis	10.00	9.7	-2.50	-5.50	-14.00	1.80	T-head axis	5.50	5.90
0.00	8.50	0.50	-5.05	1.90		Shank axis		-3.00	-5.60	-10.50	0.50		Shank axis	
-50.00	7.50	2.50	-8.80	1.50		5.80	5.20	-0.40	-4.40	-9.50	0.50		5.90	6.00
-100.00	7.40	2.80	-11.70	-2.00	11.00	7.00	5.20	-2.50	-3.60	-8.00	0.50	10.50	3.50	4.20
-150.00	8.50	3.70	-5.05	-6.30	6.50	6.50	6.10	1.30	-3.70	-7.50	-8.10	3.00	3.10	4.10

(-) sign indicates distance from the shank axis in u/s direction and distance from the T-head axis towards the river bank

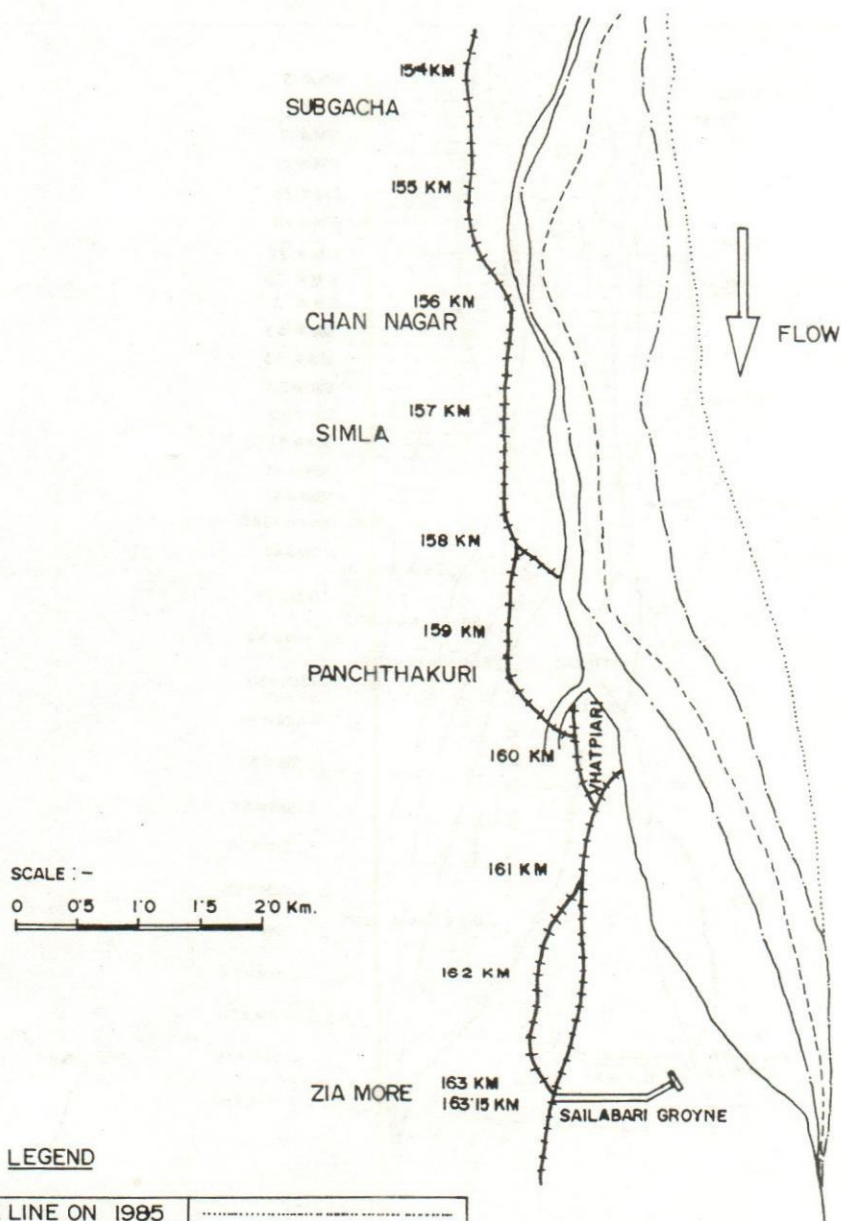
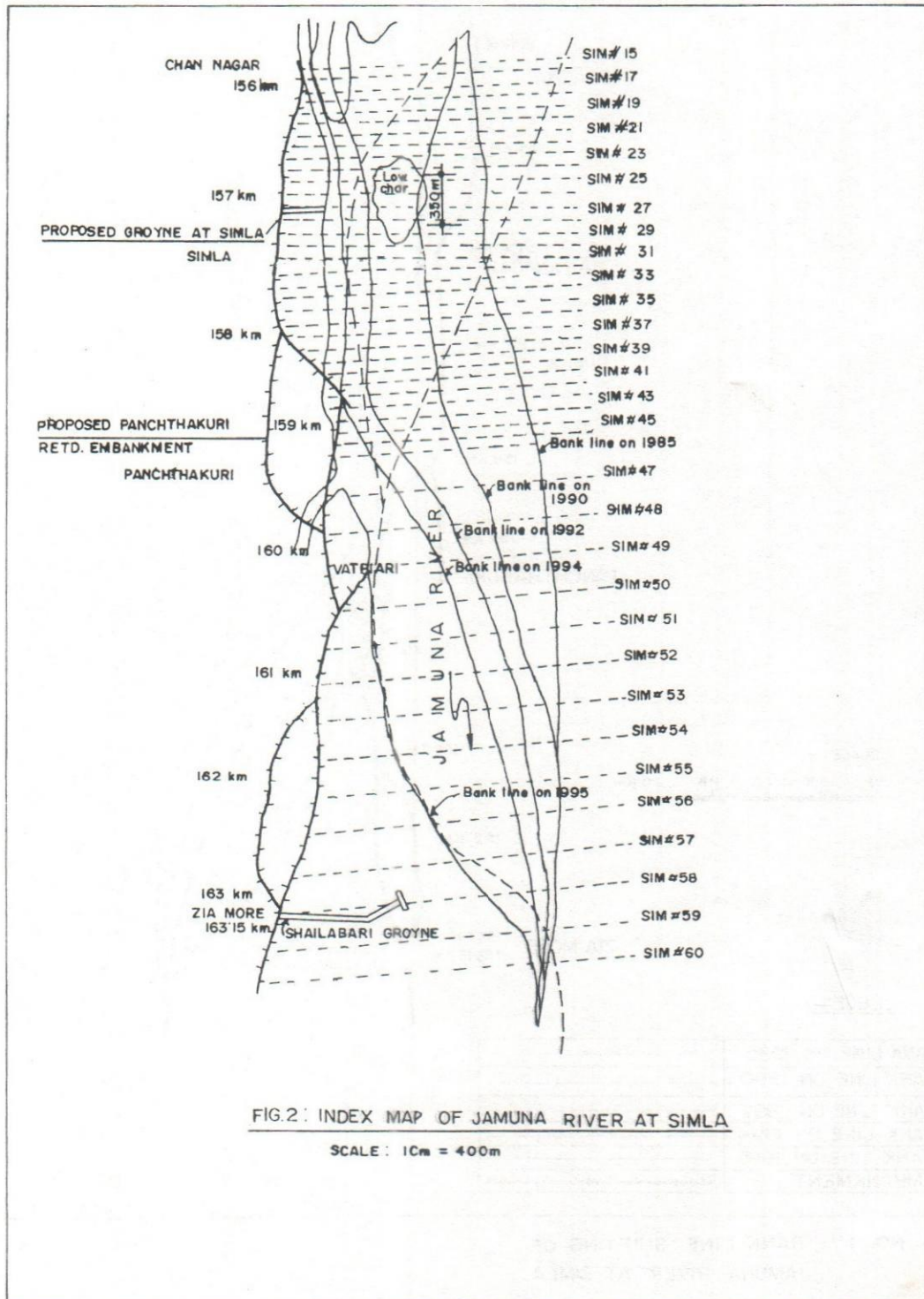
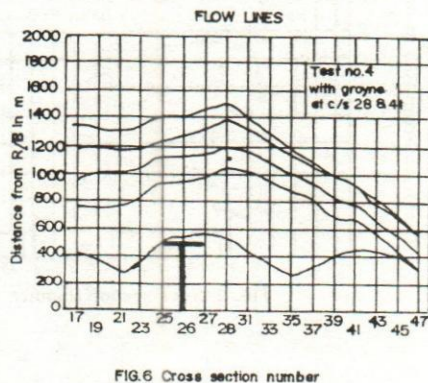
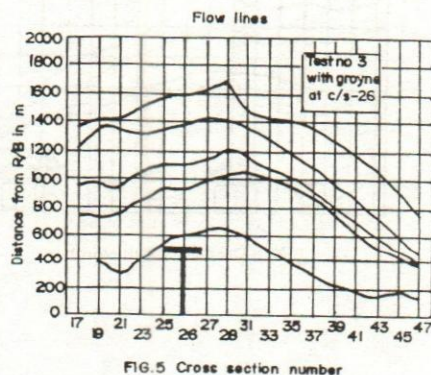
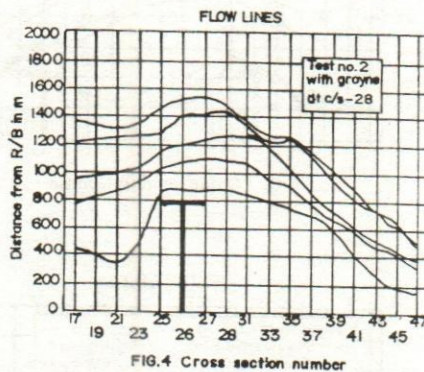
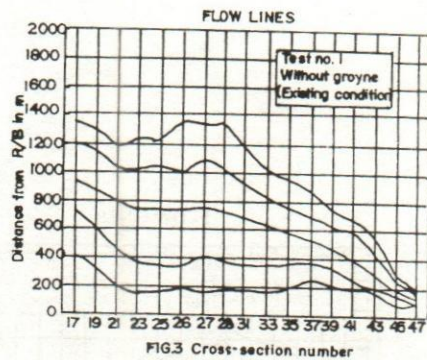


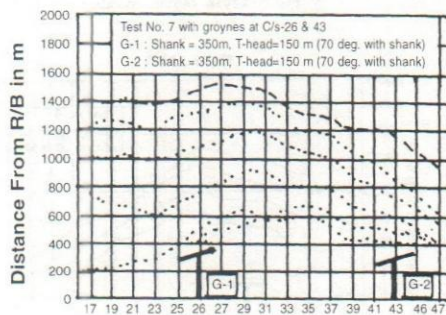
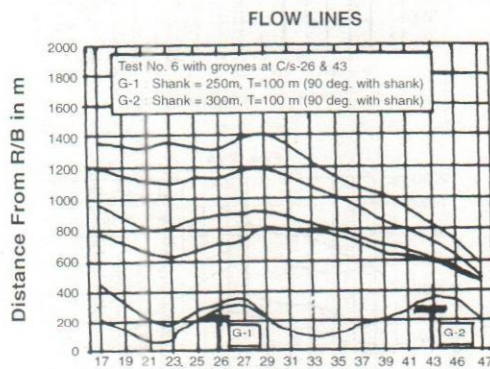
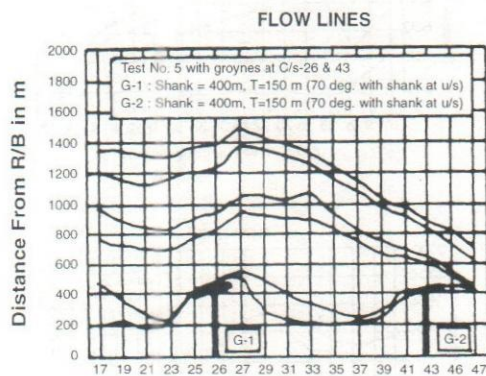
FIG. NO. 1 - BANK LINE SHIFTING OF  
JAMUNA RIVER AT SIMLA.











## Effects of Clay and Silt on the Strength Characteristics Of Different Types of Soil in Bangladesh

Mst. Anwara Jahan<sup>1</sup>

### Abstract

*This paper intends to evaluate the various established relationships between the physical and strength properties in terms of compressive strength and shear strength of different types of soil containing varying amount of clay and silt. Moreover, settlement behaviour of soil with other properties for varying percent of clay and silt content is described. Relationship between clay and silt with compressibility are outlined in brief. Various established equations and findings from different investigations are presented in concise form and their practical utility have been discussed.*

### Introduction

In designing the building, bridge, retaining wall, embankment, dam, barrage and road or air filled pavement, design engineers are concerned with the engineering properties of the different building materials and sub-soil over which the foundation of structure would be laid. Physical properties of soil in the fields vary from place to place due to geological formation and enhanced many uncertainties because the properties of soil differs from site to site.

Here the term 'Strength Characteristics' indicates only the compressive and shearing strength of soils of both cohesive and non-cohesive in nature. For foundation design, parameters related to settlement and shear strengths are most important factors which depends on content and distribution of soil ingredients in association with other physical properties.

So, for the safety of structures, the strength characteristics and the settlement behaviour of soil in foundation must be evaluated with great care. The strength characteristics and settlement behaviour of soil largely depends on the constituents of soil or particles nature in addition to the moisture content. There are certain harmful ingredients which may cause appreciable change in normal behaviour of soil. Silt is an ingredient which may have harmful effect on strength properties and compressibility as well as on stability of soil.

Foundation of structures on weak soil whose physical properties are not properly assessed may fail due to shear failure of the soil or due to excessive settlement.

---

<sup>1</sup>Scientific Officer, RRI, Faridpur.



The constituent and stratification of soil is quite different from place to place. Hence, their physical and engineering properties for foundation design must be evaluated.

An effort has been made to investigate the effect of silt and clay in varying amount with other factors such as moisture content in the soil on strength characteristics of soils.

In this paper relationship between compressive strength with other physical properties and shearing strength with other soil properties are evaluated with reference figures and relevant relationships established by various investigators.

### Soils of Bangladesh

Bangladesh forms a major portion of Bengal basin. Being located close to one of the world's major subduction fault in the north and a major transform fault in the east, the Bengal basin and its adjacent area form one of the most active tectonic regions of the world. Structural activity, primarily faulting has significantly influenced the quaternary geology (Morgan and McIntire, 1959).

The land scape of Bangladesh is mainly of a monotonous flat plain. From geological point of view, Bangladesh is located at the eastern part of Bengal basin which is an extremely flat delta consists primarily of a large alluvial basin floored with sediments deposited by three major rivers, the Ganges-Padma, the Brahmaputra-Jamuna and the Meghna and their tributaries and distributaries. Most of the part has been subsiding slowly due to tectonic forces responsible for building up the Himalays and other hilly areas. Due to the iso-static balance of the earth surface some regions have been uplifted e.g. Barind tract and some regions have a distinct trend to subside on the other hand e.g. Sylhet haor areas, Chalan beel, Faridpur beel etc.

The silt-clay materials is found extensively in Khulna district.

Distribution of soils in Bangladesh is complex and are usually heterogeneous both in vertical and horizontal direction. Soils consist of wide varieties of material ranging from gravel, poorly graded sand to silt and clay. In general there is a predominance of silt sized materials (Safiullah, 1994).

Simplified soil units of Bangladesh with their general characteristics (Safiullah, 1994 which was modified from Hunt, 1976) are shown in Table 1.

From engineering point of view, the classification of ingredients or constituents of soil is of utmost importance. Because different types of soil contain different ingredients in varying amount for which its properties varies.

Silt may be organic or inorganic. Inorganic fine grained soil shows little or no plasticity. Organic silt is a fine grained soil having more or less plastic properties. Inorganic clay is often misleading with clay for its smooth texture, but it may be readily distinguished



from clay without laboratory tests. The compressibility of organic silt is very high and permeability is low. Silt is the most unstable soil.

Table 1:

Soil Units	General Characteristics
Hill soils	Variable soil types which are function of underlying geology. Frequently sandy clays and clays grade into disintegrated rock at shallow depths.
Raised alluvial terrace deposits	Comprises a relatively homogeneous clay known as Modhupur clay and Barind clay. (LL= 30-80%, $I_p$ =12-50%. Variable depth underlain by fine to medium uniformly graded sand.
Himalayan Piedmont deposits	Mainly sandy silt in higher areas and silty clays in basin areas but often underlying fine sands at shallow depth.
Alluvial flood Plain deposits	Locally variable but in general silts and silty clays. Silt size predominant. (LL=20-50%, $I_p$ =4-30%). Fine sands abounds at depths and close to rivers. Contain mica.
Depression deposits	In the south alternating organic/clay deposits overlaying clay at depth. Elsewhere, predominantly silty clays and clays. (LL=30-40%, $I_p$ =10-16%).
Estuarine and flood plain deposits	Generally silt and silty clays. Acid sulphate soils found near coast. Organic soils close to surface in some places. Widely varies in consistency and water content.

(Source: Safiullah,1994) \*\* LL= Liquid Limit,  $I_p$  = Plasticity Index

In principle, clay is composed of particles which are colloidal in size. Clays generally are of medium to high plasticity, have considerable strength when dry, undergo extreme changes in moisture content. Clay have considerable strength in their natural state, but this strength is sharply reduced and sometimes completely destroyed when their natural structure is disturbed, i.e. when they are remolded.



## Methodology

Various equations and figures related to strength characteristics established by different investigators after performing specific soil tests are collated from different sources. Results and correlations between different soil properties are analysed and compared in short to come in a conclusion how these correlation equations can practically be used for foundation design.

### Relationship between strength and other soil properties

Compression Index ( $C_c$ ) can be related with the other properties of soil such as liquid limit, moisture content and initial void ratio.

Relationships with unconfined compression strengths ( $q_u$ ) against natural moisture content, shear strength of normally consolidated clay against effective overburden pressure are discussed.

### Compressibility:

Compressibility of the soil is of utmost importance to study the settlement behaviour of soil. The compressibility of soil depends upon many of the factors such as constituents with other physical properties.

The compressibility of the fine grained soils can be expressed by compression index,  $C_c$ , the slope of the virgin compression ( $e$ -log  $\sigma_v$ ) curve. Compression index has relationship with physical properties such as liquid limit, initial void ratio and natural moisture content.

Terzaghi and Peck (1967) found an empirical relationship between compression index and liquid limit of clay soil as

$$C_c = 0.009 (LL - 10\%)$$

Serajuddin (1970) suggested two empirical equations, for coastal zone soil of Bangladesh as

$$C_c = 0.50(e_0 - 0.50) \text{ \& } C_c = 0.0135(W - 20)$$

Where,  $C_c$  = Compression index,  $e_0$  = Initial void ratio and  $W$  = Moisture content

Plotting of compression index against initial void ratio and against natural moisture content yields two curves which is shown in Figure 1.

Analysis shows that the large portion of sub-soil consists of compressible silt-clay.

Compression index are plotted against liquid limit(LL) after experiment made by Terzaghi & Peck (1967), Skempton (1944) and Serajuddin & Alimuddin (1967) and shown in Figure 2 (source: Safiullah, 1994, ref Fig.6a). Compression index versus initial void ratio of the same soils have been plotted after experiment made by Nishida (1956), Serajuddin (1981), Serajuddin (1987) and Azzouz et. al. (1976) and shown in Figure 3 (source: Safiullah, 1994 ref. Fig.6b). For these soils  $C_c$  lies within 0.1 to 0.6. Most of the Bangladeshi soils have a  $C_c$  value ranging between 0.1 to 0.3.

Natural water contents of the major plastic clays and silts are generally less than closer to their liquid limits.

Compression Index ( $C_c$ ) determined from laboratory consolidation tests on Bangladeshi clays have been plotted against liquid limits(LL) and initial void ratios( $e_0$ ) and shown in Figures 4 & 5.

The two empirical equations are derived after Serajuddin & Alimuddin (1967) as follows:

$$C_c = 0.0078(LL - 14\%)$$

$$C_c = 0.44(e_0 - 0.30)$$

Correlations by Serajuddin (1987) made a study on the applicability of 'universal compression index' equation of Herrero (1980) to Bangladeshi plastic silts and clays and derived twelve equations. Some of them are as follows:

$$C_c = 0.2765 \left[ G_s \left( \frac{1 + e_0}{G_s} \right)^2 - 0.5171 \right]$$

$$C_c = 0.2625 e_0^{1.3678}$$

$$C_c = 0.4049(e_0 - 0.3216)$$

$$C_c = 0.0648 e^{0.382 wn}$$

Where,  $G_s$  = Specific gravity of soil,  $wn$  = Natural moisture content

These equations show the relationships between compressive index with initial void ratio and natural moisture content for plastic silts and clay. These relationships can be used for finding other soil properties.



### Compression strength as natural water content:

The compression,  $S$  of a confined stratum of normally loaded ordinary clay can be estimated from the relation:

$$S = H \frac{C_c}{1 + e_0} \log_{10} \frac{\rho_0 + \Delta \rho}{\rho_0}$$

Where,  $C_c/(1+e_0)$  is termed as the compression ratio,  $H$  is the thickness of the bed of clay under at pressure  $\rho_0$  and  $\Delta \rho$  is the pressure difference.

In order to evaluate the suitability of the clay material for a foundation it is necessary to determine its resistance to rupture under load and to determine its settlement characteristics. The shearing strength can be determined as one half of the unconfined compression strength (Serajuddin & Alimuddin, 1967). This value depends somewhat on the moisture content.

### Unconfined strength and penetration blows:

Penetration resistance in blows per foot (N-values) of the layers against unconfined compression strengths of cohesive samples obtained from the same layers has been correlated by Serajuddin and Alimuddin (1967) using Dhaka and Mymensingh clays and shown in Figure 6. This figure shows that the clay samples of medium to high plasticity follow a general trend instead of having been scattered and an unconfined compression strength of about 200 to 225 psi per blow per foot penetration would be a reasonable estimate (Serajuddin & Alimuddin, 1967).

It is well known that the influence of water on the behaviour of clay is tremendous. The unconfined strengths of clays under consideration vary widely in the range of about 1 to 44 psi and the natural water contents in the range of about 18 to 50 percent. The clays of north-west region have a general trend of higher unconfined strengths than those of any of the two regions while clays of the south-west region have a trend of low to very low unconfined compression strengths.

The unconfined compression strengths of the cohesive silt and clay soils range from about 1 psi to about 10 psi. This is not appreciable in the coastal areas for foundation and such soil is a problem for foundation engineers.

In some areas the silt-clay material is loose with low strength and in other areas it is fairly compact.

### Relationship between clay and silt with compressibility:

The values of compression index of different silt and clay soils increase consistently with increasing %clay (finer than 2 micron) as shown in Figures 7 to 9. The correlation may be defined by the equation:

$$C_c = 0.0088C_f + 0.128$$

The equation may be derived for %5 micron clay as follows:

$$C_c = 0.0034CI + 0.156$$

The correlation between ratio of %5 micron clay and % silt and compression index can be shown as follows:

$$C_c = 0.133 \text{ CI/S} + 0.19$$

Where, S = % silt, CI = %5 clay,  $C_f$  = %2 clay, CI/S = ratio of %5 micron clay and % silt.

Settlement of the strata may be determined from these equations without performing consolidation test.

### Relationship of Compression ratio with clay and silt:

Plotting of Compression ratio  $C_r/(1+e_0)$  and %2 micron clay, compression ratio and %5 micron clay and compression ratio and ratio of %5 micron clay and % silt yields three straight line relationships and shown in Figures 10 to 12. From these relationships, the values of compression ratio may be estimated only knowing the particle size.

### Shear strength:

The shearing strength can be estimated as one half of the unconfined compression strength. This value somewhat depends on the moisture content. Commonly, the shear strength of normally consolidated clays increases from zero rectilinearly with normal pressure and the curve passes through the origin.

The stability of the foundation structures built on soil depend upon the shearing resistance exerted by the soil along the probable surface of slippage.

The fundamental shear strength equation after Coulomb law is expressed as follows:

$$S = C + \sigma \tan \phi$$

Where, S = Shearing strength

C = Cohesion

$\phi$  = Angle of internal friction

$\sigma$  = Normal pressure



Skempton (1957) give a correlation for the undrained shear strength with the overburden pressure for normally consolidated clays which may be expressed as

$$S_u/P = 0.11 + 0.0037 (PI)$$

Where,  $S_u$  = Undrained shear strength of soil

$P$  = Effective overburden pressure

$PI$  = Plasticity index

$S_u/P$  = Undrained strength ratio

The Dhaka city clay is known to be overconsolidated because the undrained strength ratio values of 0.30 and 0.19 for isotropic and  $k_0$ -consolidated conditions respectively.

The low results of unconfined compression strengths and of  $\phi$  and  $c$  indicate that a large portion of the subsurface soil consists of a compressible silt-clay materials which in many locations is soft and poorly suited for supporting structures.

#### Evaluation of Undrained shear strength:

One of the major problems of design of earth structures in Bangladesh is evaluation of shear strength parameters for insitu soils. It is necessary to develop empirical relationships for undrained strength with index soil properties. Stress ratio  $S_u/\sigma'_c$  is plotted against plasticity index for soils of varying overconsolidation ratios comprising of nine different locations in Bangladesh and shown in Figure 13.

#### Discussions

It is observed that compressibility of natural soil deposit largely depends upon the silt/moisture ratio and the relationship can fairly be expressed quantitatively.

From population histogram of unconfined compressive strength and silt/moisture ratio, it is evident that maximum unconfined compression strength values occurred within the range of values for silt/moisture ratio of 2.0 to 2.5.

Initial void ratio ranges from 0.75 to 2.2 and compression index from about 0.1 to 1.28 in coastal areas in Bangladesh. The compression index on the average is quite high and the settlement of structures founded on such soils may be considerable depending upon structure dimensions, thickness of the silt-clay layer and depth of structure. The compression index of silt-clay soil is generally dependent upon the initial void ratio and so also upon natural moisture content in the saturated condition.

Skempton (1948) suggested that in normally consolidated clays, the rate of increase in shear strength with effective overburden pressure depends on the type of clay in terms of liquid limit or plasticity index.



Terzaghi and Peck have suggested that for normally consolidated clays of medium or low sensitivity there exists a close relationship between liquid limit and field compression index.

Using the figures and equations plausible correlations can be made between regional soils and if some properties are known, the other parameters for foundation design can be estimated easily. Compressive index for different zones are better correlated and the trend of the curves are somewhat homogeneous. Standard ranges of the tolerable parameters are mentioned in various text books and the findings for Bangladeshi soils are compared and the deviations can be better predicted by evaluating the equations and curves.

#### Steps to be followed in evaluating the soil:

1. Moisture content and liquid limit is to be known to estimate either the soil is preloaded.
2. The unconfined compressive strength should be estimated from different correlations.
3. Initial void ratio can be estimated by multiplying the natural moisture content by a factor 2.7 assuming the soil is totally saturated and the compression index may be determined and also amount of settlement can be determined.

4. Time for settlement can be determined from the equation:

$$t = T_v / C_v H^2$$

Where,  $t$  = Time required to reach a certain percentage of primary consolidation

$T_v$  = Time factor coefficient dependent on percentage of consolidation,

$C_v$  = Volume of compression and  $H$  = thickness of layer

5. Approximate overburden pressure should be estimated.

#### Conclusions

This paper is expected to give quick general idea to the engineers and designers dealing with soils as construction and foundation materials.

A number of correlations between compressive strength and other soil properties were made by various investigators. Of them, only a few were collated and presented. Detailed criticism were not done despite their uses. Only they are discussed in concise form enabling to the designers for preliminary guidelines. The designers can only verify the results with them.



Relationship between undrained shear strength with effective overburden pressure may be established to find out the resistance to rupture.

Compressive index, actually is described in equation forms. The equations indicate so far that compression index of the fine grained soils of Bangladesh can be better correlated to initial void ratio or natural moisture content than liquid limit. Knowing particle size, some equation also gives settlement behaviour, and as such expensive consolidation test can be avoided.

## References

1. Alimuddin, A.(1991) Effect of particle sizes of clay and silt on the compressibility and consolidation characteristics, Technical Journal, RRI, pp 43-53.
2. Azzouz, A.S., Frizek, R.J. and Corotis, R.B. (1976) Regression analysis of soil compressibility, Soils and Foundations, (16),2, 19-29.
3. Das, B.M. (1987) Advanced soil mechanics, New Delhi, India.
4. Flemming, N.L. and D.M. James (1990) Stress-deformation characteristics of Alaskan silt. Published in the Journal of Geotechnical Engineering, ASCE, Vol 116 NO.3, ISSN 0733-9410, pp 377-393.
5. Herrero, D.R.(1980) Universal compression index, Journal of Geotechnical Engineering, ASCE, (196),11,1179-1200.
6. Hunt, T.(1976) Some Geotechnical aspects of road construction in Bangladesh, Geotechnical Engineering, (7),1, 1-33.
7. Lambe, T.W.(1960) Soil Testing for Engineers, John Wiley and Sons Inc., USA.
8. Morgan, J.P. and McIntire, W.G. (1954) Quarternary Geology of the Bengal Basin, East Pakistan and India, Bulletin of the Geological Soc. of America, (70), 319-342.
9. Murthy, V.N.S.(1993) Soil Mechanics and Foundation Engineering in SI Units, Fourth edition, Newdelhi, India.
10. Nishida, Y. (1956) A brief note on compression index of soil, Journal of SMFED, ASCE, (82), SM3, 1027-1 to 1027-14.
11. Punmia, B.C.(1987) Soil mechanics & Foundations, Newdelhi, India.
12. Safiullah, A.M.M.(1994) Some geotechnical aspects of Bangladeshi soils, IEB, Bangladesh.

13. Serajuddin(1964) Correlation of some engineering properties of sub-surface soils occurring in the coastal embankment project area of Khulna district, Hydraulic Research Laboratory, EPWAPDA, East Pakistan.
14. Serajuddin, M. & Alimuddin, A. (1967) Engineering properties of soils in East Pakistan, *The Pakistan Engineer*, (7), 11, 869-892.
15. Serajuddin, M. (1970) A study of the engineering aspects of soils of coastal embankment project area in East Pakistan, Institute of Engineers, East Pakistan.
16. Serajuddin, M. (1987) Unconfined compression index equation and Bangladeshi soils, *Proc. 9th SEAGC*, 1, 5-61.
17. Skempton, A.W. (1944) Notes on the compressibility of clays, *Quarterly J. of Geol. Soc.*, London (100), 119-135.
18. Skempton, A.W. (1948) Vane tests in the alluvial plane of the river forth near Grangemouth, *Geotechnique*, Vol 1,2.
19. Skempton, A.W. (1957) Discussion on the planning and design of the New Hong Kong Airport, *Proc. ICE*, Vol 7, pp 306.
20. Terzaghi, K. & Peck, R.B. (1967) Soil mechanics in engineering practice, 2nd edition, John Wiley & Sons, Inc. New York.



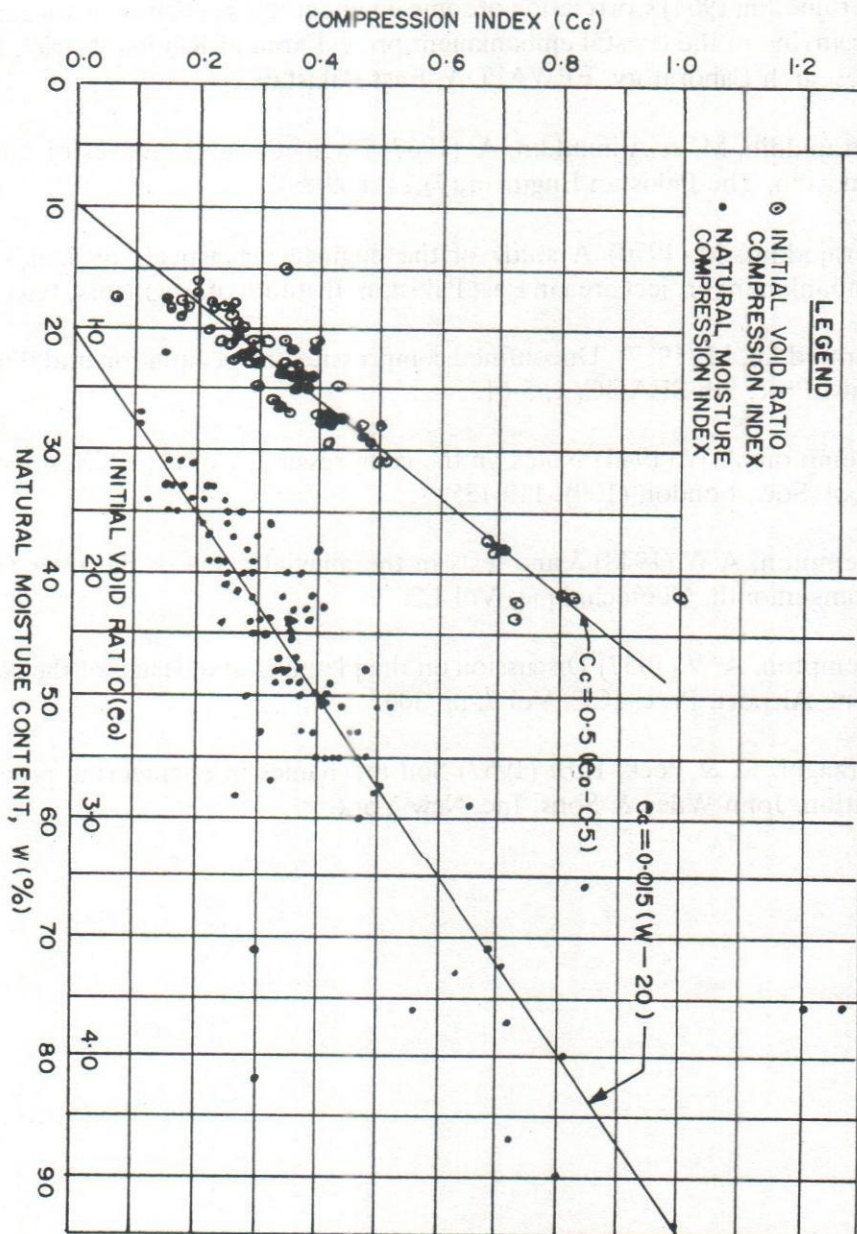


FIG.1 : CORRELATION OF COMPRESSION INDEX WITH INITIAL VOID RATIO AND NATURAL MOISTURE CONTENT

( SOURCE : SERAJUDDIN, 1969 )

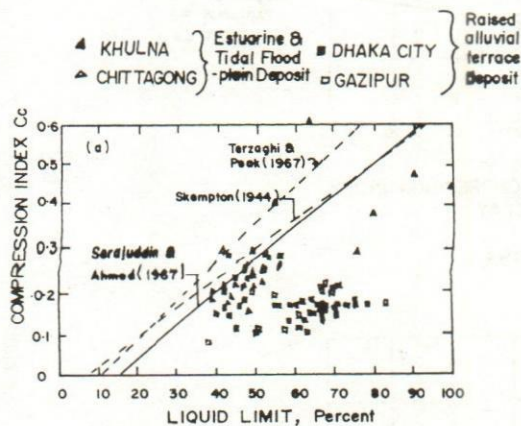


FIG. 2 : COMPRESSION INDEX Vs. LIQUID LIMIT FOR FINE GRAINED SOILS

( SOURCE : SHAFIULLAH, 1994 )

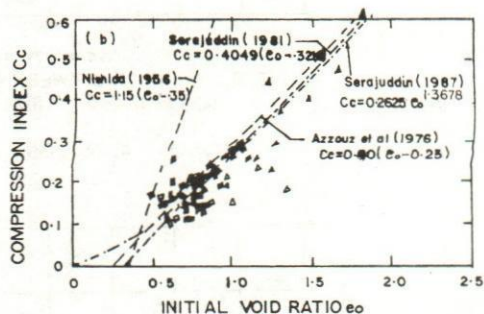


FIG. 3 : COMPRESSION INDEX Vs. INITIAL VOID RATIO RELATIONS FOR FINE GRAINED SOILS

( SOURCE : SHAFIULLAH, 1994 )

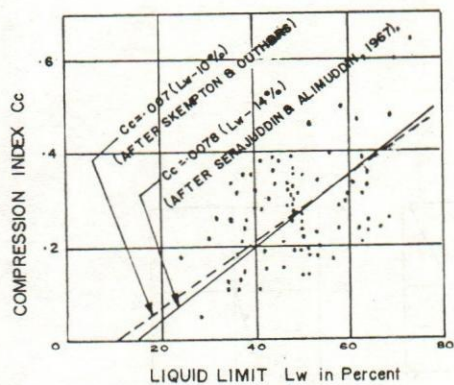


FIG. 4 : LABORATORY COMPRESSION INDEX Vs. LIQUID LIMIT

( SOURCE : SERAJUDDIN & ALIMUDDIN )

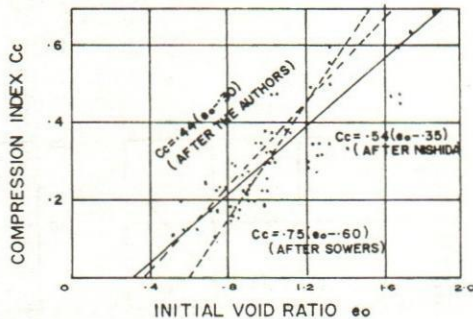


FIG. 5 : LABORATORY COMPRESSION INDEX Vs. INITIAL VOID RATIO

( SOURCE : SERAJUDDIN & ALIMUDDIN )

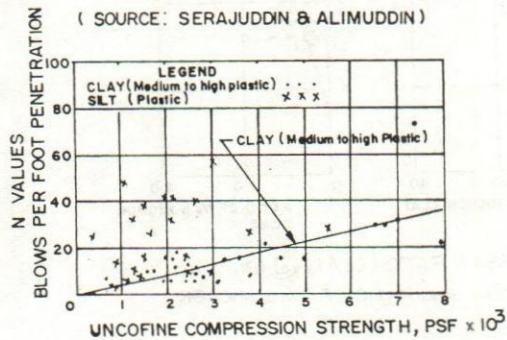


FIG. 6 : UNCONFINED COMPRESSION STRENGTH Vs. PENETRATION BLOWS OF DHAKA AND MYMENSINGH CLAYS

( SOURCE : SERAJUDDIN & ALIMUDDIN )

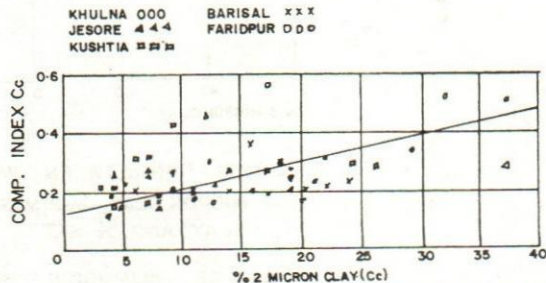


FIG. 7 : RELATION BETWEEN COMPRESSION INDEX (Cc) AND % 2 MICRON CLAY

( SOURCE : ALIMUDDIN, 1994 )



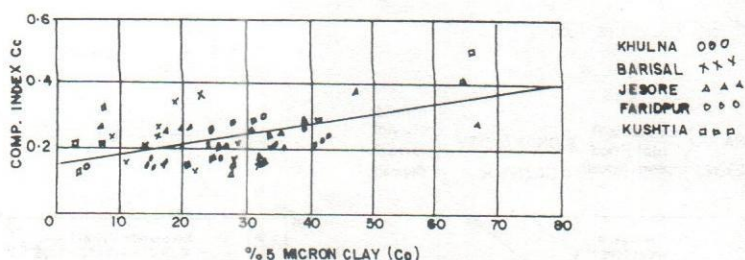


FIG. 8 : RELATION BETWEEN COMPRESSION INDEX (Cc) AND % 5 MICRON CLAY

( SOURCE : ALIMUDDIN, 1994 )

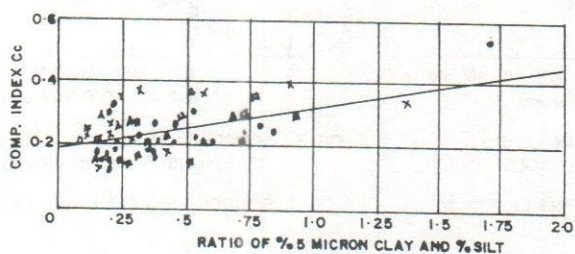


FIG. 9 : RELATION BETWEEN COMPRESSION INDEX (Cc) AND RATIO OF % 5 MICRON CLAY AND % SILT ( 74 MICRON )

( SOURCE : ALIMUDDIN, 1994 )

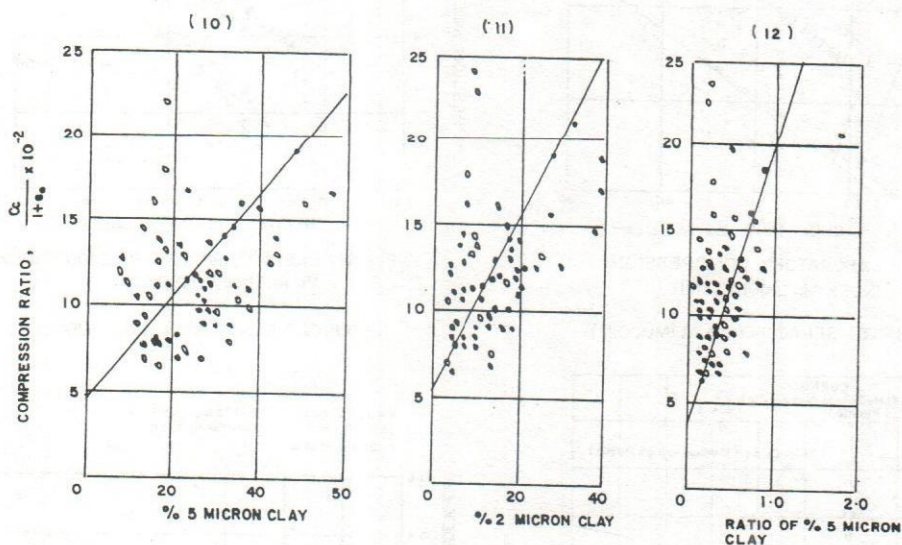


FIG. 10-12 : RELATION BETWEEN COMPRESSION RATIO (  $C_c / (1+e_o)$  ) AND % 5 MICRON CLAY, % 2 MICRON CLAY AND RATIO OF % 5 MICRON CLAY AND % SILT

( SOURCE : ALIMUDDIN, 1994 )

LEGEND

NO	LOCATION	WL (%)	Ip (%)	SOIL TYPE	CLAY
1	KOYRA	44	21	CL	18
2	SARANKHOLA	39	13	ML	15
3	KALAPARA	45	19	CL	18
4	GALACHIPA	36	6	ML	9
5	CHARFASSON	40	14	ML	14
6	CHARMADRAJ	33	4	ML	9
7	MOGNAMA	45	20	CL	15
8	ANWARA	42	15	ML	27
9	HATIA	41	16	CL	16

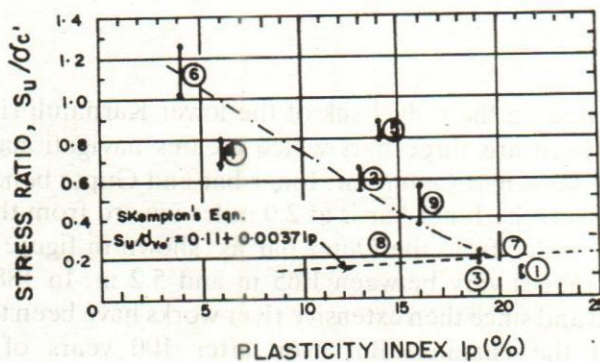


FIG. 13 : UNDRAINED SHEAR STRENGTH RATIO ( $S_u/\sigma'_{vc}$ ) ON RECOMPRESSION AGAINST PLASTICITY INDEX FOR NINE COASTAL SOILS

( SOURCE : SHAFIULLAH, 1994 )



## The Karnafuli River and It's Navigational Facilities For The Chittagong Port

Md. Lutfor Rahman<sup>1</sup>

### Abstract

*Bangladesh is a riverine country. Some of it's rivers are non-tidal and some of others are tidal. The Karnafuli river is a tidal one. This paper concerns the navigational facilities of the Karnafuli river for the Chittagong port. Hydrographic river charts of the river Karnafuli from Patenga to Kalurghat bridge is collected for the year 1982, 1984, 1986 and 1987 to conduct the present study. The length of the study reaches is about 30 km and is divided into fifty-nine equal sections at 500 m interval starting from Kalurghat bridge. The water depth at every sections are plotted on plain papers for different years and the widths for 5.5 m & 7.0 m drafts are then pointed out from the study of the plotted cross-sections along the length. The available hydrographic river charts are arranged in a systematic way so that the consecutive years of 1987 & 1986 are available for the reach between Kalurghat bridge to Sadarghat & Gupta bend to Patenga; for the year 1986 & 1984 from Sadarghat to Port jetties; and for the year 1986 & 1982 from the Port jetties to Gupta bend. A constriction exists in the Inner bar area. Care is needed so that widths do not reduce further due to siltation and bank shifting at this reach.*

### Introduction

Chittagong port is situated on the right bank of the lower Karnafuli river about 16 km from the sea-mouth. There are three bars which creates navigational hazards at the present time. These are known as Outer bar, Inner bar and Gupta bend. The Outer bar is at the mouth of the river, the Inner bar is at 2.0 miles inward from the Outer bar and the Gupta bar is at 7.4 miles from the Outer bar as shown in figure-1. The tides are semi-diurnal type and ranges vary between 1.65 m and 5.2 m. In 1888, the first port commission was formed and since then extensive river works have been taken to maintain the present course of the channel. But even after 100 years of commissioning, navigational lane width is not been to be fixed up for economical maintenance of the port channel and proper future expansion.

---

<sup>1</sup>Senior Scientific Officer, RRI, Faridpur.

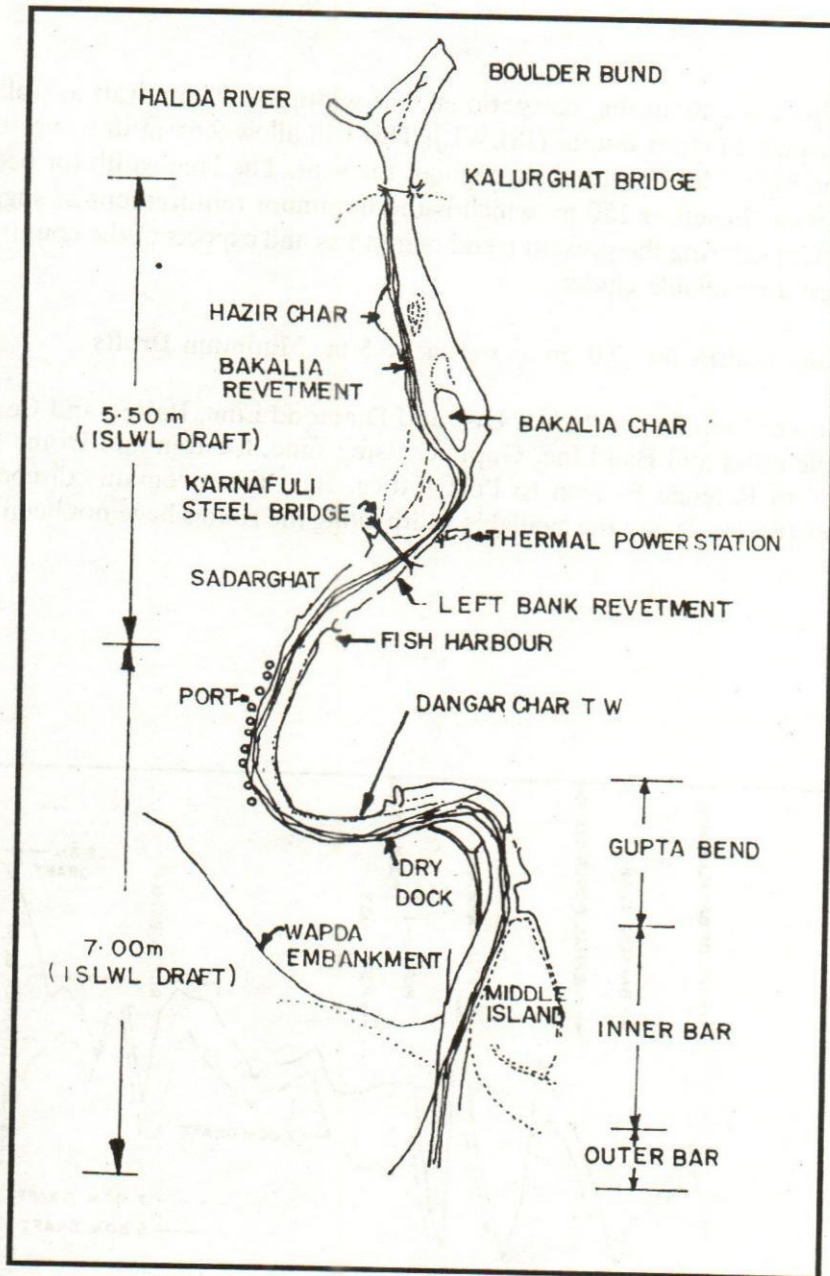


Figure-1: The Karnafuli River



This paper discusses about the navigational lane width for 7.0 m draft as well as 5.5 m draft with respect to chart datum (ISLWL). This will allow 9.65 m draft vessels to call at 95% of the high tide conditions throughout the year. The lane width for ocean going vessels has been chosen as 150 m which is the minimum requirement as suggested by NEI (1978). Considering the present trend of imports and exports of the country this can be considered a reasonable choice.

### Available Lane Widths for 7.0 m as well as 5.5 m Minimum Drafts

Few well named shipping routes like Disc and Diamond Line, Batten and Central Path Line, Triangle cross and Ball Line, Gupta crossing Line, Custom and Dome Line exist at present from Patenga Beacon to Port Jetties. But there remain discontinuity at certain places (figure-2) and the available width along the routes have not been specified.

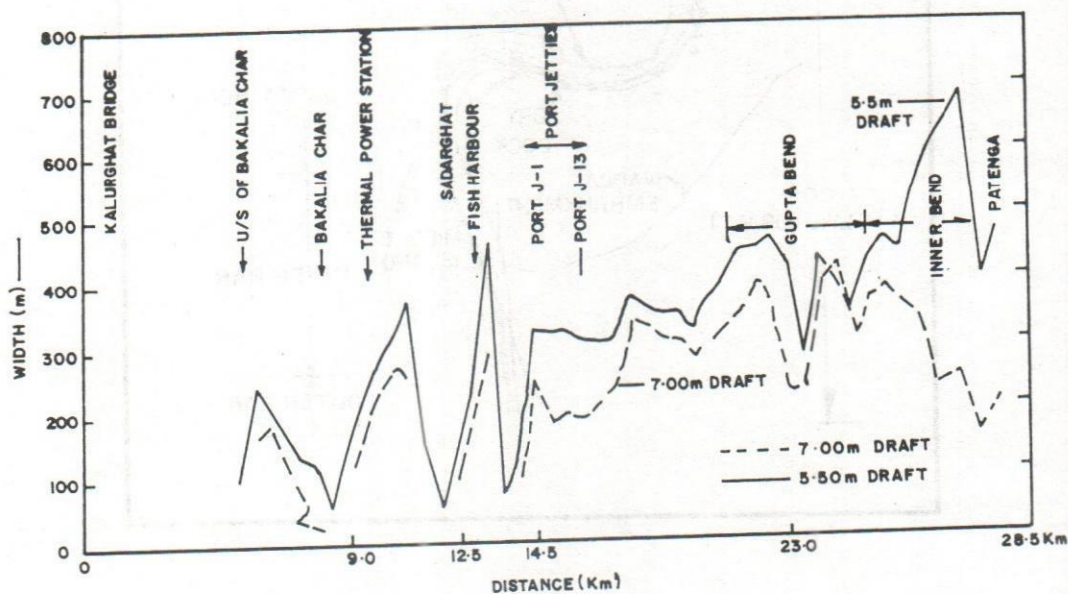


Figure-2: Longitudinal variation of widths for 5.5 m drafts and 7.0 m drafts

The navigational lane widths, therefore, have been set out in incorporating these established routes identifying the thalweg line along the channel. The upper limit of the alignment for 7.0 m draft has been extended upto the present Jetty no. 1. Beyond this point upto thermal power station, the reach is extensively used by inland marine vessels and fishing trawlers. The alignment has, therefore, been set out for this reach 5.5 m (ISLWL) draft. A steel bridge also exist at about 3.0 km upstream of Jetty no. 1 whose deck is only 15 m above the high water and thus restricts vessels having draft grater than 5.5 m draft.

In finding the existing lane widths for minimum drafts 7.0 m & 5.5 m (ISLWL), horizontal lines are drawn at these depth on the cross - sectional profiles and are plotted at 500 m intervals. From the figure, it is apparent that 150 m minimum lane width for 7.0 m minimum draft is available almost all along the channel from patenga beacon upto port jetty No. 1. A slight constriction exists in the inner bar area but this is not very alarming. A dredging is required for about 1.75 km length for 150 m minimum navigation lane width. However from jetty No. 1 upto the thermal power station (20 km downstream of kalurghat bridge) minimum 150 m lane width for draft of 5.5 m is avilable except at upstream of Jetty No. 1 and Sadarghat. The total distance of approximately 3.0 km reach length (1 km at port jetty No.1 and 2 km at Sadarghat) needs widening at these two stations.

### Discussions

This study has revealed that the conditions of the Karnafuli river for 7.0 m draft are satisfactory for navigable lane upto 150 m . A widening at Gupta bend both at the right and left bank is required for easy access. The condition at the Gupta bend is not very much unfavourable. The bend radius is 976 m. which is just 24 m short of the allowable value and can be ignored.

However, serious bank erosions exist at the opposite bank to port all through the channel. These eroded materials are causing siltation problems on the left bank of Gupta bend and downstream of it at the Inner bar and Outer bar. The problems need immediate attention and delay may cause shifting of the alignment of deep water channel by creating shoals and bars and endanger the navigation of the port.

### Conclusions

The following conclusions may be made from the present study :

- a) A 150 m wide navigational lane widths for 7.0 m minimum draft (ISLWL) is easily possible with minimal dredging works in the Karnafuli river.
- b) Serious bank erosion exist on the left bank of the Karnafuli throughout it's navigation route from Kalurghat bridge to Patenga beacon. This should be immediately checked by bank protection works like revetments etc. Otherwise the river may shift and create



further siltation problem.

c) The river reach at the Gupta bend area need careful river training and bank protection works both against scour and siltation. Continuous dredging by water jets may be helpful in this respect.

d) The present condition at inner bar is not unsatisfactory. But further shoaling and siltation may cause choking and deterioration of the navigation channel. Adequate bank protection revetment both at the upstream and downstream of the reach may be helpful in establishing the stability.

e) Extension of the navigation route from Jetty no.1 to up to kalurghat bridge for 5.5 m draft (above the existing port jetties) needs of dredging works. However, this extension should be based on proper economic justification.

### Acknowledgement

The author gratefully acknowledge the help of the hydrographic survey department of the Chittagong Port Authority (CPA) for supplying river charts needed for the study.

### References

1. Alam, M.K and Rahman, Md. Lutfor; Master Alignment for Chittagong Harbour, The Journal of NOAMI, International Scientific Series Number (ISSN)- 1027-2119, Vol. 12, No. 1 &2, December 1995.
2. BRTC, 1987, Final Report, Mathematical Model study of the river Karnafuli, 1987, Chittagong Port Authority, prepared by the Dept. of Water Resources Engineering and Bureau of Research, Testing and Consultation, Bangladesh University of Engineering & Technology, Dhaka.
3. BRTC, 1986, Final Report, Mathematical Model study of the river Karnafuli, 1986, Chittagong Port Authority, prepared by the Dept. of Water Resources Engineering and Bureau of Research, Testing and Consultation, Bangladesh University of Engineering & Technology, Dhaka.
4. CPA, 1986, Hydraugraphic River Charts from Chittagong Port Authority, 1986, Chittagong, Bangladesh
5. CPA, 1984, Hydraugraphic River Charts from Chittagong Port Authority, 1984, Chittagong, Bangladesh
6. CPA, 1982, Hydraugraphic River Charts from Chittagong Port Authority, 1982, Chittagong, Bangladesh

7. CPA, 1985, Year Book, Chittagong Port Authority, 1985, Chittagong, Bangladesh.
8. CPA, 1982, Year Book, Chittagong Port Authority, 1982, Chittagong, Bangladesh.
9. HRS, 1960, Report on Model Investigation, Part-1, Karnafuli river, Hydraulics Research Station, Wallingford, Berkshire, U.K.
10. Rahman, Md. Lutfor; Study on Master Alignment of Chittagong Port from Patenga to Kalurghat Bridge, M.Engg. Thesis, Dept. of Water Resources Engineering, BUET, Dhaka.

### Abbreviation

BIWTC	-	Bangladesh Inland Water Transport Corporation
BRTC	-	Bureau of Research ,Testing and Consultations
BUET	-	Bangladesh University of Engineering & Technology
CPA	-	Chittagong Port Authority
HRS	-	Hydraulic Research Station
ISLWL	-	Indian Spring Low Water Level
IWTA	-	Inland Water Transport Authority
NEI	-	Netherlands Economic Institute



## Importance of Using Cone Penetration Test In Solving The Problems Associated With Standard Penetration Test

Md. Hanif Mazumder<sup>1</sup>

Engr. Md. Matiar Rahman Mondol<sup>2</sup>

### Abstract

*The standard Penetration Test (SPT) is performed to determine the resistance of soil to the penetration of a standard size sampler, in order to obtain a rough estimate of the properties of soil in situ. Attempts have been made to relate N (SPT) values to shear strength parameters, bearing capacity, soil density, state of compaction, as well as relating N-values to the performance of structures. It is known that a number of problems exist with the use of SPT results rendering strength of available correlation questionable. In saturated, fine or silty, dense or very dense sands, the N-values may be abnormally great because of the tendency of such materials to dilate during shear under undrained conditions.*

*The cone penetration test (CPT) is an indispensable tool in the site investigations which consists of pushing the cone into the soil by the rod at a slow rate and measuring penetration resistance on the cone and frictional resistance on a friction sleeve. The CPT is the only available routine investigation technique that provides an accurate continuous profile of soil stratification. In this paper the problems connecting with the SPT are highlighted and it is advocated to use CPT.*

---

<sup>1</sup>Principal Scientific Officer, RRI, Faridpur.

<sup>2</sup>Scientific Officer, RRI, Faridpur.

## Scope of Standard Penetration Test

Standard penetration test is made by making use of a split spoon sampler. The method of carrying out the test is as follows :

The split spoon sampler is connected to a string of drill rods and is lowered into the bottom of the bore hole which was drilled and cleaned in advance. The sampler is driven into the soil strata by making use of drop weight weighing 140 lb. The weight is allowed to fall freely from a height of 30" (760 mm) on to an anvil fixed on the top of the drill rod. The number of blows required to penetrate every successively 6" into the strata upto a maximum total depth of 24" is countered. The number of blows required to penetrate 6" to 18" depth is termed as SPT value or N-value. The SPT is normally conducted at 5' interval. During the test with most soils, some form of disturbed sample can be obtained and this sample will be useful for identification and descriptive purpose.

## Problems Associated with SPT

In saturated, fine or silty, dense or very dense sands, the N-values may be abnormally great because of the tendency of such materials to dilate during shear under undrained conditions. Hence, in such soils, the results of standard penetration tests should be interpreted conservatively.

In addition, the values of N in cohesionless soils is influenced to some extent by the depth at which the test is made. Because of the greater confinement caused by increasing overburden pressure N-values at increasing depths may indicate larger relative densities than actually exist.

By far the most common error in connection with the standard penetration test in sand or silt occurs, however, when drilling is being done below the water table. If the water level in the drill hole is allowed to drop below ground-water level, as may easily occur, for instance where the drill rods are removed rapidly, an upward hydraulic gradient is created in the sand beneath the drill hole. Consequently, the sand may become quick and its relative density may be greatly reduced. The N-value will accordingly be much lower than that corresponding to the relative density of the undisturbed sand. Care is required to see that the water level in the drill hole is always maintained at or slightly above that corresponding to the piezometric level at the bottom of the hole. Use of the plugged, hollow-stem auger as a means for drilling in cohesionless soils below water table almost inevitably leads to alteration of the relative density; hence, N-values determined under these circumstances should not be relied on.

In deposits containing many boulders the results of the standard penetration tests may be unreliable because of the small size of the sampling spoon compared to that of the boulders.



In highly sensitive clays the standard penetration test may lead to a gross misconception of the consistency. Moreover, it is far too crude a test to justify its use for even approximating numerical values representing the strength of soft or very soft saturated clays. The ease of penetration of the sampler depends not only on the strength of the soil but also on its compressibility. Thus a strong cohesive soil with a high air content may have a substantially lower N-value than an equally strong saturated soil in which the voids cannot collapse as the sampler advances.

### Scope of Cone Penetration Test

The Cone Penetration Test (CPT), the indispensable tool in the site investigation consists of pushing into the soil, at a sufficiently slow rate, a series of cylindrical rods with a cone at the base and measuring in a continuous manner or at selected depth intervals the penetration resistance on the cone and, if required, the total penetration resistance and/or the local side friction resistance on a friction sleeve. In addition, the pore-water pressure present at the interface between penetrometer tip and soil can be measured during penetration by means of a pressure sensor in the cone. This pore-water pressure includes the pore-water pressure increase or decrease due to compression and dilation of the saturated soil around the cone arising from the penetration of the cone and the push rods into the ground.

Cone penetration tests are performed in order to obtain data on one or more of the following subjects :

1. The stratigraphy of the layers and their homogeneity over the site.
2. The depth to firm layers, the location of cavities, voids and other discontinuities.
3. Soil identification.
4. Mechanical soil characteristics.
5. Drive ability and bearing capacity of piles.

### Optimum Use of CPT in Investigation

To get the most out of soil Borings, it will generally be favourable to start the investigation with some exploratory CPT's across the site. The following example illustrates the importance of the CPT in the case of non-homogeneous soil profiles. In one investigation (carried out in the North Sea) a clay layer of about 0.5 m thickness within a sand layer was not discovered by sampling but showed up clearly in CPT results. Only after repeated attempts in new boreholes it was possible to also obtain samples from this layer. In other cases a layer of soft sandy silt may be encountered from which



only very disturbed samples, if any, can be obtained. In this case the importance of the CPT results increases and it would be favourable to increase the number of CPT's.

In sand layers undisturbed samples can not be obtained and the results of the CPT's are very helpful for estimating the in situ density of the sand. This is essential information when preparing laboratory tests on recompacted soil. For clays the undrained shear strength computed from CPT results together with the on board shear strength and density determinations on samples are routinely used for estimating in situ effective stresses and preconsolidation pressure (Andresen et al., 1979). These parameters are used for setting up test programs for triaxial, simple shear and oedometer test.

### Analysis of Data for Foundation Design

Many theories have been developed to relate the cone bearing  $q_c$  to the shear strength of the soil, i.e.  $\Phi$  in sands and  $s_u$  in clays. Complete summaries of the available methods were presented by Schmertmann (1975) and by Mitchell and Lunne (1978), to which reference is made for further information. Further advances in shear strength can be expected with the measurement of pore pressure during the penetrometer test.

### Undrained Shear Strength of Clay from Cone Resistance

Derivation of the undrained shear strength from CPT results is done either theoretically or by means of evaluated empirical correlations.

The available theories for determining undrained shear strength from CPT's can be divided into three groups :

- (i) bearing capacity solution (eg. Meyerhof. 1961) ;
- (ii) cavity expansion approach (eg. Vesic. 1975) ;
- (iii) steady penetration solution which combines the two previous approaches (Baligh 1975)

All these theories relate the cone penetration resistance,  $q_c$ , to the undrained shear strength,  $s_u$ , in the following manner :

$$q_c = N_k s_u + P$$

Where  $N_k$  = the bearing capacity number or cone factor  
 $s_u$  = undrained shear strength

$P$  = an expression of total overburden pressure.



The contribution of total overburden pressure ( $P$ ) has been interpreted as either the in situ vertical stress,  $P_o$ , or the in situ horizontal stress,  $\sigma_{ho}$ , or the in situ octahedral stress  $\sigma_{oct} = 1/3(p_o + 2\sigma_{ho})$ . Baligh et al. (1980) summarize the different theories and associated cone factors proposed in the literature.

### Drained Shear Strength of Sand

Several theories and empirical or semi-empirical correlations for the interpretation of cone resistance in sands have been published. Mitchell and Lunne (1978) compared some of the methods for obtaining the friction angle of sands and applied them to results of CPT's carried out in the North Sea and at several locations on land. They concluded that the methods suggested by Janbu and Senneset (1974), Meyerhof (1975), and Schmertmann (1975) gave the most consistent results and lend themselves best to practical applications.

### Deformation Characteristics of Sand

The cone penetration resistance of a sand is a complex function of its strength and deformation properties. Many attempts have been made to establish empirical correlations between cone resistance and deformation modulus,  $M$ . Mitchel and Gardner (1975), made a comprehensive review of the correlations developed for sands. Most of the correlations take the form  $M = \alpha q_c$ .

Where,  $M$  is the constrained modulus. The proportionality factor,  $\alpha$ , in the more recent recommendations varies between 1.5 and 4 in most cases.

### Pile Bearing Capacity

Determination of pile capacity from the CPT is one of the earliest application of the cone test. An empirical correlation for end bearing was established in Holland (Heijnen 1974) of which the validity was confirmed by other investigations (Schmertmann 1975). Nottingham (1975) developed correlation factors to determine the capacity of friction piles from the side friction of the penetrometer (Schmertmann 1975). The only recent development in the calculation of pile capacity has been the introduction of a correlation for over consolidation and gradation in cohesionless materials (Te Kanp 1977). The method is based on the result of a number of pile load tests in Holland in high  $q_c$ , over consolidated sand (Beringen et. al 1979).

## Conclusion

In comparison with the SPT, the ease and economy with which the CPT can be performed would make it be preferred method of soil investigation, provided that the results of the CPT could be conveniently interpreted and practically applied.

In River Research Institute, Faridpur, an attempt has been made to perform a research work on "The Strength Characteristics of Soils of Flood-Plain Zone with Special Reference to Faridpur Areas on the Basis of Some In situ Tests and Laboratory Shear Tests". Although initially the work is limited to Faridpur area this would be extended to other areas of Bangladesh. Distribution of soils in Bangladesh is complex and are usually heterogeneous both in vertical and horizontal direction. Soils consist of wide varieties of material ranging from gravel, poorly graded sand to silt and clay. In general there is a predominance of silt sized materials. It is already known from the previous discussions that a number of problems exist with the use of SPT results rendering strength of available correlation questionable. The CPT has proved valuable for soil profiling, as the soil type can be identified from the combined measurement of end resistance and side friction. The test lends itself furthermore for the derivation of normal soil properties, such as density, friction angle and cohesion. Various theories have been developed in the course of time and continued research in this direction is adding to the usefulness of the CPT for foundation design. So it is clear and wise decision that other method of field test i.e. CPT using International Reference Test Procedure (ICSMFE) should be used as additional correlation factors for Bangladeshi soils.

## Acknowledgement

The authors wish to express their thanks to Dr. A.M.M. Safiullah, Professor of Civil Engineering Dept. BUET, for his valuable comments to use CPT as additional correlation factors in solving the problems associated with SPT specially for research work. They also wish their appreciation to Mr. Md. Enayetur Rahman Khan, Data Entry Operator, River Research Institute, Faridpur for his typing assistance.



## References

1. De Ruiter, J. (1981), Current Penetrometer Practice.
2. Lunne, T. and kleven, A. (1981), Role of CPT in North Sea Foundation Engineering.
3. Muromachi, T. (1981), Cone Penetration Testing in Japan.
4. Murthy, V.N.S. (1993), A Text Book of Soil Mechanics and Foundation Engineering in SI Units.
5. Peck, R.B., Hanson, W.E. and Thornburn, T.H., Foundation Engineering.
6. Safiullah, A.M.M., Some Geotechnical Aspects of Bangladeshi Soils.
7. Safiullah, A.M.M., comments on Research Proposal of River Research Institute.

## Stability Test of The Patenga Coastal Embankment Near Chittagong

Md. Rafiqul Alam<sup>1</sup>

### Abstract

*This paper describes the procedure of the wave model study with the stability of the patenga coastal embankment near Chittagong. The aim of the model test is to study the behavior of the profile for different wave lengths in combination with different water levels. This test consists of wave run up test and stability test with revetment consisting of cubes and rectangles made by concrete and stones. The purpose of the wave run up test is to construct a dimensionless curve from which it is possible to determine the run up if the wave data are known. Stability test is performed to investigate the embankment at patenga i.e to verify the stability of different block units and further the influence of the arrangement of the blocks. Finally 3D stability test on the conclusion of embankment (like the head of the break water) was performed. The stability coefficient "k" = 5, from the Hudson formula for the 3D test is significantly lower than the other stability test which is realistic one.*

### Introduction

This paper describes the procedure of the model tests with the stability of the patenga Coastal Embankment near Chittagong.

The aim of the model test is to study the behavior of the profile for different wave heights in combination with different water levels. Model waves required for the hydraulic test usually belongs to small amplitude wave, which is classified in the three groups, (a) Deep water waves (b) Intermediate depth waves and (c) shallow water waves, according to the water depth (d) to wave length (L) ratio ( $d/L$ ).

1. For deep water wave  $0.5 < d/L$
2. for intermediate wave  $0.04 \leq d/L \leq 0.5$
3. For shallow water wave  $d/L < 0.04$

---

<sup>1</sup>Senior Scientific Officer/Principal Scientific Officer, RRI, Faridpur.



The wave generator is to reproduce these model waves in a test basin by the mechanical displacement of water. For this the wave generator consists of both the wave maker to displace water and the Electro-hydraulic drive system to actuate the wave maker (Mannuel for planning guide of wave generator).

The wave basin & model arrangement is shown in fig. 1, Annexure-A (Dietrich '1987).

### Test with wave run-up

This test describes the set-up. The runs and finally the treatment of the Data.

### Experimental Set-up

The revetment consists of organized placed cubes and rectangles made by concrete. The cubes have a length of around 36 cm, while the rectangles dimension is  $3.6 \times 3.6 \times 1.8 \text{ cm}^3$ . The slope of the revetment is approximately measured to be 1:4.7. In front of the revetment, the bottom was plane and sloping with a slope measured to be approximately 1:63. The width of the wave basin was 5.6 m. The longitudinal profile is shown in the fig. 2, Annexure-A (frodsoe '1988).

### Experiments

Two days of preliminary testing was performed. The water level was in all experiments 30 cm in front of the wave maker. In each run the maximum run-up  $L_1$ , was measured by a scale from a zero position at the bricks place on the crest of the embankment. After the run-up has been measured, the wave are removed and the position of the still water level  $L_2$  is measured. Now the run-up called  $R_u$  can be found from fig. 3, Annexure-A to be  $R_u = (L_2 - L_1) \sin \alpha$  (1)

where  $\alpha$  the slope of the embankment,

$$\tan \alpha = 1/4.7 \quad (2)$$

For their present slope of the embankment is found to be  $12^\circ$ , So,  $\sin \alpha = 0.21$

$$\text{Hence } R_u = (L_2 - L_1) \times 0.21 = \Delta L \times 0.21 \quad (3)$$

$$\text{Where, } \Delta L = L_2 - L_1 \quad (4)$$

The wave heights were in this Preliminary test only measured in one position and this location was in the middle of the basin. Usually the run-up is related to the wave height just in front of the toe of the embankment, which might be slightly larger than that in the middle of the basin.

**First test:**

The wave gauge was calibrated 10cm variation in water depth resulted in 4 cm deflection on the writer, So the wave height is determined by  $H = 10\text{cm} \times (z/4\text{cm})$  (5)

when  $z$  is the measured deflection on the writing paper from the waves.

The measured results are listed in table 1 below

Table-1

Exp No	Z(cm)	$L_1$ (cm)	T(sec)	$\Delta L = L_2 - L_1$ (cm)	$R_u$ (cm)	$R_u/H$	$\xi = 0.266 \left( \frac{T}{\sqrt{H}} \right)$
01	0.7	1.75	1	18	3.78	2.16	2.01
02	1.7	9.25	1	20	4.20	0.99	1.29
03	2.4	6.00	1	30	6.30	1.09	1.09
04	0.8	2.00	2	24	5.04	2.52	3.76

**2nd test:**

The Calibration of the wave gauge resulted in a 2.8 cm deflection for a 10 cm variation in water depth .

$$\text{So, } H = 10 \text{ cm} \times (Z/2.8 \text{ cm}) \quad (6)$$

(It should have be mentioned that the somewhat torque sensitivity could be wanted by adjusting the wave gain button on the wave signal generator).

The measured results are listed in table-2 (Run-up Data):

Table-2

Exp No	Z(cm)	$L_1$ (cm)	T(sec)	$\Delta L = L_2 - L_1$ (cm)	$R_u$ (cm)	$R_u/H$	$\xi = 0.266 \left( \frac{T}{\sqrt{H}} \right)$
05	0.55	1.96	1	15	3.15	1.61	1.90
06	1.25	4.46	1	27	5.67	1.27	1.26
07	0.55	1.96	2	15	3.15	1.61	3.80
08	1.15	4.11	2	28	5.88	1.43	2.62
09	0.50	1.79	3	22	4.62	2.58	5.96
10	1.08	3.86	3	39	8.19	2.12	4.06
11	1.70	6.07	2	41	8.61	1.42	2.16
12	2.30	8.21	2	40	8.40	1.02	1.85



## Data-analysis

The purpose of model tests on run-up is to construct a dimensionless curve from which it is possible to determine the run-up if the wave data are known. In general, the run-up depends on

- slope of revetment
- wave height  $H$
- Wave period  $T$
- water depth in front of the revetment

For a smooth slope, the above listed parameters can be converted to the following dimensionless relationship

$$R_w/H = \xi \quad (7)$$

where the parameter  $\xi$  is the so called surf similarity parameter or Iribarren number defined by

$$\xi = \tan \alpha / \sqrt{\frac{H}{L_0}} \quad (8)$$

where  $\tan \alpha$  = slope of revetment,  $H$  = wave height at the toe of the revetment and  $L_0$  = deep water wave length.

$$L_0 = (g/2\pi)T^2 = 1.56 T^2 \quad (9)$$

It is that the eq<sup>n</sup>  $\xi = \tan \alpha / \frac{\sqrt{H}}{L_0}$  is a measure of the ratio between the slope of the structure & wave steepness.

In table 1 and 2 the values of  $R_w/H$  and  $\xi$  respectively are tested on the measured data. For the given slope  $\alpha$ , ( $\tan = 1/4.7$ ) the eq<sup>n</sup> (8) can be written as

$$\xi = \frac{1}{4.7} \sqrt{\frac{H}{1.56 T^2}} = 0.266 \frac{T}{\sqrt{H}} \quad (10)$$

These points are plotted in fig. 4, Annexure-A.

It is seen that the points are located around a curve, the "run-up curve" which now can be used to evaluate the run up in the prototype. From the run-up curve it is seen that the deviation in the run-up curve is due to roughness and permeability of the slope.

The larger the roughness the smaller will be the run-up. Similarly a large permeability between the blocks in the revetment will reduce the run-up.

### Stability test

Preliminary stability test has been performed in order to investigate the embankment at patenga. In order to verify the stability of different block units and further the influence of the arrangement of the blocks, the embankment in the model was splitted up in four different stretches as shown in the figure  
Given below:

Interlocked rectangles 3.6X3.6X1.8cm <sup>3</sup>	Stones D<5 cm	2 Layer Dumped Cubes D=4.6 cm( Test 1) D=3.6cm(Test 2)	2 Layer Dumped rectangles 3.6X3.6X1.8cm <sup>3</sup>
--	---------------	---	---

### Structure of the revetment used in the stability test:-

Two kinds of test were performed , the main difference being different filter below the cover layer. In test no-1 the revetment was placed directly on sand (d-0.2) while in test no-2 the revetment was placed on a filter layer consisting of gravel with a mean diameter of 5mm and a thickness of around 3 cm.

The water depth in both tests was just infront of the wave maker equal 37.4 cm. The purpose of the tests was to determine the unknown constant K in the Hudson formulae  $W_r = \gamma_r H^3 \tan \alpha / k (s - 1)^3$  where  $W_r$  is the required weight of blocks in the revetment.  $\gamma_r$  is the density of the armour blocks and s is the relative density of the blocks =  $(\gamma_r / \gamma_w)$ ,  $\gamma_w$  being water density.

### Test no: 1

The experimental results of test no-1 is given below.  
Period=0.98sec.

### Wave Weight H

### Remarks

02.0 cm	No movement of Revetment
05.0 cm	No movement of Revetment
10.0 cm	Movement of Rectangles
14.3 cm	Movement of Rectangles & Boulders



Because of the preliminarily, large gaps between the successive wave heights were allowed, So the estimate of K will not be a very certain estimate. However, the results tested above suggest the following values K:

$$\text{Rectangles : } k = \frac{\gamma_r}{W_r} \tan \alpha \left( \frac{H}{(s-1)} \right)^3 \quad (\text{Jensen '1984})$$

$$\text{or with } \gamma_r = 1.6 \text{ ton/m}^3, w_r = 36 \text{ g} = 36 \times 10^{-6} \text{ ton (measured)}$$

$$S=1.6, \quad \tan \alpha = 1/4.7$$

$$\text{and } H = 0.075 \text{ m}$$

$$K=18$$

which is fairly stable protection .

## Boulders

Because the sizes of the boulders differ from each other, K is determined simply by taking the largest stone which has moved during the wave attack. For a wave-height of 14.3 cm the largest moving stone had a weight of 107 grams . The density of the stone is taken to be 2.65 tons/m<sup>3</sup> .

Hence,

$$k = \frac{2.65}{107 \times 106} \times \frac{1}{4.7} \times \frac{0.143}{(2.65-1)}$$

$$\text{or } K = 3.4$$

Which confirms that rounded stones are quite unstable due to small friction. Because the embankment was placed directly on sand, large amount of this sand was washed away during the run, resulting in large damage( settlement) of the revetment.

## Test No-2

Test No-2 was quite similar to test no-1, but now a 3cm thick filter layer was placed just below the revetment. Further the large cubes which did not move in test-1 were placed with smaller cubes(3X3X3 cm<sup>3</sup>).

The experimented results of test no-2 is given below.

<u>Period(Sec)</u>	<u>Wave Height(cm)</u>	<u>Remarks</u>
1.0	05	No Movement
1.0	06	No Movement
1.0	07	Dumped Rectangles
1.0	08	Started Moving
1.5	10	Smaller Stones(D=3cm)
1.5	12	Started Moving
1.5	14	Cubes Started Moving

This more accurate test added the following information to test no-1: The k Value for dumped rectangular blocks is slightly over estimated in test no 1. Inserting a critical wave height of 6.5 cm instead of 7.5 cm suggest that k should be reduced to

$$k = 18X(6.5/7.5)^3 = 12$$

The k-value for cubes can now be evaluated to be

$$k = r/rD^3 \tan \alpha [H/s-1]^3 \text{ (Jensen '1984)}$$

$$= \tan \alpha [H/D(s-1)]^3$$

$$k = 1/4.7 [9/3(1.6-1)]^3$$

$$= 26.6$$

Which is a fairly high k value.

The effect of the filter layer was obvious. Even though some damage was observed in the revetment. The slope of the revetment remained stable during the whole test.

**Recommendation for further stability test. (Fredsoe '1988)**

Experiments with different filter layers.

- If we call the mean diameter of the filter material  $d_f$  and the mean diameter of the armour layer in the revetment  $d_a$ , the ratio in test no -1 was

$$d_a/d_f = 3\text{cm}/0.02\text{cm} = 150$$

$$\text{in test no-2 } d_a/d_f = 3\text{cm}/0.5\text{cm} = 6$$



While test no-2 showed that ratio 6 is on the safe side, test no-2 showed that ratio 150 is on the unsafe side. Hence more experiments with other diameters in filter layer (say 1mm & 3mm) are needed.

### 3-Dimensional stability test on the conclusion of Embankment (Fredsoe '1988)

It is well known that the conclusion of a structure (like the head of a break water for instance) the blocks in the armour layer is more exposed to wave attack than the blocks in the trunks of the structure. At potenga, the revetment ends towards north in a similar rounded structure. In order to determine the stability of rectangular blocks placed on the conclusion of the embankment which is shown in the fig. 5, Annexure-A.

The embankment consisted of rectangular blocks of the size  $3.6 \times 3.6 \times 3.6 \text{ cm}^3$  in two layers, and placed on a filter layer of gravel ( $d_f = 5 \text{ mm}$ ) The filter layer was 3cm thick and placed on fine sand on the protected side of the embankment, the armour layer was made by stones. The test data are listed below

<u>Wave Heights(cm)</u>		<u>Remarks</u>
<u>Wave gauge-1</u>	<u>Wave gauge-2</u>	
3.6	3.0	Blocks starts rocking at I
5.3	4.6	Movement at I & rocking at II
9.0	7.7	Total destruction but fastest at I

### Acknowledgement

The author is grateful to Mr. Jan Dietrich, UNDP short team expert, consultant hydraulics for planning the study. The author likes to thank Mr. Jorgen Fredsoe, Estuarine and coastal Hydraulics expert of UNDP and the research personnel of RRI for carrying out the model tests at RRI. The author also likes to thank the officer and staff those who were associated with the construction and operation other model, water supply, power supply etc.

## Conclusion

From the data the following can be concluded:

Surprisingly the plane embankment at position I seems to be more unstable than the embankment on the curved part of the embankment.

This should be considered in other tests with different wave period. However in the present test the difference in the stability was very clear. It might be explained by the fact that the instability of the blocks are due to the interaction between the run-down from the former wave & the run-up from the next (popular speaking concentration of energy). On the curved part of the embankment no run-down takes place because the wave simply is travelling around the corner (Popular speaking transformation of energy), Which is shown in fig. 6, Annexure-A.

The coefficient  $k$  in the Hudson formulae can in this test on the plain part of the embankment be determined by  $k = (H/s-1)^3 1/X \tan \alpha$

Where  $X$  = vol. of the block. This gives

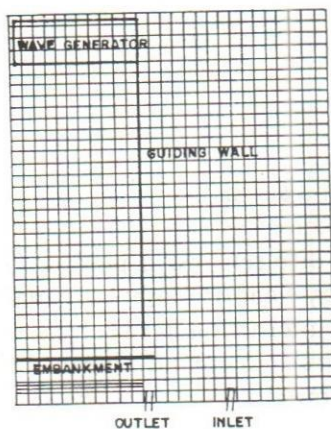
$$k = (4.6/1.6-1)^3 X 1/(3.6 \times 3.6 \times 1.8) X 1/4 = 5$$

This value is significantly lower than those obtained in stability tests before and is most realistic one.

## References

1. DIETRICH, Jan (1987), Report of model tests with Patenga Coastal Embankment. RRI, UNDTCD, BGD/81/046.
2. Fredsoe, Jorsen (1988), "Report of Tests with Embankment Protection in Wave Basin". RRI UNDTCD BGD/81/046  
Denish Hydraulic Institute.
3. Jensen, O, Juul (1984), "A monograph on Rubble Mound Breakwater". Denish Hydraulic Institute, November, '84
4. Mitsui Engineering & Ship Building Company Ltd. "Manual for planning guide of wave Generator".

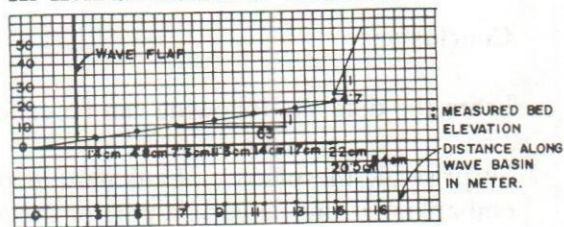




WAVE BASIN AND MODEL ARRANGMENT.

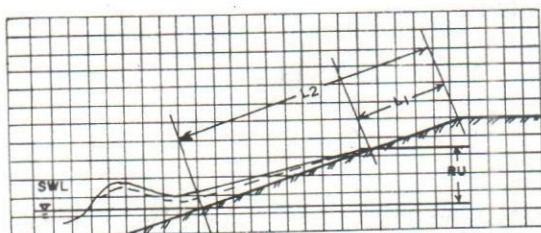
FIG. 1

BED LEVEL (Cm) LOCATION OF WAVEGAUGE



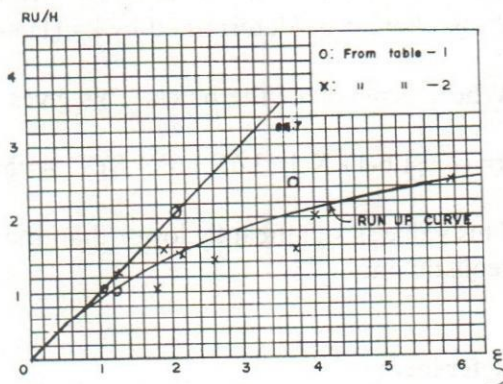
LONGITUDINAL MEASURED BED PROFILE IN WAVE-BASIN.

FIG. 2



DEFINITION OF  $L_1$ ,  $L_2$  AND THE RUN-UP  $RU$ .

FIG. 3



PLOT OF DIMENSIONLESS RUN-UP DATA.

FIG. 4

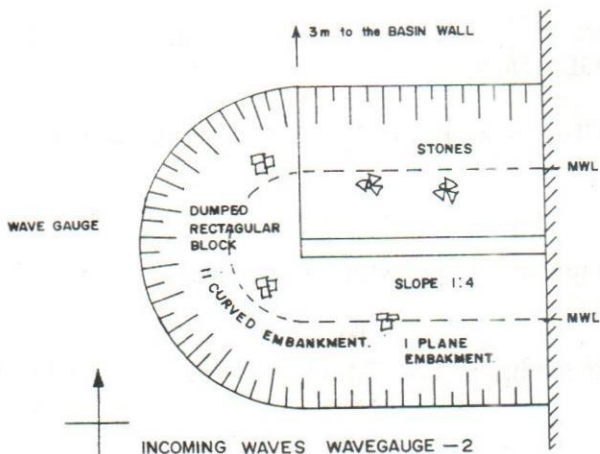
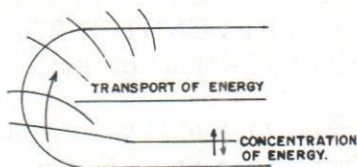


FIG. 5



MOVEMENT OF WAVE FRONTS

FIG. 6

## Development of Heat and it's Dissipation in Hardening Concrete

M. Sawlat Ali<sup>1</sup>

### Abstract

*If the temperature development and the temperature distribution of hardening concrete structures are known to the project authority is able to make suitable decisions for example, regarding time of form stripping, time of prestressing, method of curing etc. Moreover, by selecting an appropriate construction procedure, the structure may be protected against critical temperature differences and thus against thermal stress cracking.*

### Introduction

Now a-days concrete is the most important construction materials. It is composed of cement, water, fine and coarse aggregates. Among the concrete ingredients only cement and water are reactive. During the hardening process of fresh concrete, cement reacts with water chemically and thereby heat is developed in the concrete through out the hydration period of cement. During the hydration period of cement the heat development may be large and the interior temperature of the concrete structure may be very high with respect to the surrounding temperature. This difference of temperature may cause cracks in the concrete members. The intensity and dimension of cracks depend on the heat developed in the concrete. Generally at first the cracks are very small and may not be seen with naked eye. But when the concrete structural members become cooling down to normal temperature the cracks grow larger in dimensions due to the shrinkage of concrete. In the hydraulic structure it is very harmful. Through these cracks in the concrete, water in the from of atmospheric moisture enter into the concrete and thereby rap to the reinforcement. Then the reinforcement react with water to form oxide of iron and produce a volume of eight times of its original volume and damage the structure in coarse of time. The heat dissipation of concrete depends on the thickness of the structural member. "For a wall of 6" thickness 95% of heat generated during the hydration process in the concrete will be lost to the air in about 1-1/2 hours. For 5' thick wall the same amount of heat will be lost to the air in a week or more. (ACI - 207 - 112 - 26).

The concrete laboratory of RRI, Faridpur made an attempt to measure the interior temperature of hardening concrete during its hardening period of concrete poured in the six different members of concrete structure during hydration period of cement. Before commencement of casting of concrete if we test the concrete ingredients and if we determine the heat of hydration of cement, then we predetermine the heat development in concrete by simulating the properties of concrete in the CIMS (Computer Interactive Maturity System) in RRI. The concept behind the CIMS is that if we have tested out

---

<sup>1</sup>Senior Scientific Officer, RRI, Faridpur.



concrete property development in the laboratory at a constant temperature and if we simulate or measure the concrete temperature during the hydration period of concrete in the structure we are able to predict accurately the concrete strength and other properties at any given time anywhere in the concrete structure to contradict that construction complies with the assumption made in the plan.

With the existing knowledge of today, it is impossible to state the exact limits of temperature differences which are acceptable in hardening concrete cross-section. According to experiences it is wise to stay within the following limits for temperature stress.

For cooling of cross-section after stripping allowable temperature difference over the cross-section should be  $20^{\circ}\text{C}$ . For construction joint and structure with greatly varying cross-section dimensions maximum difference may be  $10^{\circ}\text{C}$  to  $20^{\circ}\text{C}$ .

In the latter case greater difference in temperature may be acceptable under certain conditions since relaxation affects in the hardening concrete may reduce temperature stress.

### Adiabatic Condition of Concrete

If the minimum dimension of a concrete structure is about 1M(3.3') or more the concrete of the structure will have almost Adiabatic Conditions i.e. no heat exchange with the surroundings. The amount of heat generated in the concrete during the hydration period of cement, generally a rule of thumb, is that, the total heat developed by OPC per  $100\text{kg/m}^3$  cement results in a temperature rise of the concrete (at adiabatic condition's) of about  $10^{\circ}\text{C}$  ( $18^{\circ}\text{F}$ ). Where the surface of the concrete structure is cast against steel molds or forms the surface temperature of concrete will be equal surroundings (air) temperature.

If the temperature gradient (difference) from the centre to the surface of the concrete structure is above  $20^{\circ}\text{C}$  ( $38^{\circ}\text{F}$ ) the thermal stress will be higher than the concrete tensile strength and the concrete will crack. At the time of cracking (Max. temp. diff.  $20^{\circ}\text{C}$ ) we can actually see the cracks. As the centre of the structure cools down, the cracks will close and again become invisible after shrinkage.

The cracks, however, are there and will serve as opening for water etc. So that the durability of the concrete structure is reduced if the concrete cross-section is not unrestrained, cracking may occur at a temperature difference of  $10^{\circ}\text{C}$  or even less (e.g. casting of wall on hardened concrete) to reduce the maximum temperature we have various options. But none of them are easy and all of them are expensive. However, it is also very expensive and difficult to repair cracks in concrete structure.



In the present work we have measured only the concrete interior temperature during the hydration period of cement (OPC) from different 6(six) Nos. (figs. 1 - 6) concrete structures to see the development of concrete interior temperature and its behaviour.

### **Measuring Concrete Temperature**

The concrete interior temperatures were measured by using digital thermometer and thermocouple

### **Placing of Thermocouple**

The thermocouple were placed at the locations where the concrete interior temperature measurement is desired during the hydration period of cement. Care has been taken to ensure that soldering points are placed at a distance from reinforcement or other materials that may disturb the temperature measurement through their size, specific heat or nature. For placing thermocouple in the green concrete we have used bamboo stick. The thermocouple were tapped with the stick, then the thermocouple with bamboo stick was mounted in the green concrete upto the desired depth. After a suitable time the bamboo-stick was drawn without any disturbances of the thermocouple.

### **Frequency of Reading**

A frequency of reading have been adopted rapidly for the first 8(eight) hours as the interior temperature was changing very first. Later on, the reading were taken of one/two hours interval. Finally after two or three days the interior temperature reading were taken three times daily.

### **Observation**

It is seen from the table no.1 that the maximum concrete interior temperature were ranging from  $46^{\circ}\text{C}$  to  $61^{\circ}\text{C}$  corresponding to time to attain the maximum temperature were ranging from 14 hours to 28 hours and the concrete mixing temperature were ranging from  $22^{\circ}\text{C}$  to  $29^{\circ}\text{C}$ . The temperature gradient were ranging from  $14.5^{\circ}\text{C}$  to  $25^{\circ}\text{C}$ . It is obviously seen that the concrete surface temperature of the hardening concrete were higher than the air temperature by  $2^{\circ}\text{C}$  to  $7^{\circ}\text{C}$  during the period around the maximum temperature raised. Knowledge of the temperature development and temperature dissipation in the hardening concrete will help the contractor an opportunity of controlling the hardening phase of the concrete in a safe and appropriate way. On the basis of temperature measurement it is possible to make the necessary decision as to striping, stressing of cables, additional insulation, curing etc. So that prescribed requirements made in the actual work conditions are observed in a financially sound way.



## Conclusion

Concrete interior temperature rises very rapidly in hot weather, where as, it is slightly slow in the cold weather. Higher the initial concrete temperature larger the maximum concrete interior temperature. Larger the concrete structural dimensions higher the maximum interior temperature.

Rise of interior temperature and its dissipation follow the same trend for the same type of cement. The differences of concrete interior temperature depends on that of the mixing temperature of the concrete for the same type of cement and mix ratio.

### STATEMENT OF CONCRETE INTERIOR TEMPERATURE BY DIGITAL THERMOMETER

Sl. No.	Test No.	Type of Cement	Concrete Mix Temp. °C	Concrete Temp. Max. °C	Surface Temp. at the time of Max. Temp °C	Depth of Reading in ft.	Temp. Difference °C	Elapsed Time to attain Max. Temp. (HRS)
1.	A	Chhatt	22	49.00	34.50	2.5	14.50	22
2.	B	Chhatt	27	51.50	35.00	2.5	16.50	16
3.	C	Chhatt	23	46.25	30.50	2.5	15.75	22
4.	D	Chhatt	24	51.00	30.50	2.5	20.50	28
5.	E	Chhatt	24	50.75	31.00	2.5	19.75	14
6.	F	Chhatt	29	61.00	36.00	2.5	25.0	14

Higher the concrete mix temperature higher the Max. temperature attained.

## Acknowledgement:

Tribute to my colleagues and Concrete Technicians who helped me in different phases of this works. My special tribute to best of Mr. M. Zahurul Islam former C.S.O. of RRI, Faridpur.

## Reference

1. WADDELL, J.J. Concrete construction hand book, 2nd Ed. Mc. Graw-Hill Book Company, New-York, U.S.A.
2. Neville, A.M. Properties of concrete 3rd Ed. 1981.
3. A.C.I. Manual of concrete practice, part-1-1983.
4. Kjaer, U. Measuring of concrete temperature, Lecture note, Dated 13.11.86.
5. Troxell, G.E. and Davis, H.E., composition and properties of concrete, Mc. Graw-Hill Book Company, New-York, U.S.A.
6. Shetty, M.S. concrete technology.



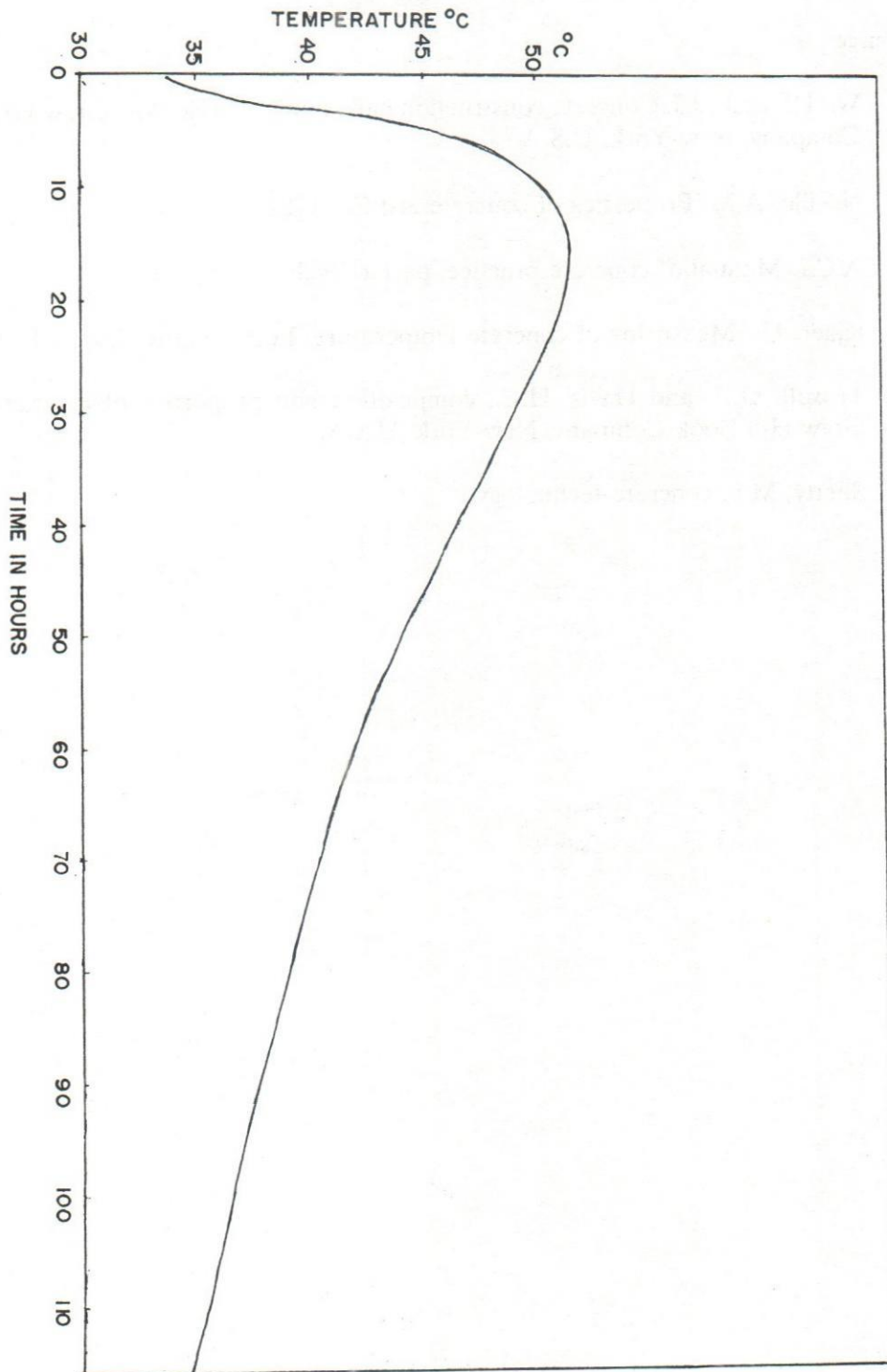


FIG. NO. I

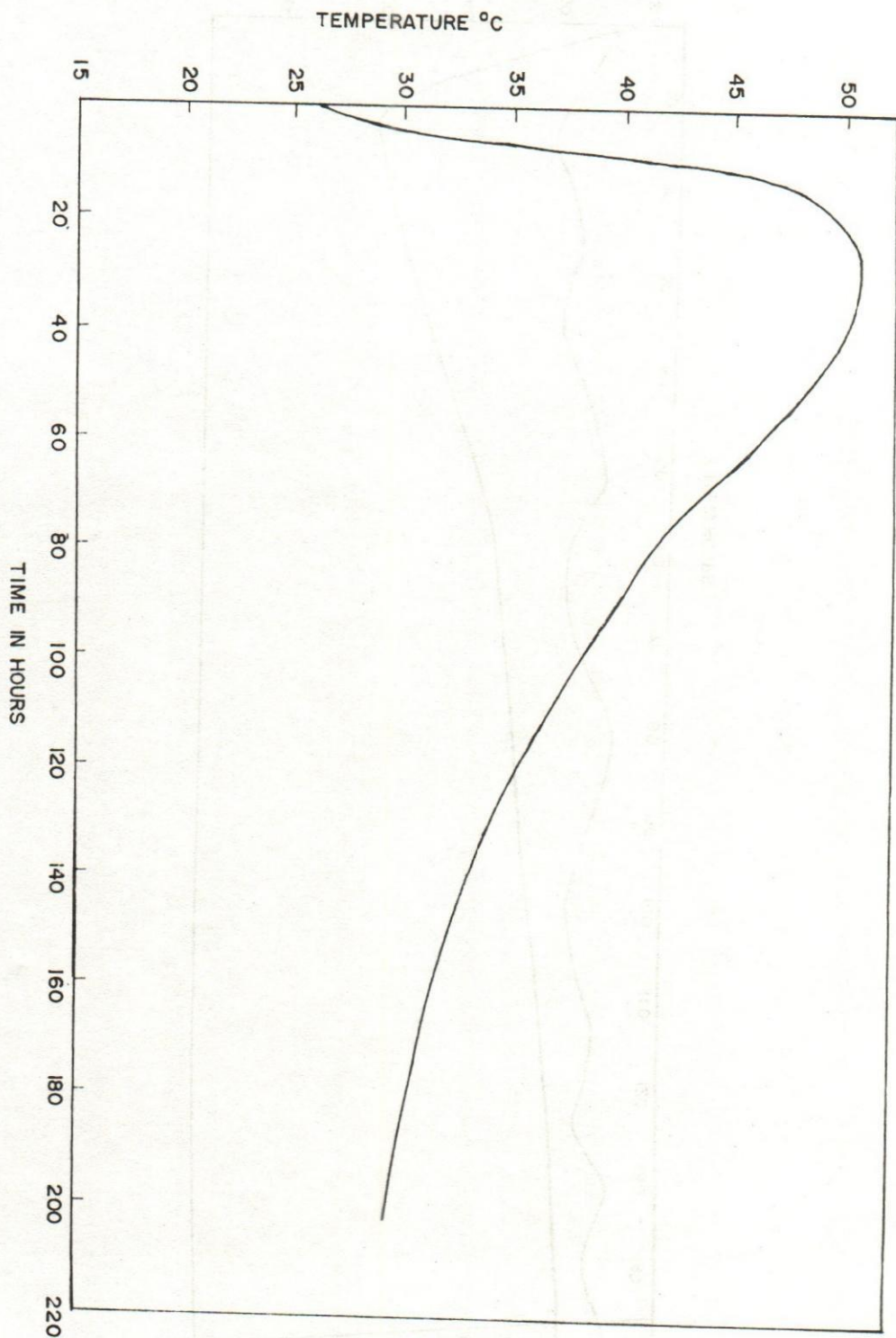


FIG. NO. 2



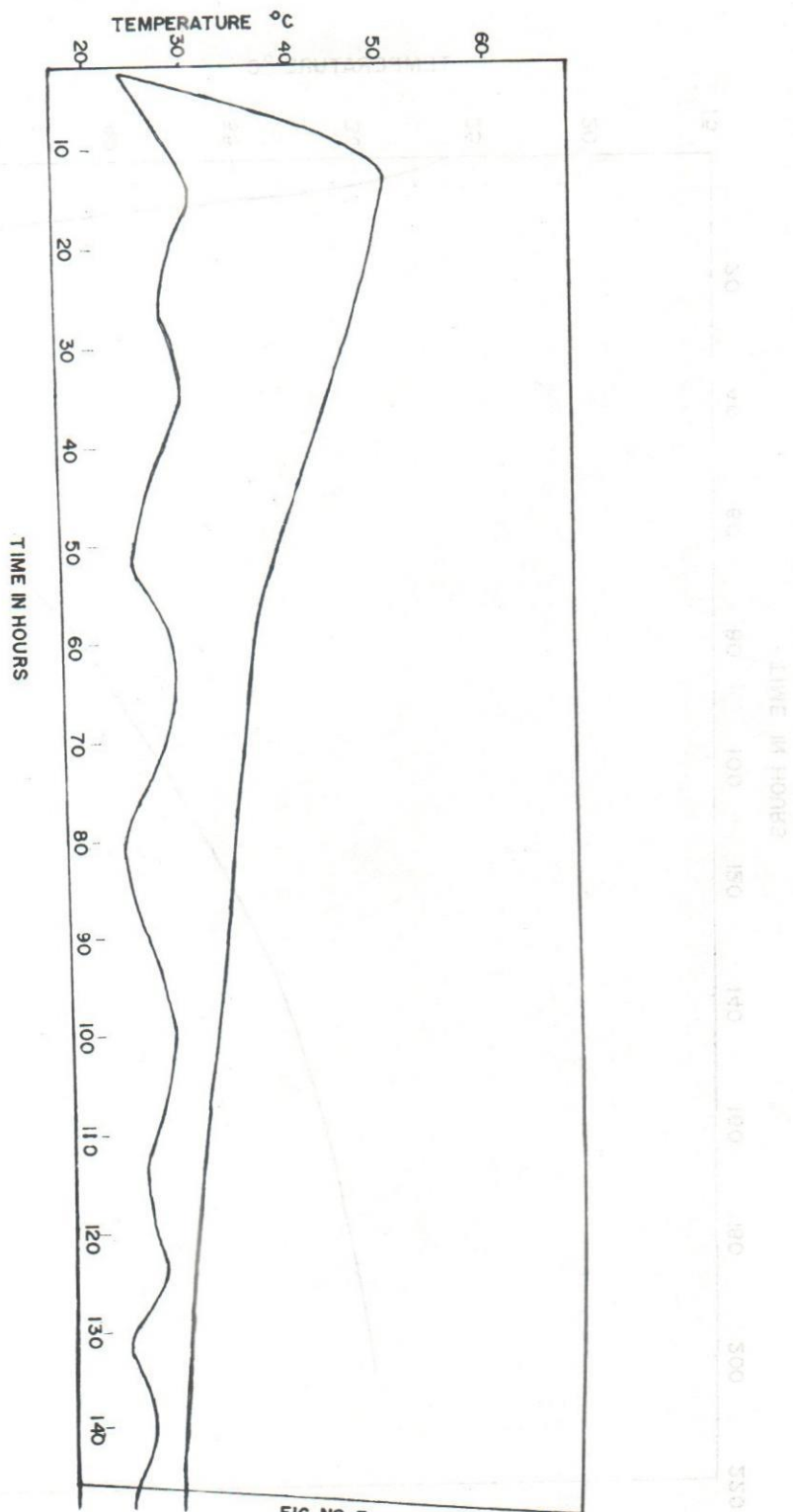


FIG. NO. 3

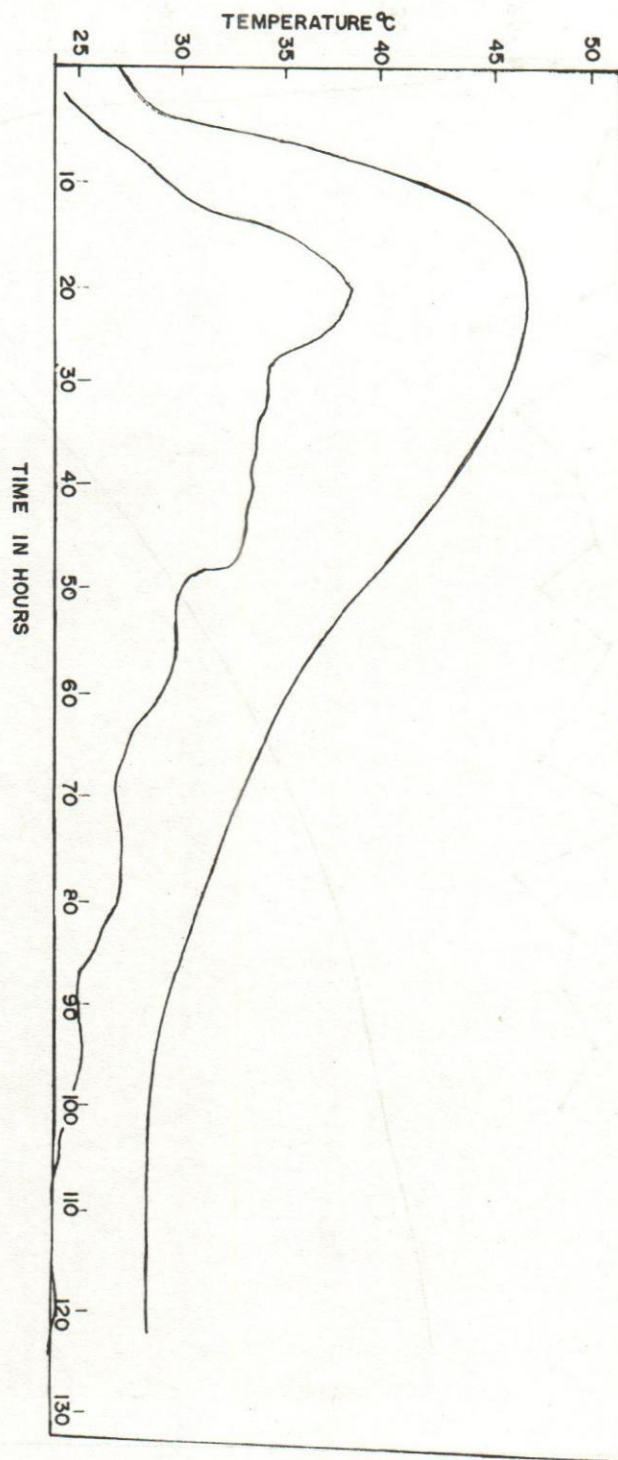


FIG. NO. 4



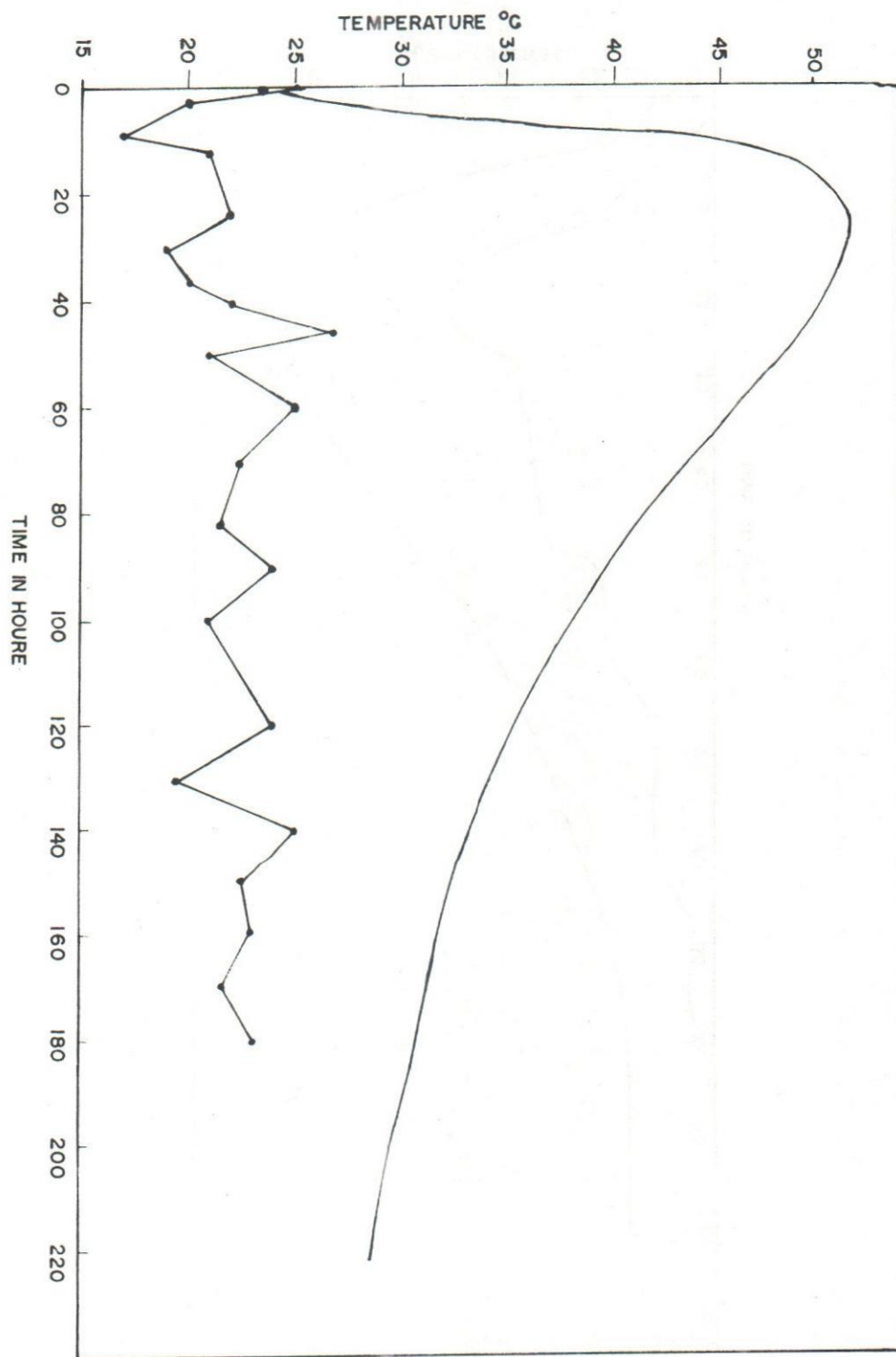


FIG. NO. 5

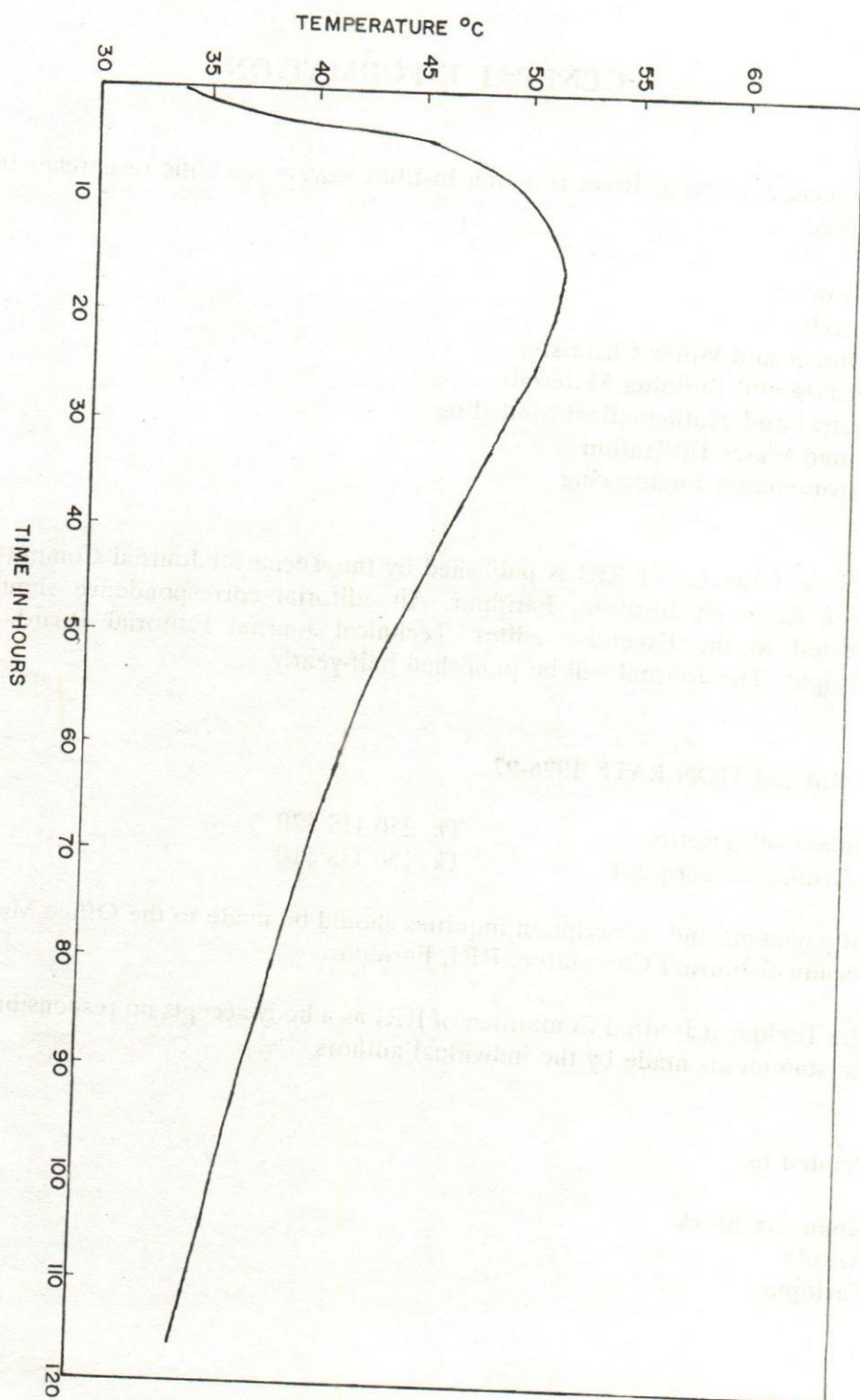


FIG. NO. 6



## **GENERAL INFORMATION**

Technical Journal of River research Institute covers scientific researches in the fields of

**Hydraulics**  
**Geotechnics**  
**Sediment and Water Chemistry**  
**Concrete and Building Materials**  
**Physical and Mathematical Modelling**  
**Ground Water Utilization**  
**Environmental Engineering**

Technical Journal of RRI is published by the Technical Journal Committee of River Research Institute, Faridpur. All editorial correspondence should be directed to the Executive editor, Technical Journal Editorial Board, RRI, Faridpur. The Journal will be published half-yearly.

### **SUBSCRIPTION RATE 1996-97**

Annual subscription:	Tk. 250 US \$20
Individual subscription:	Tk. 150 US \$10

All payments and subscription inquiries should be made to the Office Manager, Technical Journal Committee, RRI, Faridpur.

The Technical Journal Committee of RRI as a body accepts no responsibility for the statements made by the individual authors.

**Printed by:**

**Khan Art Block**  
**Niltuly**  
**Faridpur**